CHEMICAL REVIEWS

pubs.acs.org/CR

Review

Advanced Materials for Energy-Water Systems: The Central Role of Water/Solid Interfaces in Adsorption, Reactivity, and Transport

Edward Barry, Raelyn Burns, Wei Chen, Guilhem X. De Hoe, Joan Manuel Montes De Oca, Juan J. de Pablo, James Dombrowski, Jeffrey W. Elam, Alanna M. Felts, Giulia Galli, John Hack, Qiming He, Xiang He, Eli Hoenig, Aysenur Iscen, Benjamin Kash, Harold H. Kung, Nicholas H. C. Lewis, Chong Liu, Xinyou Ma, Anil Mane, Alex B. F. Martinson, Karen L. Mulfort, Julia Murphy, Kristian Mølhave, Paul Nealey, Yijun Qiao, Vepa Rozyyev, George C. Schatz, Steven J. Sibener, Dmitri Talapin, David M. Tiede, Matthew V. Tirrell, Andrei Tokmakoff, Gregory A. Voth, Zhongyang Wang, Zifan Ye, Murat Yesibolati, Nestor J. Zaluzec, and Seth B. Darling*

Cite This: *Chem. Rev.* 2021, 121, 9450–9501

Read Online

ACCESS | Metrics & More | Article Recommendations

ABSTRACT: The structure, chemistry, and charge of interfaces between materials and aqueous fluids play a central role in determining properties and performance of numerous water systems. Sensors, membranes, sorbents, and heterogeneous catalysts almost uniformly rely on specific interactions between their surfaces and components dissolved or suspended in the water—and often the water molecules themselves—to detect and mitigate contaminants. Deleterious processes in these systems such as fouling, scaling (inorganic deposits), and corrosion are also governed by interfacial phenomena. Despite the importance of these interfaces, much remains to be learned about their multiscale interactions. Developing a deeper understanding of the molecular- and mesoscale phenomena at water/solid interfaces will be essential to driving innovation to address grand challenges in supplying sufficient fit-for-purpose water in the future. In this Review, we examine the current state of knowledge surrounding adsorption, reactivity, and transport in several key classes of water/solid interfaces, drawing on a synergistic combination of theory, simulation, and experiments, and provide an outlook for prioritizing strategic research directions.

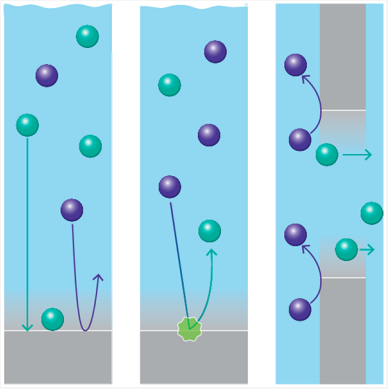

CONTENTS

Received: January 25, 2021
Published: July 2, 2021

https://doi.org/10.1021/acs.chemrev.1c00069
Chem. Rev. 2021, 121, 9450–9501

INTRODUCTION

Water is central to all aspects of life and society. Sustaining satisfactory economic production, health, education, and environmental protection relies on the availability and sustainable management of water.[1] Yet, water resources are under ever-increasing stress because of climate change, development, population growth, and other factors;[2] this is particularly true with regard to the depletion of groundwater.[3] Overcoming water stress will require progress with infrastructure and policy, and there is also a major role to play for innovations from science and technology.

Scientific and technological advances that improve our understanding and efficient use of water and energy are of critical importance. The direct connection between water and energy takes its most tangible scientific form at water/solid interfaces that mediate energy conversion and transduction processes or are designed to influence water chemistry.[4−6] Water/solid interfaces are central to a broad array of scientific and technological processes including heterogeneous catalysis and electrochemistry, life sciences and biomedical applications, and environmental and geosciences.[7] The importance of such systems cannot be overstated.[8] Yet, numerous fundamental questions in these areas remain unanswered despite decades of study. At the heart of these issues are molecular-scale questions involving the nuances of water's hydrogen bonding at interfaces with electrolyte solutions, the interfacial transfer of energy in the form of protons and electrons, the adsorption and chemical reactivity of solutes at structured and confined interfaces, and many other particulars connected to water. With the emergence of newfound capabilities to experimentally probe and computationally model these complex systems, the chemistry and physics of aqueous solution/solid interfaces has become one of the most exciting fields in science.

Structure and dynamics at water/solid interfaces, rife with entropic complexity, necessarily involve multiple length scales. Atomic-level insights govern attractive and repulsive molecular and electrostatic forces related to wetting, with nanoscale structure influencing binding and interfacial reactivity through shaping of the local environment, and still larger length scales dictating how these interactions couple with cohesive forces and translate into fluid transport in the vicinity of interfaces. In some cases, length scales for a given phenomenon (e.g., Debye length) can vary by orders of magnitude, depending on the environment. Two major challenges in deciphering interfacial phenomena are (1) pulling out local influences that become washed out in ensemble measurements of heterogeneous systems and (2) distinguishing interfacial behavior from that in the bulk. To address these challenges, it is necessary to bring together researchers with a convergence of expertise in theory/modeling/simulation, materials synthesis/fabrication, and advanced characterization enabled by world-class facilities. The U.S. Department of Energy's 2017 Basic Research Needs Workshop for Energy and Water highlighted the timeliness and importance of new fundamental science studies to help address burgeoning challenges related to water both nationally and globally.[9]

Interfaces in water systems participate in a host of processes, each representing a fascinating subject for study and carrying considerable relevance for applications. Here we will focus on the three fundamental aspects of aqueous solution−solid interaction: (i) adsorption, (ii) reactivity, and (iii) transport (Figure 1). Each of these three topics has been studied for many years and in many different contexts, yet much remains to be learned.

Adsorption phenomena in aqueous systems, despite the apparent simplicity of excluding chemical reactions, are surprisingly complex. Even the adsorption of water itself onto solid surfaces remains something of a mystery—this is particularly true as one examines layers beyond the initial hydration layer, where interactions between water molecules in dissimilar local environments dominate.[7] Capture of certain classes of solutes from aqueous systems receives special attention because of their toxicity or other harmful characteristics. Heavy metals fall into this category, and substantial research effort has been directed at their adsorption.[10,11] Adsorption of polymers at interfaces, and especially of charged polymers (due to their high solubility in water), has generated tremendous interest in the community. As with other species, adsorption will occur spontaneously from solution if the interaction between the polymer and the surface is more favorable than that of the water with the surface. Ideal solid surfaces are impenetrable to these polymer chains and are flat, electrically neutral, and chemically homogeneous.[12] Departures from these idealities add increasing levels of complexity, but understanding all these competing interactions at various length scales will be critical to revealing fundamental mechanisms associated with fouling—a ubiquitous phenomenon in water systems.[13]

Catalysis and reactivity in aqueous systems, including the reactivity of water itself, is a deep and broad field for which it is impossible to do justice in a brief summary. Much work has been done in the area of solar fuels, with water oxidation representing perhaps the most challenging aspect, whether by heterogeneous electrocatalysis at electrode surfaces, heterogeneous catalysis by oxidic bulk materials, homogeneous catalysis using transition metal complexes, or biocatalytic strategies related to photosynthesis.[14] While efforts to identify efficient and effective processes for splitting water using sunlight as an energy source are ongoing,[15] there are opportunities to exploit the advances in catalytic science gained in those studies to create new catalytic

https://doi.org/10.1021/acs.chemrev.1c00069
Chem. Rev. 2021, 121, 9450−9501

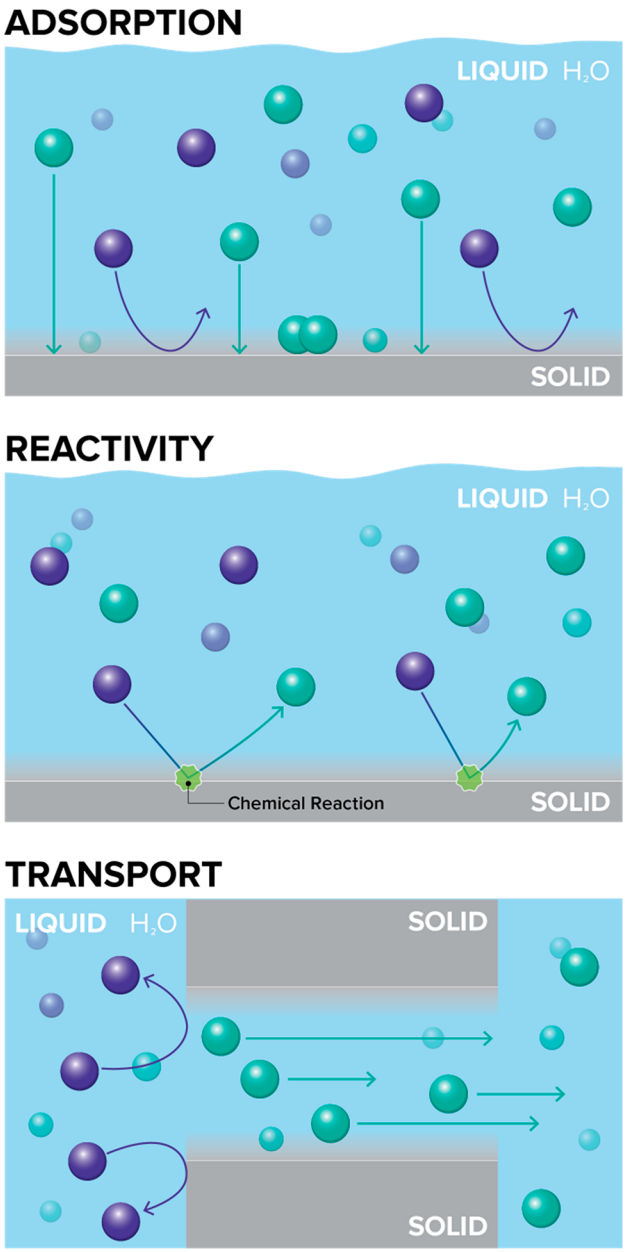

Figure 1. Schematic representations of three categories of water/solid interface processes: adsorption, reactivity, and transport.

materials and reaction pathways to generate reactive species in water with potential use in remediation. Heterogeneous water phase catalysis for water treatment is a burgeoning field of study rich with fundamental science questions remaining to be answered.[16,17]

Flow and transport in porous media have long been of interest to researchers and technologists alike. In general, transport processes in porous media can be divided into three levels: molecular, mesoscale, and macroscale. At the large scales, pore networks for investigations of multiphase flow first appeared in the 1950s,[18] later complemented by percolation theory[19] and models based on pore-space geometry.[20,21] Mesoscale modeling generally deals with flow, rejection, flux, and fluidic transport. When a medium is porous and aqueous fluid flow is laminar, hydrodynamic theories can be applied and solved using existing frameworks.[22] Application of a specific model depends on the pore structure factors such as pore size, shape, porosity, average capillary length, pore-size distribution, surface area, and tortuosity.[23] Diffusion processes are also often relevant to transport through porous media, driven by solute concentration gradients. Commonly adopted models, especially in cases involving ions, are those based on the Extended Nernst−Planck equation with the Donnan steric equilibrium at water/solid interfaces.[24,25] On the molecular scale, numerical simulations are often carried out. Molecular dynamics (MD) is one such tool where the physical motion of atoms and molecules is simulated. Newtonian equations of motion are solved numerically for a system of interacting particles, and the forces between particles are defined by interatomic potentials.[26]

Water/solid interfaces represent a broad array of research topics, far too diverse to fully address in one paper. In this Review, we will address the state-of-the-art in each of the topical areas discussed above and identify exciting and important knowledge gaps. Water/solid interfaces are the unifying theme, and the Review is structured according to principles of adsorption, reactivity, and transport associated with these interfaces.

1. ADSORPTION

1.1. Introduction/Overview

Adsorption phenomena in aqueous systems are surprisingly complex, yet controlling and harnessing such behavior is of critical importance across a range of energy-water systems. From the health and well-being of individuals who depend on clean drinking water, to fit-for-purpose water across industrial sectors, adsorption plays a key role in addressing ongoing challenges. Such challenges include the selective capture of toxic or other harmful substances, including heavy metals and emerging contaminants such as lead and per- and polyfluoroalkyl substances, and the prevention of fouling and scaling (deposition of inorganic materials) processes. Notwithstanding its applied significance, adsorption is characterized by complex interfacial interactions in confined geometries for which much of our scientific understanding remains lacking. In this section, we review research in the field of adsorption for energy-water systems and its impact on generating a detailed understanding of the solid/water interface as obtained through complementary techniques of materials synthesis, in situ characterization tools, computational modeling, and analysis. Such research seeks to elucidate many of the molecular-scale interactions involved in adsorption, including nonspecific and specific forces of chemical and electrostatic origin, and correlating these interactions with key factors in adsorptive processes such as geometrical constraints of confinement. By gaining a fundamental understanding of the factors that govern interfacial interactions in model systems, it is possible to design materials with superior performance in applied systems and provide a better understanding of the delicate interplay between material form (e.g., pore size) and function (e.g., chemical functionality) from the Ångstrom to the mesoscopic length scales.

At the molecular scale, surface adsorption and site-specific binding of ions and molecules from aqueous solution depend on a complex three-way interplay of interactions between surface, adsorbate, and water. These multiple competing effects are determined by electrostatics, hydrogen bonding, solvation dynamics, and surface morphology, as well as less intuitive factors such as hydrophobicity and entropic forces from crowding and depletion. Even in bulk solution, the interplay of these factors is complex, which is reflected in the fact we are still

https://doi.org/10.1021/acs.chemrev.1c00069
Chem. Rev. 2021, 121, 9450−9501

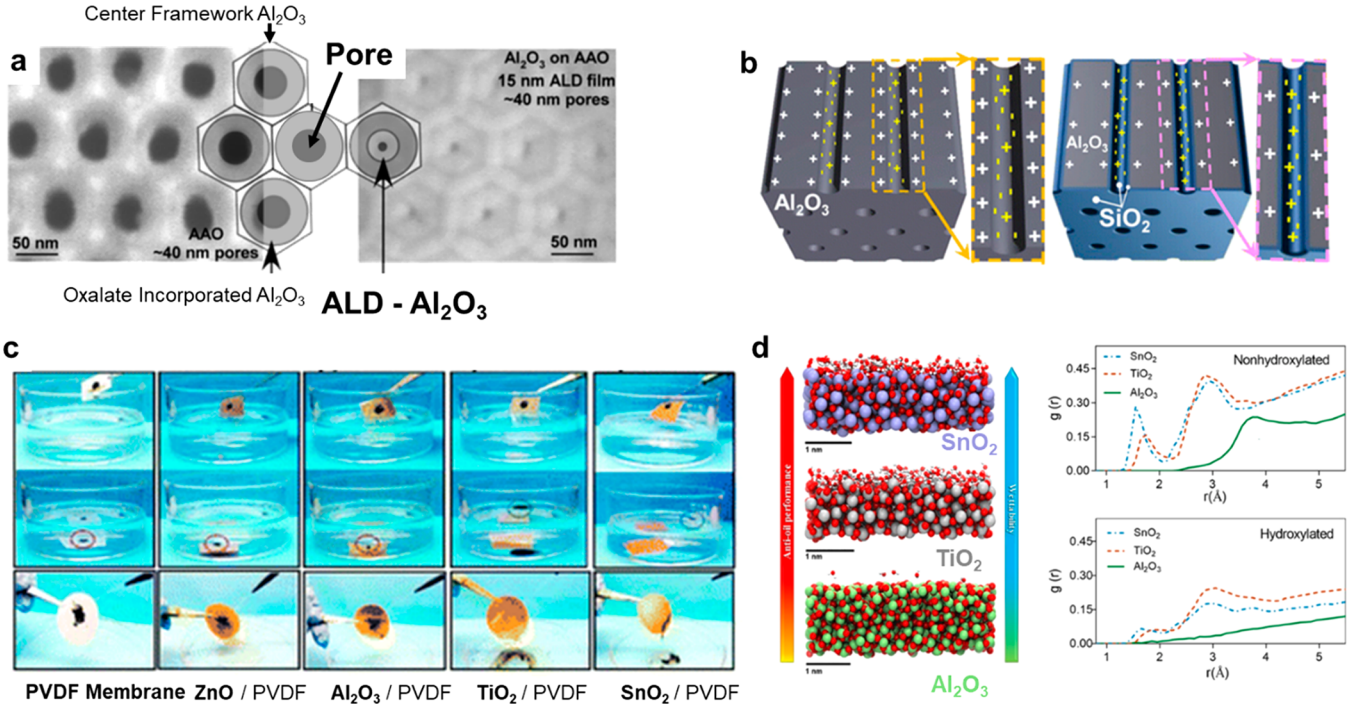

Figure 2. SEM top view micrographs of (a) an uncoated (left) and 15 nm alumina-coated (right) anodic aluminum oxide (AAO) membrane showing 10 nm pores remaining after the ALD coating. The SEM image of the uncoated membrane shows regions of differing contrast associated with compositional changes that affect the secondary electron yields. The bright regions are from what is suggested to be relatively pure alumina, while the gray portion has incorporated oxalate anions from the anodization solution. The dark portions are the pores themselves. Reprinted with permission from ref 37. Copyright 2005 American Chemical Society. (b) Schematic of surface charges on pure AAO and SiO_2-coated AAO membranes. Reprinted with permission from ref 39. Copyright 2013 American Chemical Society. (c) Anticrude-oil performance of membranes coated with different oxides by ALD. (d) Molecular Dynamics simulation snapshots showing three different amorphous oxide layers and water molecules that are within 3.4 Å above their surfaces. The atoms are colored by their types, i.e., O (red), H (white), Sn (purple), Ti (gray), and Al (green). From bottom to top, the wettability of these amorphous oxide layers increases, which is characterized by the water−oxide radial distribution functions, g(r), shown in top graph for nonhydroxylated (pristine) and in bottom graph for hydroxylated oxide layers. Reprinted with permission from ref 40. Copyright 2018 American Chemical Society.

missing a molecular theory of solubility in water.[27] At the root of all adsorption problems are the concepts of aqueous solvation, solubility, and the rapidly changing hydrogen-bond network of water, which dynamically organizes itself to accommodate solutes and adapt to extended surfaces. Many such features have been captured nicely in a series of model and applied experimental systems, but further development of experimental and theoretical methods is required to better explain the interplay of many competing noncovalent interactions for aqueous solutions in the boundary layers with solid interfaces.

1.2. Material Platforms for Probing Adsorption Phenomena

There is no shortage in the number of substrates, materials, and synthetic techniques that have been employed to study processes of adsorption in aqueous media. While the list included here is some small subset of the many possibilities, the techniques included enable access to a diverse set of finely tunable chemical and electrostatic environments through highly tailorable interfacial properties. At the same time, there is great potential for complementarity in their approach to understand—and ultimately control—a range of adsorption phenomena. The specific platforms considered include atomic layer deposition (ALD), two-dimensional (2D) materials, and polymer brushes, spanning multiple material classes such as small molecules bound to oxide substrates, charged polymer brushes, and functionalized 2D layered materials. ALD (or more generally, atomic layer processing, which includes ALD, molecular layer deposition (MLD), and vapor phase grafting) offers great versatility via direct control over interfacial chemistries and geometries. At the same time, ALD-coated surfaces can be used to introduce subsequent functionality through the covalent binding of chemical moieties. Substrates based on 2D materials, such as graphene and molybdenum disulfide, are an exciting class of new materials for energy-water systems with high surface area and tailorable surface properties. Polymeric brushes, in particular those with charged groups, are another class of materials that can be leveraged to imbue bulk materials (e.g., polymer membranes and inorganic substrates) with superior resistance to fouling and/or selective ion-sequestration.[28−30] While such materials and methods are well-known in a variety of different fields throughout the research community, they have only recently been explored for water-based applications.[31]

1.2.1. Atomic Layer Deposition. Atomic layer deposition (ALD) is a conformal, Ångstrom-scale controlled, interface functionalization technique, offering direct control over interfacial chemistry and tunable film composition. ALD is performed by subjecting a solid surface to sequential exposures of precursor vapors that chemically react on the surface in a self-limiting fashion resulting in the layer-by-layer growth of an inorganic coating.[32−34] The self-limiting chemistry, coupled with gaseous diffusion of the precursor vapors, allows for highly conformal coating of high-aspect-ratio and high-surface-area substrates including porous membranes. Such features render ALD a highly promising technique for interfacial engineering

https://doi.org/10.1021/acs.chemrev.1c00069
Chem. Rev. 2021, 121, 9450−9501

within energy-water systems in confined geometries. Recent advancements in ALD-based interfacial membrane engineering[35,36] highlight a particular area where ALD can be applied with versatility and great promise in energy-water systems to control interfacial interactions with atomic- and molecular-scale precision. Whereas ALD uses organometallic precursors and inorganic compounds (such as H_2O) to grow inorganic coatings, MLD uses exclusively organic vapor compounds to grow organic coatings in an atomic layer-by-layer manner and shares many of the desirable attributes of ALD.

Transition-metal oxides, such as aluminum oxide (Al_2O_3) and titanium dioxide (TiO_2), are prototypical ALD materials that can be deposited over a broad range of conditions, including low temperatures compatible with polymer substrates. When these coatings are applied to a membrane, they directly modify the material's surface chemistry, and thus the interface, while leaving the bulk unchanged. In the case of anodic aluminum oxide (AAO) membranes, ALD can shrink the AAO pore diameter in a layer-by-layer fashion over the entire pore length[37−39] (Figure 2a,b). Similarly, these oxide-based coatings can impart chemical-based functionalities. In one example, stark differences in the oil-repellent properties of ALD-coated polyvinylidene fluoride (PVDF) membranes were associated with the metallic center of the oxide coating ($SnO_2/Al_2O_3/ZnO/TiO_2$) and the resulting hydration layers[40] (Figure 2c,d). Such studies highlight the extent to which atomic-interfacial interactions, and specifically direct control over them, can be used to tailor more macroscopic behavior. Of the oxides, TiO_2 is an excellent example of a material that is generally embedded in the selective layer of membranes or adhered to membrane surfaces in the form of nanoparticles. In recent work, researchers demonstrated how TiO_2 coatings can be deposited via methods of ALD on commercial ceramic membranes using alternating doses of a titanium tetrachloride ($TiCl_4$) precursor and water (H_2O) as an oxygen source, leading to higher inorganic surface coverage compared with blending inorganic components into a casting solution.[41] In a further step, nitrogen doping into the TiO_2 lattice was achieved via doses of ammonium hydroxide (NH_4OH) during the ALD process and was shown to shift the band gap to optical wavelengths, resulting in a visible-light-activated photocatalytic film with antifouling properties. Such features suggest a novel new strategy to combat membrane fouling during continuous filtration and real-time membrane self-cleaning utilizing low-cost light sources—including potentially sunlight.[41] Notwithstanding its potential importance within applied settings, these works demonstrate some of the unique efficacy of ALD in creating atomically precise coatings to modify both chemical and physical properties of membranes.

In another set of examples, researchers demonstrated the possibility of two-step functionalization using ALD coatings acting as a type of intermediate layer.[42] A particularly promising route for oxide-based coatings is the subsequent binding of organosilane-based moieties. Organosilanes have myriad functionalities that can impart surfaces with a diverse range of properties, including charged residues, hydrophobic, hydrophilic, and oleophilic properties. Research into this area continues to expand rapidly. One recent example builds upon methods of ALD, and a closely related approach based on sequential infiltration synthesis (SIS), to highlight the efficacy of such an approach to create a reusable oil adsorbent material based on polyurethane foam. Polyurethane as a base starting material has no affinity toward organosilane functionalization, but a thin (nanometer) coating applied to the polymeric filaments enables the covalent attachment of oleophilic moieties.[43] In this way, ALD-based oxide coatings serve as a type of intermediate binding layer, and a means by which to introduce suitable binding sites for subsequent functionality exhibiting selective adsorption.

While there exist many opportunities within the field of ALD-based interfacial engineering, it is important to note that ALD is predicated by favorable interactions between surface functional groups and gaseous precursors. In this way, ALD is not applicable to many polymeric membranes that lack appropriate surface functional groups and are based on inert materials such as simple hydrocarbons (polypropylene, polyethylene, etc.).[44] While sensitization strategies exist, including oxidative plasmas or acids to introduce reactive sites, many have met with limited success because they are difficult to control or damage the structural integrity of the membranes. A recent study has highlighted a facile liquid-phase dip-coating method to overcome this limitation using tannic acid. Similar to other phenols, tannic acid was found to effectively sensitize hydrophobic polymer membranes to TiO_2 ALD coatings. Tannic acid-sensitized ALD-coated membranes were found to exhibit outstanding underwater crude oil repulsion and rigorous mechanical stability through bending and rinsing tests.[44]

Taken as a whole, ALD has the ability to enable a new synthetic paradigm for interfacial membrane engineering, and in particular controlling interfacial water-energy interactions with great precision. Other noteworthy examples include Janus membranes for ionic rectification or nanofiltration,[44] suggesting a versatile synthetic strategy for hybrid inorganic/organic membranes,[45] combining favorable features of polymeric membranes such as low cost, tunable porous structure, and scalability, with features more associated with inorganic (e.g., ceramic) membranes such as superior hydrophilicity and structural stability.[46] Not only can ALD achieve a higher inorganic surface coverage compared with blending inorganic components into casting solution, it can also be achieved with molecular-scale precision and control.

We close this section by noting that improvements in energy−water systems will necessitate fabrication of high-performance separation membranes, and ALD as a synthetic toolkit to do so provides an appealing new strategy. Excitingly, such research has yet to fully exploit the broad spectrum of ALD-based coatings with respect to dielectrics, conductive oxides and nitrides, metals, and even organics which could have a profound impact on the ability to precisely and selectively engineer membrane interfaces.

1.2.2. Two-Dimensional Materials. Whereas ALD and related methods offer tremendous flexibility in modifying interfaces for study and use within aqueous systems, some materials themselves can offer a diverse palette of physical and chemical properties at their surface(s). Two-dimensional (2D) materials such as graphene have had a profound influence in a variety of physical and applied fields. More recently, they have begun to make a similar impact on energy-water systems. The family of 2D materials continues to expand rapidly. Excitingly, its breadth has extended beyond graphene to transition metal dichalcogenides (TMDs), hexagonal boron nitride (h-BN), MXenes, black phosphorene (b-P), graphitic carbon nitride, silicates (mica), and layered double hydroxides (LDHs). The chemical tunability of 2D materials has led to their use as sorbents, membranes, and capacitors in water research. 2D materials are intrinsically promising to study interfacial phenomena because of their chemical selectivity and high

https://doi.org/10.1021/acs.chemrev.1c00069
Chem. Rev. 2021, 121, 9450−9501

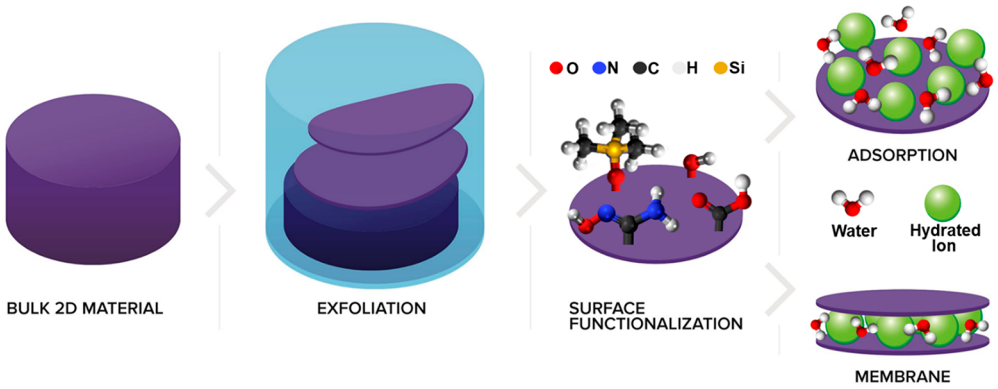

Figure 3. Schematics showing the synthesis of surface functionalized 2D materials from exfoliated suspensions obtained from their bulk material. Surface functionalized 2D materials can be used for selective adsorption or as laminated membranes for selective separation.

specific surface area from 636 m^2/g of MoS_2 to 2630 m^2/g of graphene.[47−50] Selectivity can be achieved through the manipulation of surface chemistry (Figure 3).

The synthesis of 2D materials includes two routes: top-down (exfoliation) and bottom-up (chemical vapor deposition). Both methods are potentially scalable and can lead to the production of large quantities of single-to-few layers of 2D materials. Here, we will focus on exfoliated 2D materials. Synthetic top-down methods of 2D materials include oxidation-assisted exfoliation,[51−54] intercalation-assisted exfoliation,[55,56] solid reaction with mechanical shearing,[57] chemical etching,[58,59] direct ultrasonication with different solvents,[60−64] electrochemical exfoliation,[65−67] and supercritical fluid expansion and exfoliation.[68,69] Surface functionalization of 2D materials can be achieved through covalent functionalization and noncovalent adsorption; various composite materials can also be formed. With its abundant oxygen-containing groups, graphene oxide (GO) is easily covalently functionalized. Procedures include organosilane reactions with hydroxyl groups,[70−72] acyl chloride and amine reactions with carboxylic acid groups,[73−76] and hydrazide and amine reactions with carbonyl groups.[73,77] The other 2D materials' basal planes are more inert. Covalent functionalization of TMDs can be achieved by creating S−C bond using organoiodide or by using thiol-containing molecules to fill in the S vacancies.[78−84] Similar strategies can be employed to other 2D materials after adding an initial step to create surface defects or oxygen-containing groups.[64,85−91]

In energy-water systems, 2D materials have been widely used as sorbents for water remediation (Figure 3). Various GO architectures have shown high adsorption capacities of 200−1000 mg/g for the removal of cationic and anionic pollutants, radionuclides, and organic small molecules.[92−99] GO also preferentially adsorbs certain heavy metal ions in the order Pb > Cu > Cd > Zn.[92,100] This order correlates well with these metals' relative binding affinities to carboxylic functional groups. Selective removal of U-(VI) was demonstrated through the attachment of phosphate or polyaniline groups on GO.[101,102] Improved Pb removal was achieved through amino silane functionalization.[103] Additionally, electrochemical methods can be applied to 2D materials for water/ion separations. Capacitive deionization has been shown with GO,[104−107] MoS_2,[108,109] C_3N_4,[110] and MXenes.[111−113] Surface-functionalization-assisted electrodeposition was also introduced using a GO electrode, which showed a 2 orders of magnitude higher removal efficiency of heavy metal ions than in passive adsorption experiments.[100]

Following the discovery of molecular sieving in layered GO films,[114] 2D materials have been applied to various membrane-based separations. Laminated membranes can be fabricated through the assembly of 2D materials stacks (Figure 3). Sieving of ions from water, or ions from other ions, depends on the interlayer spacing between two 2D sheets, as well as the material's surface chemistry. In typical 2D channels, the two water/solid interfaces are separated by only ∼1 nm, giving rise to new interfacial phenomena. Such phenomena have a profound influence not only on adsorptive properties but also on the structure and dynamics of confined molecules and ions, as described below. Water takes a layered form when confined in 2D channels; below 1 nm, up to three discrete layers of water molecules can exist.[115] The 2D confinement gives rise to extreme water properties. For example, 2D-confined water in a channel between graphite and hBN with a height of ∼1 nm showed an out-of-plane dielectric constant of 2 comparing to 80 for bulk water.[116,117] In contrast, the parallel dielectric constant under confinement of ∼1 nm between graphene layers can be as high as >100.[118] The density of water within these 2D channels varies from 4 to 6 g/cm^3 to virtually 0 because of the discrete nature of the water arrangement.[119]

Surface chemistry plays a crucial role in determining the number of layers at equilibrium and, when water acts as molecular spacers, can also affect the interlayer spacing.[120] Extraordinary transport behaviors were observed within 2D channels for both water molecules and hydrated ions.[121,122] Monovalent ions, especially Li, diffuse faster in graphene channels (without surface charge) relative to ions in bulk electrolytes of the same concentration; the transport of divalent and trivalent cations is hindered, however.[123] Different conductivity between cations and anions was also discovered in 2D materials. This cationic selectivity has been utilized for energy generation across a concentration gradient.[124−129] As the family of 2D materials—and the ability to tune their structure, chemistry, and charge—continue to expand, this class will serve as a powerful platform for elucidating and exploiting adsorption phenomena.

1.2.3. Polymers and Polymer Electrolyte Brushes. Embedding selective adsorption sites in porous media poses a considerable synthetic challenge. While both the methods described above offer direct control at water/solid interfaces, there is a great need for soft materials that adopt more fluid- or liquid-like properties that can be engineered with the same degree of chemical versatility. ALD and 2D materials use a library of primarily inorganic species to engineer interfaces; even

https://doi.org/10.1021/acs.chemrev.1c00069
Chem. Rev. 2021, 121, 9450−9501

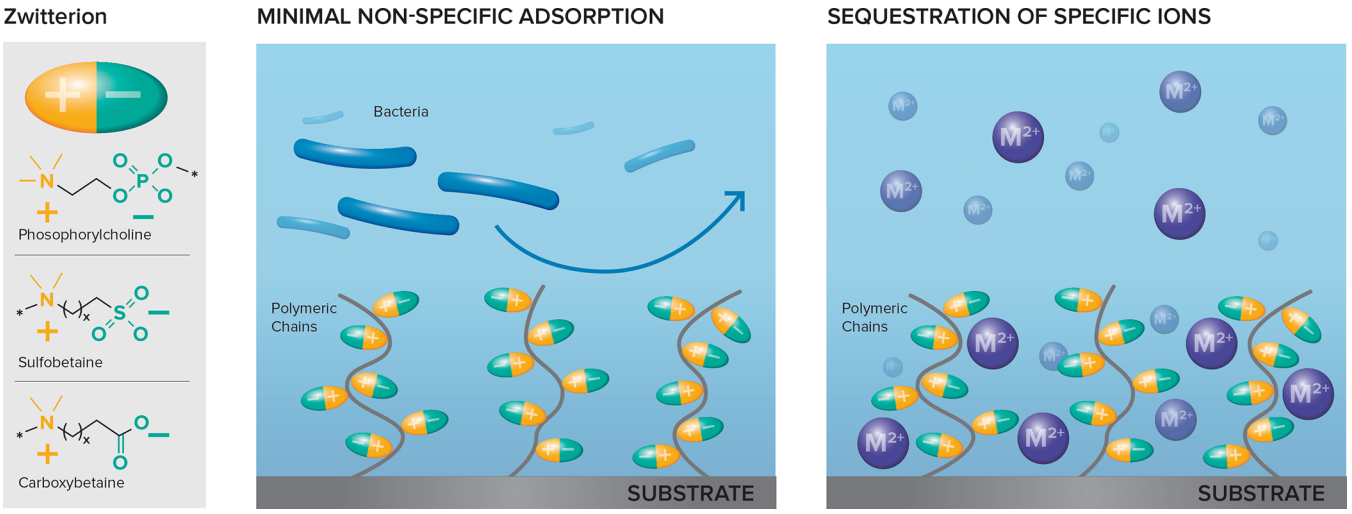

Figure 4. Schematic depicting the three common classes of zwitterionic groups (left) and their applications in polymer brush coatings to mitigate biofouling (middle) or sequestering specific ions (right).

greater flexibility can be drawn from the introduction of organic moieties. Bulk polymer materials and polymeric surface coatings have a high degree of versatility and can be engineered to reduce or enhance their interfacial interactions with organic matter and thus tune important adsorption properties. Of these, coatings are more advantageous in the sense that bulk properties of the material (e.g., ceramic membrane) can be retained while tuning the surface properties. Most explored in the past several decades is the design and optimization of surface coatings that impart biocompatibility and/or resistance to the adsorption of biological matter. Such properties are essential to prevent fouling, a critical challenge in applied systems. It is important to note that biocompatibility and/or resistance to the adsorption of biological matter are not necessarily synonymous, and we refer to the latter as "antifouling" with the disclaimer that a rigorous definition of this term should also include nonbiological matter. Antifouling is particularly important for interfaces in aqueous media such as those found in water treatment or marine applications.

When compared to chemically similar monolayer treatments, the attachment of polymers to surfaces generally offers improved stability and resistance to biofouling.[130] These so-called polymer "brushes" are either physically tethered (physiosorbed) or chemically tethered to the substrate. Covalently bound polymer brushes are more stable and are obtained by either grafting-to or grafting-from surfaces. The grafting-from approach provides higher brush surface density—this is best for antifouling—and is usually achieved using surface-initiated controlled radical polymerization.[131]

Typically, the chemical groups associated with effective antifouling are those that can be strongly hydrated such as oligo- or poly ethylene oxides, saccharides, zwitterions, and hydroxyl-containing acrylates and acrylamides.[132,133] The strong hydration and net neutral charge of these groups substantially decrease the energy gain from foulant−surface interactions—which come at the cost of displacing the interfacial water—and effectively mitigate biofouling.[134] Zwitterionic brushes have several advantages over these other groups: they are more salt-resistant, and their (ionic) solvation is most similar to bulk water, which translates to a lower net energy gain from displacement of the solvated water (i.e., better antifouling).[134] Several zwitterionic moieties have emerged as effective and easily accessible for polymer brushes: phosphorylcholines, carboxybetaines, sulfobetaines, and even amino acids (Figure 4).[134]

Antifouling polymer brushes have minimal nonspecific interactions with biological matter, but they can also be engineered to simultaneously promote specific interactions like ion-binding[135] or (bio)molecular recognition (Figure 4).[136] Of particular interest to the water treatment community is the use of such brushes to modify nanodevices and membranes, enabling manipulation of their ion-transport properties. For example, ionic mobility through nanochannels and nanopores coated with zwitterionic brushes can be tuned via environmental pH, brush density, and pore size.[137−139] Using nanofiltration membranes functionalized with similar antifouling polymer brushes, several groups have demonstrated effective monovalent salt separation in the presence of multivalent salts, neutral organic compounds, or antibiotics.[140−142] The high selectivity of these membranes was achieved while maintaining high flux; as such, these examples illustrate great promise for the use of antifouling polymer brushes in food, desalination, and biological separation processes.

1.3. Characterization Methods for Adsorption Processes

Adsorptive processes such as those outlined above encompass a range of different length-scales from the Ångstrom to the mesoscopic and thus necessitate characterization spanning these disparate length scales. In this section, we review two characterization methods based on X-rays and vibrational spectroscopies. While the true spectrum of characterization techniques remains beyond the scope of this Review, both X-rays and vibrational spectroscopies probe in excellent detail adsorptive interactions and mechanisms at molecular and atomic levels. Importantly, both methods can be used in situ/operando to depict in detail molecular behaviors and structural dynamics. Anomalous X-ray scattering provides a wealth of information by combining both interface- and element-specificity in X-ray characterization. Unlike other characterization tools including laser-, electron-, X-ray-, and neutron-based techniques, anomalous X-ray scattering probes ion adsorption properties using both total electron density distributions and element-specific substructures at solid−liquid interfaces. Importantly, it is possible to minimize spectral interference from either the solution or the bulk substrate

https://doi.org/10.1021/acs.chemrev.1c00069
Chem. Rev. 2021, 121, 9450−9501

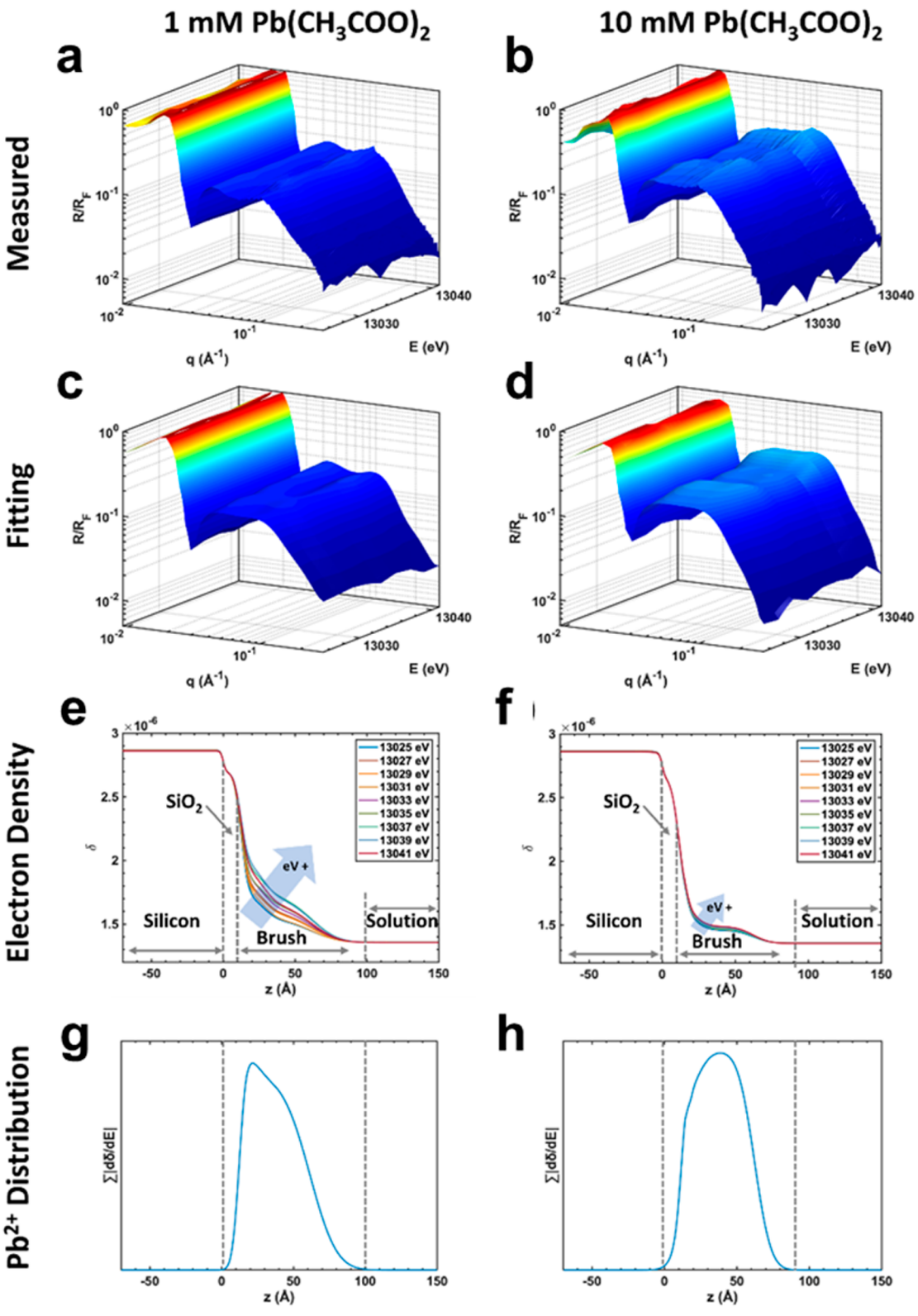

Figure 5. Analysis of poly(cysteine methacrylate) brushes in the presence of Pb^{2+}. Resonant anomalous X-ray reflectivity data of poly(cysteine methacrylate) brushes in (a) 1 mM (b) 10 mM $Pb(CH_3COO)_2$ solution. All measurements were under energies ranging from 13025 to 13041 eV with a 2 eV increment step. (c,d) Best fitting profiles of raw RAXRR data. (e,f) Electron density profiles based on the fitting results. (g,h) Derivates of electron density to energy as a function of brush depth. Reprinted with permission from ref 135. Copyright 2019 American Chemical Society.

through the use of resonant anomalous X-ray scattering and analyze simultaneously both geometric and spectroscopic structures. Vibrational spectroscopies provide useful techniques for studying both the adsorption of ions from solution, as well as the more fundamental properties of the solid−liquid interfaces that are ubiquitous in sorption technologies. Techniques such as infrared (IR) absorption, vibrational sum frequency generation (vSFG), and ultrafast 2D IR spectroscopies are able to make use

https://doi.org/10.1021/acs.chemrev.1c00069
Chem. Rev. 2021, 121, 9450−9501

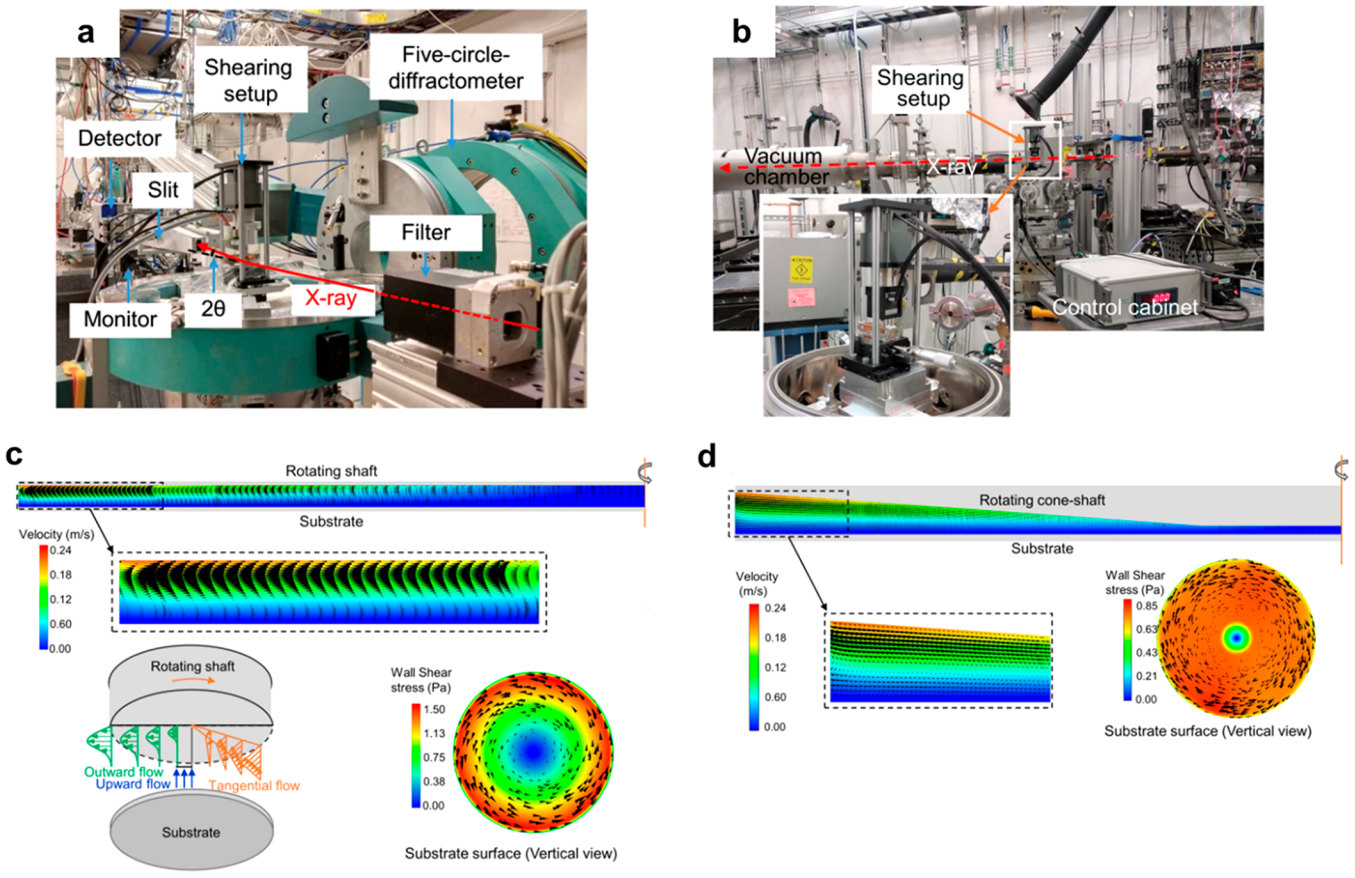

Figure 6. In situ shearing X-ray measurement system at the Advanced Photon Source (APS) beamline 12-ID-D (a) and 8-ID-E (b). Computational fluid dynamics (CFD) simulations of the flow field in the *x*-*z* plane in the parallel-plate geometry and the cone−plate geometry are shown in (c) and (d), respectively. The colormap represents the velocity value, and the black arrows represent the in-plane velocity direction. The enlarged views are given in the dashed box. The bottom left inset of (c) shows a schematic of the flow in the gap of the parallel plates. The tangential, outward, and upward flows are marked by orange, green, and blue arrows, respectively. The bottom right inset of (c) and (d) represent the flow field at the surface of the silicon substrate. The colormap represents the shear stress. The black arrows represent the in-plane velocity direction. Reprinted with permission from ref 185. Copyright 2020 AIP Publishing.

of the details of local molecular structures to probe the specific interactions important for ion adsorption, to determine the impact of the ions on the structure of the adsorption material, and to study the structure and structural dynamics of water and ions in the vicinity of the interface. Importantly, vibrational spectroscopic techniques are capable of probing not just the adsorption process itself but additionally the details of the environment in which the adsorption occurs, potentially providing important insight toward the broader context of the adsorption process.

1.3.1. X-rays. The adsorption of ions to aqueous interfaces is a phenomenon that profoundly influences vital processes in water treatment and process engineering. Many tools, including laser-, electron-, X-ray-, and neutron-based techniques (e.g., sum frequency generation spectroscopy,[143−147] spectroscopic ellipsometry,[148,149] low-energy electron diffraction,[150] and X-ray spectroscopy[151−154]) have been valuable for revealing surfaces structures.[155,156] However, the ideal technique for probing ion adsorption is one that provides both total electron density distributions and element-specific substructures at solid−liquid interfaces. These both are attributes of an X-ray technique combining interface-specificity of high resolution X-ray scattering and element specificity of X-ray absorption spectroscopy: resonant anomalous X-ray scattering.[157−161] Importantly, through the use of resonant anomalous X-ray scattering it is possible to minimize spectral interference from either the solution or the bulk substrate components[162] and analyze simultaneously both geometric and spectroscopic structures through model-dependent analysis.[163] This technique has been applied to probe the organization of interfacial "hydration layers" and the important role of adsorbed ions at mineral-water interfaces.[158,160,161,164−167] In what follows, we highlight the efficacy of this technique in describing the adsorption properties of polymer brushes.

As described above, interfacial characteristics and adsorptive properties can be altered by polymer brushes (polymer chains tethered to a surface via one chain-end).[157,168] Researchers have used amino acid-based zwitterionic poly(cysteine methacrylate) polymer brushes for improving ion selectivity for the design and optimization of antifouling water treatment membranes and applied resonant anomalous X-ray reflectivity (RAXRR) near the Pb K-absorption edge (13.035 keV) to understand electrostatic interactions of charged groups within and between chains with Pb^{2+} ions in aqueous solutions.[135] The changes of electron density depth distribution as a function of the photon energies are correlated to the relative concentration of resonant Pb ions in brushes, thereby reflecting the enrichment and distribution of Pb^{2+} ions at the solid−liquid interface (Figure 5).

The static properties of polymer brushes are well understood through extensive theoretical,[169] computer simulation,[170,171]

https://doi.org/10.1021/acs.chemrev.1c00069
Chem. Rev. 2021, 121, 9450−9501

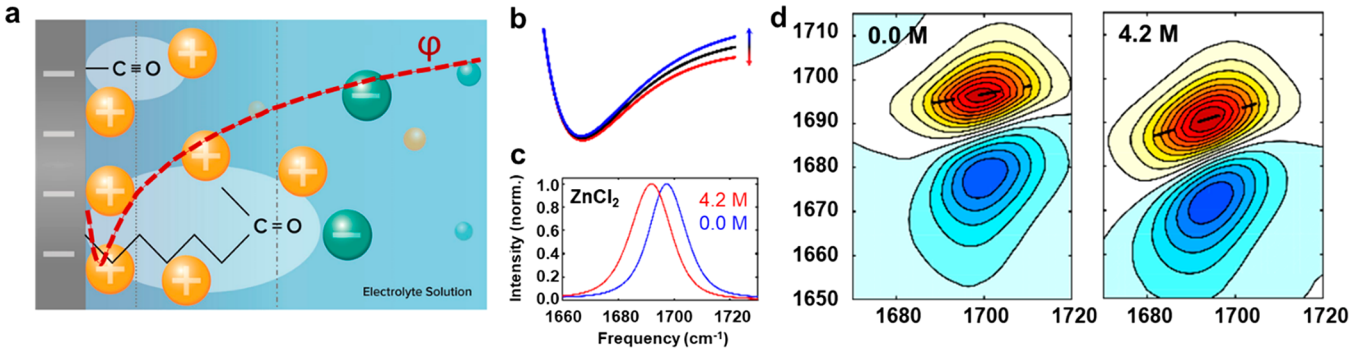

Figure 7. (a) Cartoon illustrating how vibrational probes tethered to an electrode could be used to sense ion distributions and electrostatic potential φ. (b) Schematic illustrating the effect of an electrostatic field E on the vibrational potential, with FTIR spectra of a carbonyl stretch showing the effect of adding 4.2 M $ZnCl_2$ to D_2O. (c,d) 2D IR spectra of carbonyl stretch at early waiting time showing the increased inhomogeneity due to adding 4.2 M $ZnCl_2$.

and experimental studies,[172−176] but the properties of such a soft interface can be switched by weak external stimuli.[177−179] The knowledge of polymer brushes in nonequilibrium and under flow is still incomplete, even though it is crucial for the design of the aforementioned antifouling water treatment membranes. Numerous simulations and theoretical methods have been applied, but researchers have drawn opposite conclusions—for both swelling[180,181] and collapse[182−184]—concerning the behavior of polymer brushes under shearing. More persuasive evidence from in situ/operando experiments is required to depict the detail of the molecular behaviors and structural dynamics. Chen et al. designed and implemented an in situ shearing X-ray measurement system, equipped with both inline parallel-plate and cone-and-plate shearing setups and operated at the Advanced Photon Source (APS) at Argonne National Laboratory, to investigate the structures and dynamics of end-tethered polymers at the solid−liquid interface (Figure 6).[185] By comparing the swelling behaviors between amino acid-based poly(acetylcysteine methacrylate) and poly(cysteine methacrylate) brushes on flat silicon substrates, the considerable influence of electrostatic interactions on the shear response of polymer brushes was demonstrated. Moreover, the interparticle interactions of polyzwitterionic poly(2-methacryloyloxyethyl phosphorylcholine) brushes grafted on silicon dioxide nanospheres with curved interfaces was evaluated and revealed a uniform distribution, but a less aggregated status, under shearing. The successful application of the in situ shearing X-ray measurement system provides an extra view to gain insights into the dynamics in soft interfaces under shearing processes.

1.3.2. IR Spectroscopy. A common approach that has been used broadly in many different scenarios is the use of localized vibrational modes as a probe for the local electrostatic environment in a complex material, taking advantage of spectral shifts induced by the vibrational Stark effect[186,187] and the modulation of coupling between vibrational modes in close proximity to one another induced by changes in the local structure by the adsorption of ions.[188,189] With the Stark effect, the local vibration being used as a probe will experience an electrostatic field imparted upon it by the local environment, which will induce shifts in the frequency of the probe. These environment-dependent shifts can then be used to infer information about charge distributions even in complex adsorption materials such as biological ion channels.[190] The interpretation of these measurements relies critically on the accuracy of the maps that connect the frequency of the reporter mode to the local electrostatic field, which may become problematic in complex environments where nonelectrostatic effects might be varying along with the electrostatic distribution.

One of the predominant tools for spectroscopically studying interfacial systems is vSFG, a second-order technique that is considered to be surface-specific due to the cancellation of the second-order nonlinear susceptibility $\chi^{(2)}$ in isotropic media under the dipole approximation. This makes vSFG a particularly useful tool for studying the structure of the water and ions in an electrolyte solution in the interfacial layer between the bulk and the interface, allowing for studies of changes in the double-layer structure due to the electrolyte composition and the surface charge of a mineral or electrode.[191,192] By combining this approach with the use of a vibrational probe tethered to the electrode (Figure 7a), this technique can be used to measure the electrostatic potential at the electrode interface as a function of solvent or applied bias (Figure 7b,c), and it has been demonstrated that the fields can be highly spatially inhomogeneous with significant effects from the sign of the potential and the chemical nature of the probe.[193−195] vSFG spectra can at times be difficult to interpret due to the complicated selection rules and effects of molecular orientation, but it has proven to be a useful technique for studying the solvent and ion structuring within the solid−liquid interface.

By taking advantage of ultrafast spectroscopies such as 2D IR, it is possible to obtain information about the effect of adsorption on the distributions of local solvation environments and the dynamics of the solvation and orientational fluctuations of the vibrational probe. This technique provides the change in a vibrational spectrum at frequency ω_3 as a function of excitation frequency ω_1 in a femtosecond (fs) time-resolved manner and can be considered as a vibrational analog of 2D NMR correlation spectroscopies (Figure 7d). One of the major advantages of 2D IR spectroscopy over linear spectroscopic techniques is its ability to separate homogeneous and inhomogeneous contributions to the line broadening of a transition on time scales faster than typical solvation dynamics. This makes it possible to quantify the degree of local structural inhomogeneity in a molecular system, and to observe the time scale over which the distribution remains inhomogeneous. This is made possible by the separation of homogeneous and inhomogeneous contributions to the line width onto the antidiagonal and diagonal directions of the 2D spectrum at early waiting times, and the relative significance of these components can be quantified by the degree of elongation of the spectral band.[196]

By observing the dynamics of the spectral elongation, it is possible to directly measure the time scales on which the local

https://doi.org/10.1021/acs.chemrev.1c00069
Chem. Rev. 2021, 121, 9450−9501

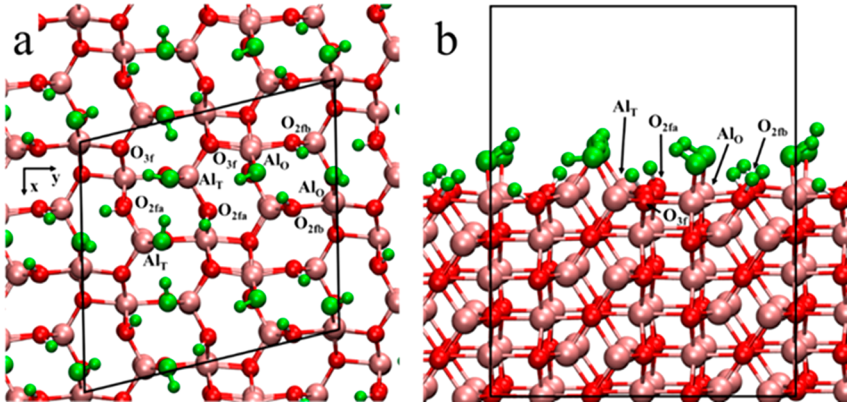

Figure 8. (a) Top view and (b) side view of (2 × 1) unit cell of hydroxylated θ-Al_2O_3(010). Al_T: tetrahedral Al; Al_O: octahedral Al; O_{2fa} and O_{2fb}: 2-fold coordinated O; O_{3f}: 3-fold coordinated O. Al and O are in pink and red, respectively. The −OH and −H are highlighted in green. Nonbonded waters have been removed for clarity. Reprinted with permission from ref 209. Copyright 2019 American Chemical Society.

solvation environment fluctuates. If the vibrational band contains contributions from multiple structures, which may be incompletely resolved, then these line shape dynamics can reveal the time scale for the exchange processes between these structures. This could involve, for example, configurations where the probe molecule is hydrogen bonded to water versus coordinated to an ion, perhaps weakly. The specific ion configurations and motions that contribute to the inhomogeneity can be determined in tandem with molecular dynamics simulations. Importantly, these dynamics can be observed on a fs to picosecond (ps) time scale, much faster than is accessible to NMR measurements, thereby making this an important complementary technique for the study of fast processes in disordered solution-phase environments.

Recently, 2D IR spectroscopy has been increasingly applied to surface systems of various kinds,[197−199] demonstrating the promise of this emerging technique. For example, a 2D IR study of a model rhenium carbonyl catalyst immobilized on an ITO surface demonstrated that the identity of the solvent could induce reversible structural changes in the monolayer on the time scale of hours,[200] illustrating how this technique can resolve the structural properties of the interface. It can also be used to study the interaction between the interface and the solvent, such as in a recent study of SiOH groups on the surface of amorphous silica exposed to various organic solvents, where the time scale for the solvent exchange between CCl_4 and benzene could be observed through their impact on the hydroxyl stretch band.[201] By utilizing different types of vibrational probes tethered to the solid−liquid interface, it is possible to design experiments that are sensitive to different kinds of species in solution, and in principle to specifically probe the solvent and the various ions in solution and how these interact with the surface.

1.4. Simulations of Molecules and Ions in Water

The synthesis and characterization approaches outlined above rely on theory and modeling to complete the picture and better understand water/solid interfaces. In some cases, such efforts are needed to interpret the experimental data given the complexity of scales and the highly dynamic nature of an aqueous environment. Importantly, theory and modeling can capture phenomena that are inaccessible to experimental methods. As an example, the rapidly changing (on the 10 fs time scale) hydrogen-bond network of water, which is at the root of all aqueous solvation, solubility, and adsorption problems, can dynamically organize itself to accommodate solutes and adapt to extended surfaces. Most measurements detect average structural information, so one needs simulations to determine if fluctuations are important to the interpretation. This played a role in a recent study of salt effects in the solvation of acetone by water.[202] Here it was found that sodium ions and water molecules competed with each other in interacting with the carbonyl oxygen, leading to noticeable effects in the Stark modeling of IR spectra. Here, experimental and theoretical methods were complementary to one another, providing an excellent tool for explaining the interplay of competing noncovalent interactions.

1.4.1. Theory and Modeling of Molecules at Aqueous Interfaces. A variety of computational methods have been successfully employed by researchers to describe molecular-scale interactions in the adsorption of small molecules on surfaces. Molecular dynamics (MD) simulation, which describe the time evolution of a system with the use of empirical force fields, is one of the most extensively used methods to study adsorption on surfaces for understanding structural changes that occur on short time scales not accessible with experimental methods. For example, a study of homopolypeptides in aqueous solution on a gold surface showed that the peptide's interaction with the surface is related to how stable the molecule is in solution.[203] The binding of peptides in aqueous solution near gold and palladium has also been investigated, suggesting that conformational changes play a large role in the strength of bonding interactions,[204,205] as well as the structure and conformation of the amino acids.[206,207] Additionally, the mechanism of ionic permeation into alkanethiol monolayers on a gold surface has been explored.[208] Simulating soft matter systems such as these is essential for guidance and interpretation of polymer brush functionalization strategies such as those discussed above.

An alternative to empirical force fields involves using density functional theory (DFT) in the context of quantum mechanics/molecular mechanics (QM/MM) calculations, where DFT is used for a small portion of the system and empirical force fields for the rest. This approach is often used to describe reactions in proteins, and there is also much interest in first-principles or ab initio MD, where DFT is used to define forces for the entire system being studied. The latter method plays an important role later in this Review. However, for adsorption involving aqueous interfaces, DFT studies with just a few water molecules have often been used. For example, a previous study investigated the structure of water on a metal surface,[7] revealing information

https://doi.org/10.1021/acs.chemrev.1c00069
Chem. Rev. 2021, 121, 9450−9501

about the formation of small clusters of water molecules and its dependence on the size of the water cluster and the metal surface. In a combined theoretical and experimental study (Figure 8), researchers explored methanol adsorption on hydrated θ-Al_2O_3 surfaces with the use of DFT calculations to provide a detailed analysis of the surface and a mechanistic understanding of the energetics associated with adsorption that is of interest not only for simple adsorption studies but also in development of heterogeneous catalysts.[209] In this study, the effect of hydration for modeling reactions at 300 °C involved adding explicit hydroxides at the surface.

Other interfaces have also been studied using MD simulations using classical force fields or DFT. Mineral interfaces are often useful models and can also have direct relevance for geochemistry investigations. Studies have found that the adsorption behavior of cations on quartz and corundum is dependent on the cation size, with opposite trends for each surface.[210] The behavior of water within ordered and disordered silica pores has been examined both in DFT and MD simulations.[211] First-principles MD simulations have been used to study binding and adsorption behavior of charged functional groups found in amino acids on quartz.[212]

2D materials offer tremendous promise for both fundamental and applied studies in water-energy systems, and interfaces dominate their behavior. The interface between graphene and aqueous solution is a particularly well-studied area. Many studies have examined graphene's potential for water desalination and for forward osmosis membranes.[213−217] Others have focused on the effect of functionalization of the graphene surface on the water interaction with both the surface and nanopores.[218−221] These methods have the potential to provide analogous insight into the broader classes of 2D materials being explored experimentally.

2. REACTIVITY

2.1. Introduction/Overview

Adsorption phenomena outlined in the previous sections typically represent physical interactions at interfaces, governed in many cases by electrostatic, hydrophobic, and dipolar forces. Covalent chemistry also carries important functions at these interfaces. Like adsorption, the design, characterization, and study of reactive interfaces play an essential role in energy-water systems. Here, we refer to "reactivity" as the group of catalytic and electrocatalytic processes on surfaces and near-surfaces of solid−liquid interfaces, which in turn has a profound effect on transitioning more passive processes of adsorption to more active and/or responsive sets of activity. Notable examples include the design of active antifouling membranes and degradative mechanisms that build on purely passive properties of sorbents or electrocatalysis. Like adsorption, reactive processes depend critically on the organizational structure of interfacial water in confined spaces. Research capable of generating sufficient knowledge of this phenomena, and thus the development and utilization of reactivity-surface chemistries, forms an active component of ongoing activities.

Despite the ubiquity of aqueous reactive interfaces, models that capture the full structural and chemical complexity of these interfaces remain largely in their infancy. This state of affairs is compounded by the need for experimental systems that can probe the wide range of pertinent length- and time-scales involved, as well as the underlying atomic scale structure and chemical complexity. For example, water can act as a reactant, as a modifier of surface species, as coordinating ligand of ions in solution, as adsorbate on surfaces, and as a way to screen strong electric fields. Other pressing gaps in aqueous phase (electro)-catalysis include the role of extreme confinement and the existence of competing, and sometimes conflicting, requirements for efficient or optimal interfacial processes that lead to well-known volcano plots of reactivity−property relationships in heterogeneous[222,223] and electrocatalysis.[224,225] Such features form an important role in the design of antifouling materials, a critical challenge in applied water systems.

Oxidative degradation is one of the most effective means to remove organic and bioactive contaminants from polluted water. Practically all oxidation reactions of organic compounds using molecular oxygen are thermodynamically favorable, but the chemical stability of the ground state of O_2 renders these reactions slow. Activation of O_2 to form much more reactive, transient oxidants such as peroxy and OH radicals and O atoms can be achieved in photochemical or electrochemical processes or catalytically as in advanced oxidation processes (AOPs), but these processes are energy-intensive, requiring heating large volumes of contaminated water or using an energy-intensive light source or large areas of retainment if solar radiation is used. A more desirable, atom-efficient approach would be one in which the organic pollutants are degraded by oxidative reactions with molecular oxygen at room temperature, and the excess energy released is used to generate a stable but reactive oxidizing agent, such as H_2O_2 that can be used further to oxidize other, more calcitrant pollutants as well as acting as a disinfectant. A demonstrated laboratory example is the production of H_2O_2 with a one-to-one stoichiometry during the oxidation of 1,2-propanediol[226] or during the oxidation of glycerol,[227] present in wastewater from biomass processing. At present, these reactions proceed effectively only in quite basic solutions, which severely limits their applications.

In spite of their technological importance, detailed understanding of reactions critical to water remediation is lacking. In the catalytic oxidation processes, especially those near ambient temperatures and pressures, how O_2 is activated and how the energetics of this step depends on the aqueous surrounding is not well understood. The electronic structure of the catalyst surface is critical to the binding of O_2, yet there is little information on the influence of coadsorption of ions and dipolar molecules or the stabilizing effects of the solvation sphere on this step. If the reaction involves proton transfer, the role of proton mobility at the solid−liquid interface needs to be assessed. For electrochemical remediation, the additional effects of an applied potential on adsorption and activation of O_2 and the subsequent reactions need to be included, as well as the organization of water molecules and ion distribution at the solid−liquid interface and their effects on the electron transfer across the interface. In what follows, we review some of these features as they pertain to ongoing research in materials for energy water systems.

2.2. Synthesis and Fabrication of Reactive Water/Solid Interfaces

To investigate reactivity in energy-water systems, researchers have introduced a wide variety of substrates and materials. In this section, we review materials based on conductive oxides and zeolites, and additional methods of molecular immobilization. Conductive oxide materials offer a rich platform to investigate the role of potential-dependent reactivity, while zeolites are an exciting class of materials with tunable chemical functionalities.

https://doi.org/10.1021/acs.chemrev.1c00069
Chem. Rev. 2021, 121, 9450−9501

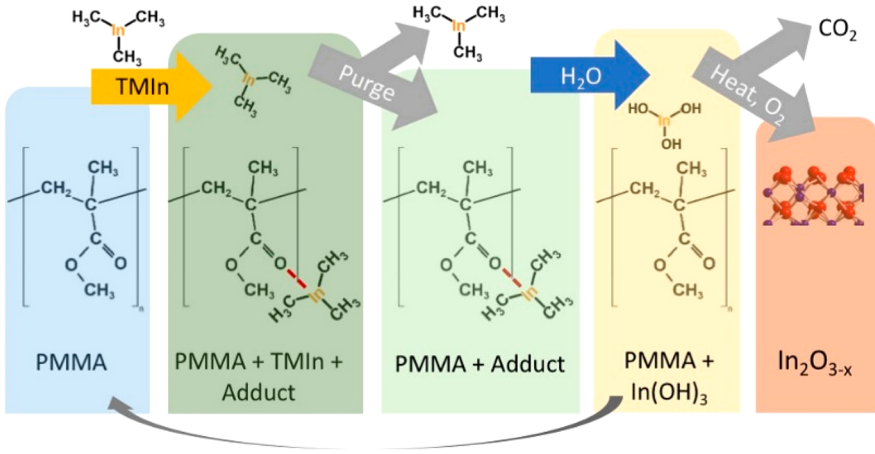

Figure 9. Idealized schematic of one SIS process in which trimethylindium (TMIn) is infiltrated into PMMA to ultimately result in an In_2O_3 solid.

The concept of molecular immobilization, and the binding of functional moieties to model and functionalize substrates, provides additional chemical control. Notwithstanding the significance of reactivity from a chemical perspective, geometrical considerations play a decidedly important role. High-surface-area, porous catalysts and electrocatalysts are employed to enhance specific (per unit weight) or areal (per unit physical area) rates of (electro)catalysis. As an example, zeolites are high-surface-area crystalline solids with well-defined nanoscale cavities and channels that are widely used in the process industry. The technologically important zeolites often possess negatively charged frameworks with charge-balancing protons, creating solid acids. The catalytic activity is determined by the acidity of the proton, which depends on the extent of hydration in addition to the zeolite framework composition and structure. Whereas information on the thermodynamic energies of these protons has emerged in recent years, their mobility and the relationship to reaction kinetics are not yet known. It is of particular interest to understand the influence of close proximity of the crystalline wall on the properties of these protons and the solvating water molecules.

Electrically conducting materials are needed to efficiently supply charge to electrocatalysts. For this purpose, electrically conducting porous oxides are preferred over porous metals owing to their stability in aqueous environments (they are already oxidized) and their wide tailorability through surface modification via anchoring of various functional groups and metal−organic complexes. Well-defined hierarchical porosity can be templated in conducting oxides. Two highly versatile templating approaches outlined in this Review are the conformal coating of or infiltration of precursor into a substrate via ALD or SIS, respectively. By using these techniques, it is possible to capitalize on the vast literature available to prepare polymeric or oxidic substrates of different pore dimensions, three-dimensional pore structures, and connectivity to serve as templates for conducting electrocatalyst interfaces of the same structures and pore properties. This approach enables the study of ion diffusion and solid-ion interaction with unprecedented material and size control.

Both the surface hydroxyl groups and terminal metal sites of these oxide surfaces provide sites for surface modification. Several well-established techniques, including silylation, condensation, and esterification can be used to anchor functional molecules to these surfaces. A high areal density of molecular complexes can be achieved through tethering to the well-defined pore walls of zeolites and other porous solids, including conducting porous oxides. These assemblies can be used to investigate the effect of confinement on (electro)catalytic reactions to answer questions pertaining to the effect of water structure and ion distribution on the overpotential of reactions that are catalyzed by these complexes.

2.2.1. 3D Conductive Oxide Electrode Design. Both industrial and analytical electrocatalysis require the relatively low-resistance delivery of electric charge to electrochemically active interfaces. Low electrical resistance is required in industrial settings to reduce ohmic losses and thereby increase power efficiency. In the lab, low resistance (<100 ohm) electrical pathways minimize the electrical resistance potential drop that would otherwise result in an electrochemically active interface with applied potential different from that set by the potentiostat. While this *iR* loss can be compensated in some specific cases, high-surface-area electrodes in which confined electrocatalysis are applied may present a voltage-loss gradient across the sample that is difficult or impossible to compensate evenly. Therefore, common substrates are composed of conductive materials including zerovalent metals, conductive carbons, and degenerately doped metal oxides. While many metals and their alloys are highly conductive, aqueous electrolytes often include non-neutral pH and concentrated salts—conditions that are prone to oxidize all but the most noble metals. Insulating or unstable surface oxides result in voltage loss or an irreproducible electrochemically active interface. Therefore, degenerately doped conductive metal oxides, in which metals already exist in a highly oxidized state, are an attractive platform for aqueous electrocatalysis. As no further oxidation is likely, a more stable and conductive surface is often maintained throughout electrocatalytic investigations. Many metal oxides have the additional advantage of visible light transmission for applications in photoelectrocatalysis as well as suitable surface chemistry for binding of molecular catalysts (see section 2.2) through readily accessible and robust linkages including carboxylate, phosphonate, siloxane, and others.

Several conductive metal oxides, including indium tin oxide (ITO) and fluorine-doped tin oxide (FTO), are commercially available as planar (2D) films deposited on glass or plastic substrates, which are prolifically employed for electrocatalytic studies and applications. However, electrocatalysis in confinement will require conductive 3D electrodes with precise control of features sizes from 1 to 100 nm. The strong electric fields present in nanoscale pores are expected to concentrate ions.[228]

https://doi.org/10.1021/acs.chemrev.1c00069
Chem. Rev. 2021, 121, 9450−9501

The effect may be used, for example, to systematically examine the effects of localized ion concentration on substrate reactivity and product selectivity. A central challenge for the development of electrochemical methods for efficiently scrubbing micropollutants and pharmaceuticals from freshwater sources is the low ionic strength. Counterion accumulation effects in nanoporous electrochemical cells offer significant local ion accumulation for more efficiently addressing low-concentration impurities. 3D conductive oxide electrode designs include ALD of ultrathin ITO films over AAO as well as sintered ITO- and SnO_2-based nanoparticle scaffolds. AAO membranes can be fabricated with a much lower dispersity of pore size and spacing compared with sintered nanoparticle networks. However, the large volume fraction of nonconductive Al_2O_3 framework in AAO limits the surface area of these frameworks.

An alternative route to generate high-surface-area and well-ordered 3D electrodes is SIS that was described in section 1.2.1.[229−233] SIS is related to ALD in that it utilizes gas-phase chemical precursors in a self-limiting reaction with solids to precisely deposit a wide range of materials. However, in SIS, the reactions occur *inside* a permeable organic template (often a polymer) to form an inorganic 3D network (Figure 9), in contrast to ALD in which deposition occurs *upon* a solid substrate to form an ultrathin 2D film. For example, a simple homopolymer thin film (e.g., 140 nm PMMA) may be converted to a microporous metal oxide film (e.g., 80 nm In_2O_3) after SIS and subsequent burnout of the polymer phase.[229] Both pore fraction and micropore size distribution may be controlled by choice of SIS process conditions. Furthermore, when SIS is applied to block copolymer templates (for which the SIS is selective for only one polymer block), meso- to macro-porous features can be further templated. For example, Figure 10a shows a ∼ 30 nm-thick symmetric vertical-lamella-forming poly(styrene-*block*-methyl methacrylate) (PS-*b*-PMMA) block copolymer thin film. A neutral surface energy copolymer mat was used to promote the vertical-lamella morphology.[234] The inset of this image shows the phase-separated block copolymer film before SIS. Five cycles of In_2O_3 SIS followed by thermal sintering and polymer burnout reveal In_2O_3 nanowires that directly correspond to the original PMMA domains. SIS applied to the matrix domains of block copolymers that form vertical cylinder blocks (Figure 9b) may be especially useful as 3D electrodes with hierarchical porosity.

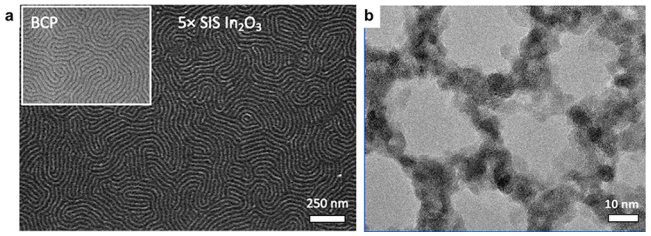

Figure 10. (a) SEM image of SIS of In_2O_3 in vertical-lamella-forming PS-*b*-PMMA block copolymer followed by thermal annealing for polymer removal. The inset of the block copolymer film before processing shows that the original phase-separated morphology is retained after SIS processing. Reprinted with permission from ref 229. Copyright 2019 American Chemical Society. (b) TEM image of three cycles In_2O_3 SIS in cylinder-forming PS-*b*-PMMA block copolymer followed by thermal annealing for polymer removal. Indium oxide deposition is restricted to the PMMA and not in the PS through the judicious choice of TMIn purge time.

2.2.2. Zeolites. The water-energy nexus extends beyond the use and transduction of energy for treatment of water. Many energy technologies are also intimately interconnected with water. The applications for aluminosilicate zeolites as solid-acid catalysts, for example, are widespread in industry and include cracking reactions, biofuel up-conversion, and dehydration reactions, among others.[235−239] The presence of water is a common factor in this chemistry, where it is often deleterious to catalytic activity by enhancing dealumination and other structural changes[239] or by competitively binding with substrates for active sites.[240,241] However, examples of zeolite-catalyzed reactions that benefit from the controlled presence of water have been reported including cyclohexanol dehydration[242] and hydride transfer reactions,[243,244] and a growing interest in aqueous acid catalysis for the biofuel industry[237] has generated a desire to understand the behavior of hydrated acidic zeolites.

Fourier-transform infrared spectroscopy (FTIR) has been widely utilized to probe the hydration behavior of acidic protons in zeolites. In particular, industrially relevant HZSM-5, an aluminosilicate zeolite having MFI framework topology, has been well-investigated.[245−251] A general picture of speciation at low hydration levels of this zeolite has emerged where a first equivalent of water relative to aluminum atoms forms a hydrogen-bonding structure with the adsorbed water molecule located between the bridging-hydroxyl of the surface-bound proton and a framework oxygen, generating so-called A, B, C-triplet bands in the infrared spectrum.[248,252−255] A second equivalent leads to formation of a Zundel-like structure whose flanking waters are still strongly interacting with surface oxygen.[255−258] With additional equivalents, speciation becomes complicated and challenging to interpret, with proposals of stable tetramers[256] and cage-dependent clusters.[259] Variable-temperature FTIR has been used to probe dynamics of hydrated protons in HZSM-5 and suggested at least two mechanisms of proton-shuttling operable at high and low degrees of hydration.[250] However, the dynamic behavior of zeolitic protons under hydration remains relatively underexplored and presents an open opportunity for further study.

Aluminosilicate zeolites, having crystalline microporous channels smaller than those found in amorphous mesoporous silicas, an absence of fixed hydrate structures, and availability of highly acidic surface protons for hydration, provide unique substrates for the study of aqueous acid under extreme confinement. The impact of these properties on pore-confined water can be observed by comparison of gas phase proton affinities (PAs) for small hydrated proton clusters versus similar species in HZSM-5. The PA of a single water molecule is well-established to be ∼165 kcal/mol.[260−269] PAs for 2−6 water molecule clusters have been calculated at the B3LYP/cc-pVTZ level of theory to be 199, 212, 220, 221, and 227 kcal/mol,[268] respectively, in general agreement with values calculated at other levels,[270−272] with the limiting proton affinity of bulk water[262,273,274] assigned to ∼265.9 kcal/mol. The proton affinity of the anhydrous HZSM-5 framework aluminum site, for comparison, is quite high. PA of the isolated site is estimated as 329 kcal/mol using gradient-corrected DFT for geometry optimizations, B3LYP for exchange and correlation energies, and 6-31G(O,H)/ECP(Si/Al) basis sets[275] with variation between ∼280 and 330 kcal/mol depending on the proximity of other Al species or silanol defects. These results are generally consistent with other reports of variable PA based on T-site

https://doi.org/10.1021/acs.chemrev.1c00069
Chem. Rev. 2021, 121, 9450−9501

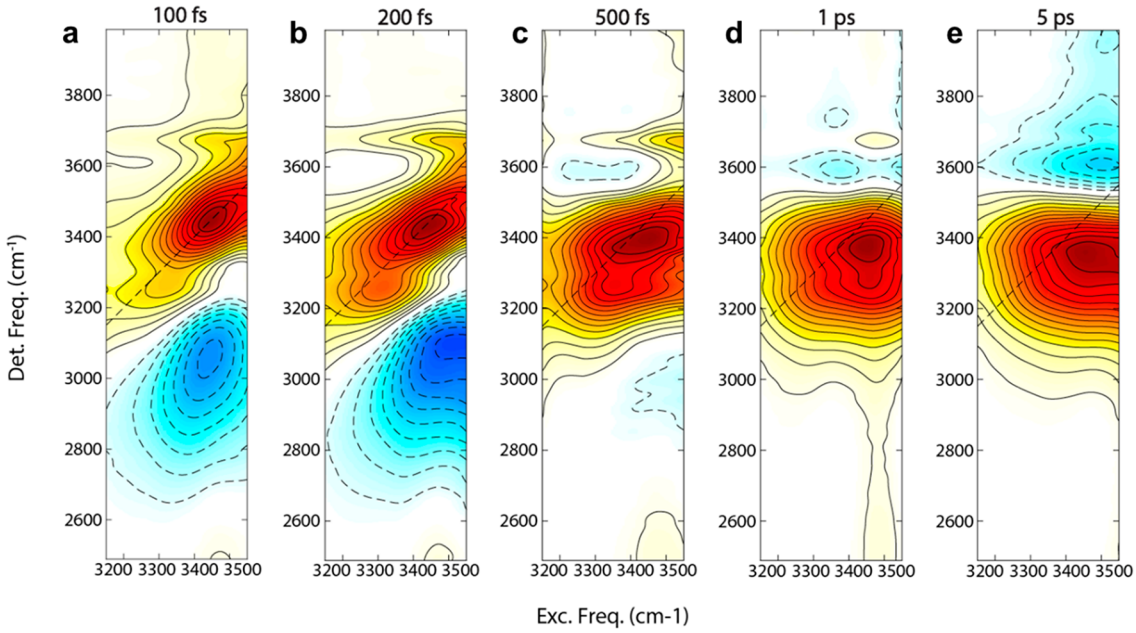

Figure 11. Isotropic 2D IR spectra of hydrated proton-form ZSM-5 taken at 100 fs, 200 fs, 500 fs, 1 ps, and 5 ps pump−probe delay. Spectra were excited by a pulse centered at 3250 cm^{-1} and show the rapid relaxation of the initial vibrational excitation and the subsequent growth of the hot ground state feature.

location of Al and proximity of silanols, aluminum Brønsted-acid sites, or aluminum defects.[276−278]

Computational, microcalorimetric, and temperature-programmed desorption analyses of HZSM-5 indicate many interesting aspects of its hydration. Heats of adsorption for water on HZSM-5 and Silicalite-1 are anomalously higher than expected from linear trends of PA for various probe molecules, which suggest the presence of water aggregation around aluminum even at low coverages, reactivity with siloxane bridges, or hydrogen bonding with silanol nests.[279] As the PA of the framework is substantially higher than that of small water clusters, additional stabilizing effects of the hydrated proton must contribute to the formation of protonated water clusters in HZSM-5. One component could be combined dispersion forces and electrostatic fields of the framework, a "confinement" effect, calculated as ∼15 kJ/mol for Silicalite-1 and 15−25 kJ/mol for HZSM-5 based on argon, CO, and N_2 adsorption studies.[280,281] Cluster formation around Al-sites is supported computationally and experimentally for $H(H_2O)_n$ (n = 1, 2) species in HZSM-5 where heats of formation have been calculated and experimentally measured to be approximately −12 to 20 and −8 to 15 kcal/mol for one and two waters, respectively,[282,283] with variations in the adsorption energy of the dimer due in part to differences in hydrogen-bonding arrangements and stability of the ion-form versus dimer hydrogen-bonded to a framework acid site.[257,258] The ranges reported could be attributed to experimental error, different levels of theory, or different aluminum and defect contents in the samples studied.[284,285] Microcalorimetric measurements have indicated unique stability to the $H(H_2O)_4$ cluster in HZSM-5 similar to proposed first-shell proton hydrates (Eigen structure) in bulk acid solution.[256,286] Interestingly, the heat of adsorption of water in HZSM-5 approaches the heat of water condensation (q_{liq} = 44 kj/mol) at a H_2O:Al ratio of ∼8,[285,286] consistent with recent proposals of a maximal cluster size in cages at the intersection of the sinusoidal and linear channels of MFI.[259] Much of the work on identifying hydrated proton clusters in HZSM-5 and describing their behavior is computational or relies on bulk measurements of adsorption, so the possibility of directly probing the vibrations and dynamic behavior of clusters formed at different hydration levels in HZSM-5 using 2DIR should be a major contribution to this area of research, especially in comparison to reported vibrational structures of gas-phase hydrated proton clusters.[287] As described in this Review, ultrafast 2DIR spectroscopy can determine vibrational correlations between water vibrational resonances and resolve their energetic relaxation over femtosecond time scales following vibrational excitation.

While time-dependent vibrational behavior of zeolites has been investigated by early pump−probe transient spectroscopies on picosecond time scales,[288−296] advancements in ultrafast IR spectroscopy present the opportunity for studying the femtosecond-time scale dynamics of these systems, as well as correlations between vibrations using 2DIR techniques. This improvement in time resolution allows for the measurement of hydrogen bonding dynamics. 2DIR investigations of a highly hydrated (H_2O: Al ≈ 13:1) proton-form ZSM-5 sample indicate correlation between proposed terminal, non-hydrogen-bonded hydroxyls with hydrogen-bonded hydroxyls in water clusters observed (Figure 11). The presence of these coupled OH-stretches suggests the formation of water clusters in isolation within the zeolite. The time-evolution of the spectrum from a pump−probe delay of 100 fs to 5 ps shows that energy relaxes from the OH-stretch to low-frequency modes, producing a hot ground state feature similar to the feature observed in bulk H_2O,[297,298] indicating the presence of an extended network of hydrogen-bonded water inside the zeolite under these conditions.

2.2.3. Molecular Immobilization for Catalytic Interfaces. Zeolites and conductive oxide materials span a rich platform in which to investigate the impact of spatial confinement on the structure of water, protons, small charged ions, and other aqueous solutes. The immobilization of molecular complexes within the pores and bound to the

https://doi.org/10.1021/acs.chemrev.1c00069
Chem. Rev. 2021, 121, 9450−9501

accessible surfaces of these materials provides an additional synthetic tool to manipulate their surface structure and interfacial chemical reactivity. Outstanding work in molecular immobilization and surface structure manipulation of substrates[299,300] like nanoparticles,[301,302] metal oxide thin films,[303−305] graphene or carbon,[306,307] mesoporous silica,[308,309] and metal−organic frameworks[310,311] using an extraordinary diversity of molecules and anchoring chemistry highlights the vast opportunities of this approach to access new hybrid materials. This section provides a brief overview of the scientific literature on molecular immobilization, with a particular focus on zeolites and conductive oxide substrates, and further refined to examine reactivity and (electro)catalysis in water.

The immobilization of molecular complexes on or in electron- and proton-conducting materials has many attractive properties. A focus on molecular complexes or catalysts allows researchers to tune the molecular structure with atomic resolution and conduct structure−activity-mechanism studies with extremely high precision. In the context of water remediation catalysis, this allows the opportunity to selectively target specific bonds or functional groups of contaminants. Furthermore, in comparison to heterogeneous catalyst materials, molecular catalysts are essentially defect-free and enjoy high metal-atom efficiency. Anchoring molecular catalysts to a surface provides opportunities to manipulate how the catalytic center interacts with other system components by coimmobilizing substrate docking sites or avoiding bimolecular and diffusional deactivation pathways. In the context of electrocatalysis, the principal reason for immobilizing molecular catalysts to electronically conducting materials is to develop direct and tunable pathways for interfacial electron transfer as a fast source or sink of electrons. Examples of immobilized molecular catalysts on electrode surfaces are prolific in the artificial photosynthesis community. High-surface-area metal oxide substrates have been employed extensively in the investigation of surface-bound multielectron redox catalysis and the development of dye-sensitized photoelectrochemical cells (DSPECs).[312,313] DSPEC and dye-sensitized solar cell (DSSC)[314,315] architectures allow detailed kinetic mapping of interfacial electron transfer between immobilized molecules and semiconducting oxides using time-resolved spectroscopies or electrochemical methods to generate system design principles to optimize efficiency and stability.

It is important to recognize that a significant limitation of molecular catalysts in water remediation applications is their relative instability under extreme conditions of pH or applied voltage as compared to their metal oxide counterparts. A specific concern for the implementation of immobilized complexes is the stability of the anchoring group, several examples of which are shown in Figure 12. Most of the early and ongoing work in molecular immobilization on semiconducting metal oxides employed carboxylic acids or phosphonic acids as anchoring acids.[316] These are deprotonated at mild pH values and therefore readily bind to metal oxide surfaces through nucleophilic attack by the negatively charged oxygen atom. These anchor groups are synthetically tractable and therefore are broadly used for molecular immobilization, but their limited stability in water at neutral or alkaline pH levels limits their utility in aqueous environments. More recently, hydroxamic acid[317] and hydroxyquinoline[318] functional groups have emerged as anchoring chemistries with enhanced stability and versatility as compared with the inorganic acids, and covalent bonds to metal oxide surfaces can be achieved by terminal silanes or silatranes[319] and the electroreduction of diazonium

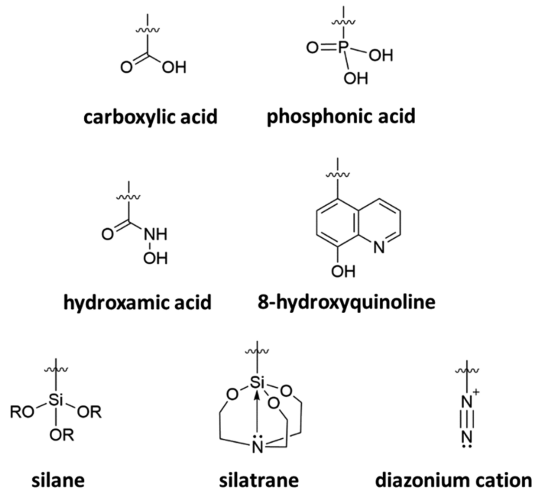

Figure 12. Chemical structures of common anchoring groups used in molecular immobilization on metal-oxide surfaces. R groups on silanes are typically $-CH_3$ or $-CH_2CH_3$.

cations.[320] Another strategy to stabilize molecular complexes anchored to metal oxide substrates and prevent desorption is via "mummification" of immobilized molecules by ALD.[321,322] As described in section 1.2, ALD is a critical tool for thin film synthesis as it can generate atomically precise conformal metal oxide thin films. Of relevance to stabilizing immobilized molecular complexes, the traditional solution deposition is followed by just a few cycles of ALD (typically fewer than 10) to protect the anchoring groups from any interaction with the ambient solution. This combination of molecular design and materials synthesis has yielded immobilized molecular assemblies with substantially higher resistance to thermal degradation and desorption at extreme pH values,[323] as well as increased yield of interfacial electron injection by disrupting deleterious surface-bound molecular aggregation.[324]

Water remediation catalysis is a constantly evolving challenge as new substrates (contaminants) are introduced into water sources with disheartening frequency. In this way, pinpointing the ultimate catalyst material is not likely the most useful pursuit, but rather identifying a suite of catalysts that operate under common conditions to attack all of the existing and emerging pollutants is perhaps a more effective strategy for comprehensive water remediation. The use of zeolites and related materials to host AOPs has recently been reviewed,[325] and there are many recent reviews on heterogeneous materials for water remediation, so here we will highlight molecular catalysts for water remediation processes (Figure 13).

Iron-TAML (TAML = tetraamido macrocyclic ligands) and closely related complexes support high-valent Fe-oxo states and are particularly effective at H_2O_2 activation that can then go on to degrade an extraordinarily broad range of aqueous pollutants.[326−329] Importantly, the Fe-TAML catalysts avoid the limitations of traditional Fenton catalysts that only are catalytic in a narrow pH range, and outside acidic conditions, ferric oxide precipitates are no longer catalytic and require removal by filtration. The majority of work on Fe-TAML water remediation catalysts has been in homogeneous systems, but a study where a Fe-TAML complex is immobilized on graphitic carbon shows that they are active for electrocatalytic water oxidation where the analogous solution-phase system deactivates quickly and suggests the promise for expanding the activity of Fe-TAML in immobilized systems.[330]

https://doi.org/10.1021/acs.chemrev.1c00069
Chem. Rev. 2021, 121, 9450−9501

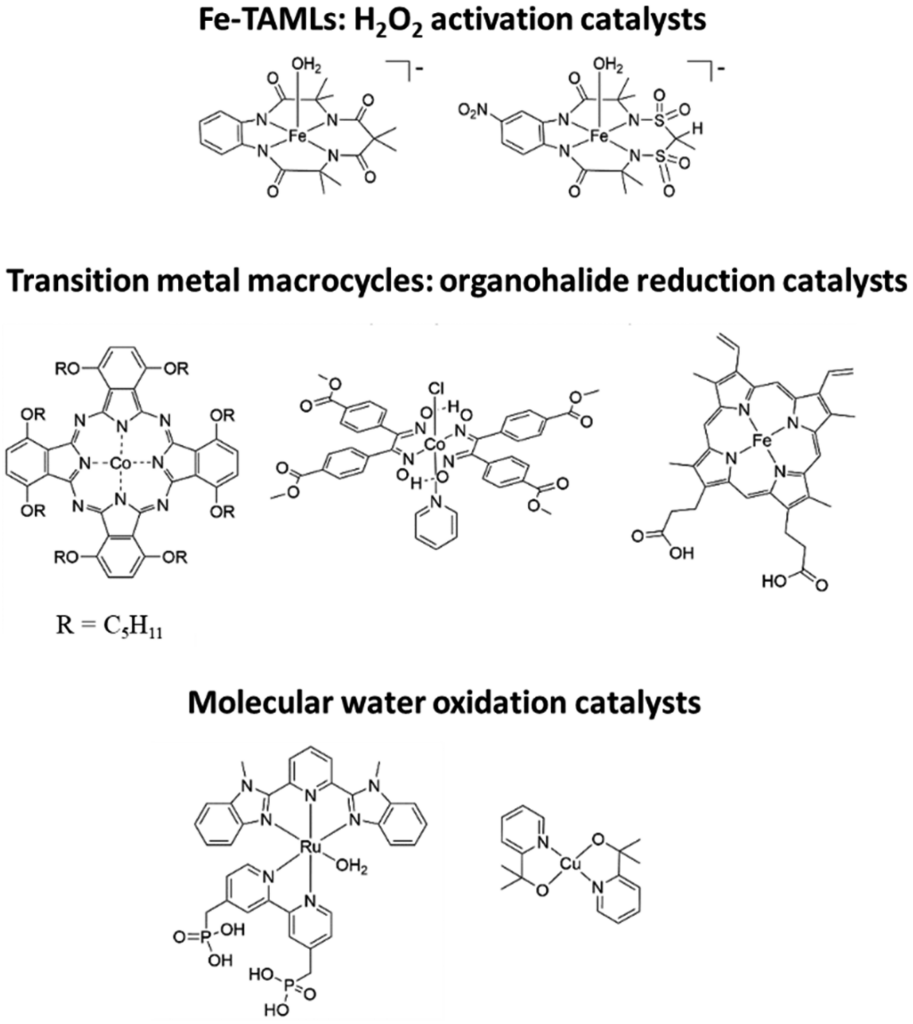

Figure 13. Chemical structures of selected molecular catalysts used for water remediation processes including activation of hydrogen peroxide, organohalide reduction, and water oxidation.

A number of transition metal macrocycles have shown promise in catalytic reductive dehalogenation, an important transformation to degrade many common water pollutants. Cobalt macrocycles,[331] including cobalt phthalocyanines[332] and cobaloximes,[333,334] have shown promise in electrocatalytically reducing chlorinated compounds. Cobalt and iron porphyrins immobilized on TiO_2 nanoparticles make use of favorable interfacial kinetics to support multiple electron transfer and enable photocatalytic C−Cl bond breaking following visible-light excitation.[335−337] Recognizing that these examples are productive toward carbon−halogen bond breaking, these molecular catalysts may be a good place to look for developing treatment systems for the degradation of particularly challenging per- and polyfluoroalkyl substances (PFAS) pollutants.

Given the intense interest in developing and understanding molecular catalysts for light- and electrode-driven water oxidation, building upon this literature is another possible avenue to explore for oxidative water remediation catalysis. The mechanisms for water oxidation by molecular catalysts are readily probed by a variety of in situ spectroscopies and are fairly well understood, but these catalysts often require high overpotential to access the $4e^-/4H^+$ oxidation of water.[338] However, this observation suggests that the oxo, peroxo, and hydroperoxo intermediates that are accessed at moderate potentials could facilitate less demanding $1e^-$ or $2e^-$ bond-breaking transformations. An example of a catalyst developed for water oxidation but applied for the oxidation of aqueous solutes is demonstrated by the oxidation of benzyl alcohol by a $[Ru(II)(Mebimpy)(4,4'\text{-}((HO)_2OPCH_2)_2\text{-}bpy)(OH_2)]$ catalyst (where Mebimpy = 2,6-bis(1-methylbenzimidazol-2-yl)-pyridine; $4,4'\text{-}((HO)_2OPCH_2)_2\text{-}bpy$ = 4,4′-bismethylenephosphonato-2,2′-bipyridine) immobilized on nanostructured ITO.[339] We note that a critical challenge for any molecular oxidation catalyst is to design the catalysts such that any metal-coordinating organic ligands are resistant to oxidation themselves. Along these lines, molecular complexes with a 2-pyridyl-2-propanoate ("pyalk") ligand can support the typically unstable Ir(IV) oxidation state,[340] and Cu(II) complexes with the pyalk ligand are competent electrocatalysts for homogeneous water oxidation at basic pH.[341]

The strategies for molecular immobilization on metal oxide surfaces are well-established, but ongoing work continues to yield more stable anchoring groups under a wide array of solution conditions and enable fast interfacial electron transfer. Additionally, the development of molecular catalysts for water remediation provides abundant opportunities to manipulate selectivity and activity through fine adjustments to the chemical structure and to understand the mechanistic details by multiple

https://doi.org/10.1021/acs.chemrev.1c00069
Chem. Rev. 2021, 121, 9450−9501

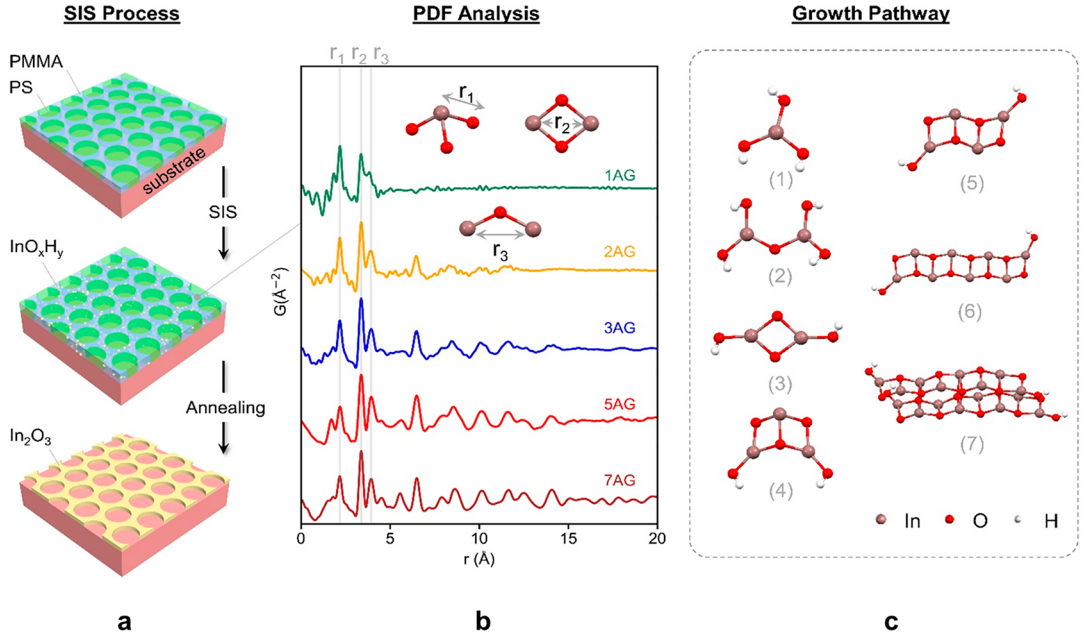

Figure 14. (a) SIS Process: An example of the synthesis of metal oxide thin film using SIS with block copolymer template; (b) PDF analysis: Experimental HEXS-PDF characterizing InO_xH_y clusters formed in PMMA thin films with the increased number of SIS cycles. The inset illustrates the first-shell In−O, second-shell In-$(\mu$-O$)_2$-In, and In−O−In bonding structures that contribute to the first three PDF peaks labeled as r1, r2, and r3, respectively; (c) Growth Pathway: The as-derived pathway for the growth of indium indium oxyhydroxide clusters in PMMA based on the PDF analysis. Reproduced from ref 351. Copyright 2020 American Chemical Society.

steady-state and in situ spectroscopic techniques. Hybrid materials based on molecular catalysts immobilized on electroactive, perfectly porous surfaces will allow researchers to investigate the effects of surface chemistry and molecular confinement on electrocatalytic remediation activity and provide the fundamental knowledge that will underpin development of complete systems for pollutant degradation.

2.3. Methods for Characterization of Water/Solid Interface Reactivity

In chemical reactivity, tracking the hierarchy of structure and structural dynamics for mesoporous materials and correlating surface-tailored structures to (electro)chemical reactivity is of great importance. The scope of this research begins with an interrogation of atomic structures for surface-modified mesoporous materials, and extends to an interrogation of the multiple nanoscale dimensions into the electric double layer for pore-confined aqueous solutions. Of particular interest are comparisons of (electro)chemical activities with interfacial structure for porous materials with buried interfaces that are modified with atomic charged sites, catalysts, and electrochemically applied potentials. Chemical reactivity derives from electronic structures of frontier orbitals determined by ligand field structures across the inner and outer coordination spheres. For interfacial catalysis, ligand fields and local structures are modified by charged sites, applied potentials, and solution structure and dynamics, including the distribution and transport of ions and solutes across the electrical double layer.[342−346]

Emerging work is showing how interfacial structure and solution confinement with dimensions comparable to those of the electrical double layer can combine to significantly modify chemical reactivity compared with a comparable planar surface.[342−346] A key challenge lies in gaining sufficiently precise information on the electronic and atom structures for deep interfaces for the development of predictive theory and the design of mesoporous materials with optimized chemical reactivity. In what follows, approaches to these challenges using a combination of advanced characterization tools, including X-ray scattering/absorption and electrochemistry, are described.

2.3.1. X-rays. Reciprocal-space grazing-incidence X-ray techniques, and a variety of spectroscopy and real-space electron, X-ray, and scanning probe microscopy techniques have provided approaches for resolving specific aspects of structure across the solid-aqueous interface. In particular, X-ray reflectivity and truncation rod analysis have provided powerful approaches for mapping electron density distributions along the profile of the solid−liquid interface, yielding information on the atomic structure at the interface and profiles of solvent and counterions as a function of distance into the solution double layer.[347−349] However, X-ray reflectivity approaches lose resolution with nonplanar porous and disordered or noncrystalline interfacial materials. Further, electron density mapping along the profile does not directly inform on atom-pair correlations, for example on the correlations between metal atoms and ligands at catalyst sites, nor directly on ion pairing distances in solution. The resolution of these features is key for understanding the fundamental basis underlying interfacial chemical reactivity. Grazing incidence X-ray scattering, including small- and wide-angle X-ray scattering (GISAXS and GIWAXS), provides versatile approaches for structure characterization of mesoporous and spatially complex interfacial 2D materials. New developments are described in the preceding section 1.3. One limitation for soft and hard X-ray GISAXS and GIWAXS lies in the limits of structure resolution at the atomic scale.

To achieve a mapping of structure in mesoporous materials and the confined liquid double layer with the highest possible spatial resolution, extended X-ray absorption fine structure (EXAFS) and high-energy (50−100 keV) X-ray scattering (HEXS) with pair distribution function (PDF) for the analysis of

https://doi.org/10.1021/acs.chemrev.1c00069
Chem. Rev. 2021, 121, 9450−9501

mesoporous catalyst materials under functional conditions have been developed. Both techniques probe structure with subatomic, ≥0.1 Å, spatial resolution and allow quantitative structure analyses by comparison to structures predicted by theory.[350−363] The combination of EXAFS and HEXS-PDF together with operando electrochemical analyses provides an approach to reveal the structure and dynamics that are directly linked in interfacial chemical reactivity and have sufficient atomic-scale resolution to serve as discriminating databases for the development of quantitative theory.

EXAFS has been widely applied for interrogating coordination structures for 2D and mesoporous catalysis materials under operando conditions.[364−372] However, EXAFS typically has limited ability to detect atomic-pair distances beyond the first and second coordination shells for molecular complexes or amorphous and disordered crystalline materials.[350] HEXS-PDF offers a useful complement to EXAFS by providing an all-atom measure of pair distances measured with a spatial resolution comparable to EXAFS, but with a resolution range that extends from the first- and outer-shell coordination distances to the few-nanometer scale.[350−363]

To illustrate opportunities for tracking the hierarchy of structure underlying function in mesoporous thin film materials, we have used combined EXAFS and HEXS-PDF to analyze the nucleating metal clusters and growth mechanisms that are responsible for the fabrication of meso-structured transition metal oxides[351] using advances in SIS.[229,230,373] The PDF profiles in Figure 14 shows the structural characteristics of the InO_xH_y clusters formed in a PMMA host matrix following individual growth cycles during SIS.[351] After the first cycle, labeled 1AG, the nucleating clusters are seen to have a discrete structure with pair distances encompassing three coordination shells, labeled r1, r2, r3, corresponding to the In−O bonding distance, the di-μ-oxo-bridged In atomic pair distance, and the distance for a mono-oxo bridged In atom pairs, respectively (Figure 14, inset). Modeling studies have shown that the experimental PDF could be fit with a specific combination of mono-, di-, and trinuclear InO_xH_y clusters. The analysis provided a unique means to track the mechanisms for SIS metal cluster nucleation and SIS cycle-dependent growth.[351] With an increasing number of SIS cycles, the nucleating clusters are seen to grow in a mechanistically characteristic fashion, indicated in Figure 14 by the increases seen in pair correlations with increasing distance for samples exposed to an increasing number of SIS cycles.

Comparison of EXAFS and HEXS-PDF experiments to explicit coordinate models yielded a detailed picture of the SIS nucleation and growth mechanism, summarized in Figure 14.[351] A notable feature is that the nucleating and growing SIS clusters are found to share a common core structure that is related to the bonding pattern seen in In_2O_3, but with discrete sizes and with mono-μ-oxo bridges between the di-μ-oxo linked InO_xH_y clusters.[351] Thermal annealing of the amorphous InO_xH_y cluster/PMMA hybrid architecture was found to transform the amorphous material to nanocrystalline In_2O_3 domains, with dimensions that are modulated by the number of SIS cycles.[351] The detection of discrete, size-tunable host matrices is a notable feature of SIS. A range of amorphous, defect, and surface termination sites have been proposed to be responsible for catalytic activity in nanocrystalline In_2O_3. The X-ray analysis of the SIS InO_xH_y clusters in PMMA suggests opportunities to use SIS for the creation of hybrid metal oxo cluster/polymer films with enhanced chemical reactivity in water treatment applications.

Finally, we note that the capability for achieving a detailed tracking of atomic structures within ultrathin SIS films has been enabled by the emergence of new synchrotron-based approaches for achieving microfocused high-energy X-rays and grazing incidence PDF analyses.[351,374−376] The resolution of the SIS amorphous InO_xH_y clusters in PMMA was achieved for approximately 150 nm-thick PMMA films containing an In atom content only of 1%−2% loading.[229] Ongoing difference HEXS-PDF approaches are demonstrating opportunities for detecting fine structure changes at chemically active sites[350,352] and confined solvents in mesoporous 2D materials. The linkage of the high-resolution X-ray with electrochemical analyses, described below, is poised to provide experimental benchmarks that document structure correlations to interfacial chemical reactivity with sufficient precision to serve as discriminating databases for the development of quantitative theory.

2.3.2. Electrochemistry. Electrochemical analysis of thin films and catalytic interfaces yields information not only on the relevant redox potentials for a given material but also on its conductivity, density of active sites, and mechanisms of adsorption and catalysis. The breadth of electrochemical techniques and materials studied fills dozens of dedicated review articles and textbooks.[377] Therefore, in this section, we will highlight the electrochemical techniques and properties relevant to understanding molecularly defined catalytic interfaces.

Cyclic voltammetry (CV) is arguably the most routine electrochemical measurement performed and typically the first insight into the redox properties of molecular systems.[378] In an ideal situation, the heterogeneous electron transfer between an electrode and a dissolved molecule results in the classic voltammogram "duck shape," which is the result of diffusional, heterogeneous interaction between the molecule and the electrode surface and is governed by the Nernst equation. Quantitative analysis of CVs can yield information on both the thermodynamics and kinetics of a given electron-transfer process and its chemical and electrochemical reversibility. In evaluating a molecular complex for electrocatalytic activity, CV can be particularly instructive in understanding reaction rates, mechanistic details, and distinguishing the identity of a precatalyst structure from the active catalyst.[379,380] However, for a surface-immobilized complex, the situation can become more complicated. For example, molecular complexes have been shown to convert from the standard outer-sphere electron-transfer processes to inner-sphere electron transfer when immobilized on conductive graphite electrodes.[381] Additionally, the electrical conductivity of the anchoring group used for molecular immobilization is an important consideration in assessing the kinetics of an electron transfer since there is no diffusional component to facilitate electron transfer.

When evaluating the molecule-solid interface, the electrical double layer (Figure 15) plays an outstanding role in determining activity and mechanism, particularly in (electro)-catalytic processes.[382−384] From many experimental approaches and theoretical models, it is well-established that the electrical double layer emanating from flat electrodes is a function of the bulk concentration of the electrolyte.[377,383] As the synthesis and fabrication methods for electro-active materials with precise pores on the Ångstrom-to-nanometer scale are developed,[229] it is relevant to note that the spacing between charged surfaces can become competitive with the length of the electrical double

https://doi.org/10.1021/acs.chemrev.1c00069
Chem. Rev. 2021, 121, 9450−9501

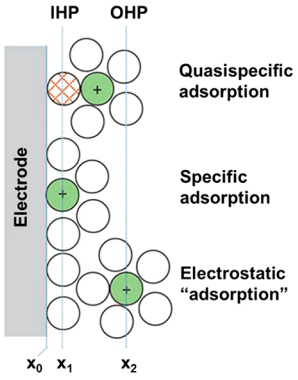

Figure 15. View of the double layer at a negatively charged electrode surface. Specifically adsorbed anions occupy the inner Helmholtz layer (IHP); quasi-specific and electrostatically adsorbed anions occupy the outer Helmholtz layer (OHP). Reprinted with permission from ref 383. Copyright 2019 AIP Publishing.

layer.[385,386] These works point to interesting, unusual possibilities to tune the reactivity of water and aqueous solutes as the reaction flask moves from the bulk solution, to the interfacial regime, to confinement where interfacial effects dominate activity and mechanisms.

Stark spectroscopy has become an important tool to experimentally visualize the width of the double layer by monitoring the changes to the electronic or vibrational signature of molecules adsorbed or immobilized on an electrode surface. In a recent study, the adsorption of diisocyanide-functionalized molecules with varying length onto Au electrodes provided a convenient handle to probe the depth of the Helmholtz layer (Figure 16a).[387] As the electrode potential was tuned from +0.1 to −0.7 V vs Ag/AgCl, the prominent isocyanide N≡C stretch of these compounds shifts nearly 40 cm^{-1} and was used to calculate the Helmholtz layer to be 7−10 Å, indicating that the bulk electrolyte in solution penetrates the monolayers of the longer compounds. In another example, Ru(II)poly(pyridyl) complexes were immobilized onto nanocrystalline TiO_2 thin films, and the change in their characteristic metal-to-ligand charge transfer (MLCT) absorbance was monitored in response to applied potential (Figure 16b).[388] The electric field experienced at the complex decreased with increasing length of the rigid anchors, where the complex with the shortest anchor was presumed to reside within the Helmholtz layer and also exhibited the fastest rates of charge recombination following photoinduced charge injection into the TiO_2 film. Additionally, interfacial electric fields have been shown to have a dramatic impact on selectivity for carbene rearrangements and epoxide formation catalysis.[389−391] We anticipate that these examples will help to guide the development of electrode surfaces, anchoring chemistry, and catalyst structure by revealing the fundamental physical chemistry of these systems and establishing the underlying principles to develop effective materials for surface-bound electrocatalysis processes.

2.3.3. Spectroscopy. For aqueous solutions, ultrafast 2DIR spectroscopy techniques—introduced in the context of adsorption phenomena earlier in this Review—have emerged as unique tools for the investigation of hydrated excess protons due to their capability to resolve dynamic behavior of hydrogen bonds and establish vibrational correlations. By studying the 2DIR spectra of bulk aqueous HCl solutions, evidence for the dominant fundamental unit (or core structure) of the hydrated excess proton in aqueous HCl solutions has been found to be a relatively long-lived "Zundel-like" species or complex with flanking waters that had a minimal lifetime of 480 fs.[392] This result was subsequently built upon[393] to confirm the predominance of the Zundel-like complex through the characteristic inverted anharmonicity of the proton stretching vibration. There remains some disagreement, however, concerning detailed structure of this complex, and whether it is properly considered as a symmetric Zundel ion or as an asymmetric Zundel-like $H_5O_2^+$ species existing between the limits of traditional symmetric Zundel- or Eigen-type structures.[394]

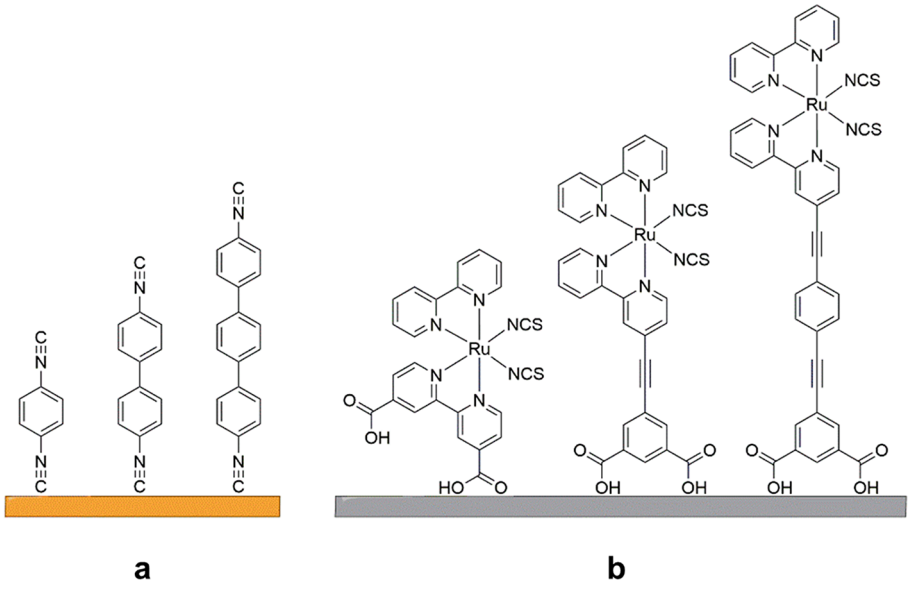

Figure 16. Examples of molecular probes used in Stark spectroscopy experiments to evaluate the size of Helmholtz layer. (a) Diisocyanate molecules adsorbed on Au electrode, monitored by changes to NC stretch as a function of applied potential and number of phenyl spacers. (b) Ru(II)poly(pyridyl) complexes immobilized on TiO_2 thin films, monitored by changes to MLCT absorbance as a function of applied potential and anchor length.

https://doi.org/10.1021/acs.chemrev.1c00069
Chem. Rev. 2021, 121, 9450−9501

Given the successes in using 2DIR methods to investigate aqueous acid solutions, the study of hydrated excess protons under confinement is an interesting extension and suggest that it might shed light into the structural details of protonated water clusters in the types of zeolite systems discussed above. Given the limited prior work on investigating solid systems using these techniques,[395−398] new methodologies specific to the study of zeolites have been developed as part of ongoing research activities. Recent studies have used 2DIR techniques to investigate water in the solid calcium sulfate hydrates bassanite and gypsum,[395] mesoporous silica MCM-41,[396] as well as at the surface of Na-exchanged Nafion membranes[397] observing slow dynamics relative to bulk water near the surface of Nafion and MCM-41, rigid hydrate structures for gypsum, and orientational disorder of water in the 5.5 Å channels of bassanite. These 2DIR results indicate the effects of confinement on water depend on the surface interactions and void sizes present and are consistent with the large body of literature in this field.[6,399−402]

2.4. Simulations of Aqueous Electrochemical Interfaces

The design and optimization of electrochemically reactive interfaces are among the open challenges in developing sustainable, advanced materials that handle, process, and treat water.[8,403−405] Theoretical models and computational studies play an important role in overcoming these challenges by providing predictions of optimal materials interfaced with water to be used in, for example, water treatment devices and purification membranes.[406−408] At the same time, they are a necessary component to elucidate many aspects of experimental investigations and help guide future experimental studies, including most notably those described above. However, to date, computational screening schemes for materials properties have mostly focused on bulk properties of candidate systems, thus neglecting the structure and chemistry of surfaces and interfaces with the liquid, except in recent first-principles studies.[409] In addition, most simulations of interfaces have been conducted in the absence of applied biases, with some notable exceptions.[410−413] The importance of interfaces cannot be overemphasized.

In the last 50 years, the condensed matter physics community has developed methods to study solid/liquid interfaces and to identify, at least for simple systems, atomic-electronic structure relations.[414−416] The latter may in turn be used to understand complex phenomena such as electronic and mass transport across interfaces and electro-[417] and photoelectrochemical reactions.[409,414] The method of choice to describe interatomic interaction and structural models for both the solid and liquid has been DFT,[418] at various levels of sophistication, combined, in the last 20 to 30 years with methods that originated in the quantum chemistry community; these methods were utilized to define so-called hybrid functionals.[418−421] About three decades ago, DFT was coupled to molecular dynamics, a simulation technique used to investigate both dynamical and thermodynamic properties of matter (ordered and disordered solids, and liquids); this coupling[422] (now known as first-principles or ab initio MD) has enabled studies of the structural and vibrational properties of water and aqueous solutions interfaced with solid surfaces, including surfaces of semiconductors such as Si[409] and SiC[423] and oxides such as tungsten oxides,[414,417] titanium oxides,[424] and bismuth vanadate.[425,426] Recently, the use of advanced electronic structure theories beyond DFT[427] has made possible accurate calculations of optoelectronic properties of defective interfaces and hence the interpretation of complex experiments and the prediction of X-ray reflectivity signatures of aqueous solutions interfaced with oxides.[428] These predictions may provide key information about spectroscopic monitoring of ions or more complex species at solid interfaces and under confinement.[429]

2.4.1. Reactive Molecular Dynamics. Multiscale reactive molecular dynamics (MS-RMD) is a method developed by Voth et al. in the computer simulation of the hydrated excess proton in a variety of environments.[430−435] The MS-RMD approach was preceded by the more empirical Multistate Empirical Valence Bond (MS-EVB) model. The MS-RMD method allows the excess proton to hop between neighboring water molecules through the hydrogen-bond network, that is, the Grotthuss shuttling mechanism,[436,437] via rearranging chemical bond topology. The ground-state reactive potential energy surface (PES) in the MS-RMD/EVB method is a linear combination of several nonreactive PES to yield an overall PES with a dynamically rearranging bonding topology along the trajectory, thus simulating chemical reactivity as a function of time in the MD. As such, the excess protonic charge defect is allowed to delocalize in its solvation structure across multiple water molecules and undergo Grotthuss shuttling. More detail on the MS-RMD method can be found in refs 430−435. Compared with the MS-RMD/EVB method, the conventional MD empirical force field method, in which the bonding topology is fixed and invariant, fails to describe the proton Grotthuss shuttling, while ab initio molecular dynamics (AIMD) simulation,[422] which treats the electronic degrees of freedom explicitly and calculates the forces on the nuclei "on-the-fly," is limited in both length and time scale due to its demanding computational cost.

The MS-RMD/EVB method has been successfully used to study the solvation and transport of the hydrated excess proton in various systems, such as bulk water and water interfaces, materials, and proteins. Over the last two decades, MS-RMD/EVB simulations have also provided an in-depth understanding of hydrated excess proton under confinement, for example, in a carbon nanotube (CNT) channel. For example, previous studies reported that the hydrated excess proton shuttles through a single proton wire in a CNT ∼ 10 times faster than in bulk water.[438,439] It was subsequently discovered there is a unique "trapping-wetting-permeation" mechanism for proton transport through a d = 0.8 nm CNT (6,6) nanopore.[440] A recent study[441] has investigated the confinement effects on the hydrated excess proton solvation and transport with CNTs of various diameters and topologies and found that the proton transport into a CNT (6,6) nanopore occurs solely via Grotthuss shuttling at the nanopore opening.

Aluminosilicate zeolite HZSM-5, with a defined crystal structure and similar nanoporous channel diameters to a CNT (6,6),[442] naturally contains a framework proton near the aluminum substitution site. As a side product of catalytic reactions, water molecules reside in the zeolite nanopores (Figure 17) and play an important role in the proton reactivity.[255,443−448] Both neutron diffraction experiments[447] and NMR spectroscopy[446] show remarkable proton mobility with the presence of water, where the proton transfers from the zeolite acidic site to the water solvation shells and then becomes a hydrated "excess" proton. Complex impedance spectroscopy has shown that high H_2O concentration in ZSM-5 improves proton transport through the zeolite lattice, via an assumed Grotthuss shuttling mechanism.[449] Computationally, water in the ZSM-5 framework acidic site has been investigated with ab

https://doi.org/10.1021/acs.chemrev.1c00069
Chem. Rev. 2021, 121, 9450−9501

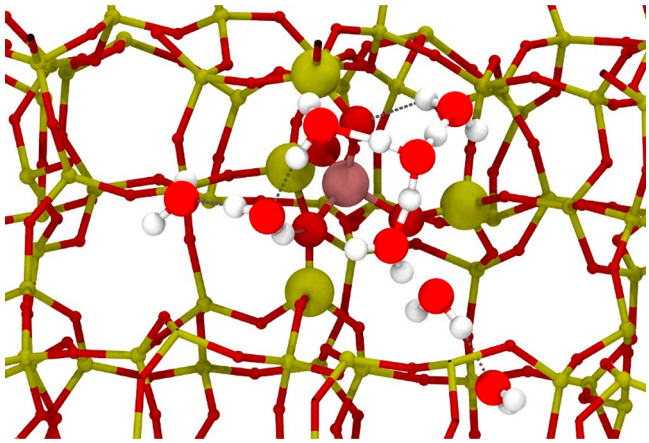

Figure 17. Trajectory snapshot from the DFT-MD simulation of HZSM-5·$(H_2O)_8$ shows a protonated water structure formed on top of the Al tetrahedron with two terminal water molecules (left and bottom right) as free rotors.

initio,[251,255,257,275,444,450−453] QM/MM,[454] and ONIOM[455] methods, most of which focused on the deprotonation energy (DPE), proton affinity (PA), and reaction enthalpy by identifying stationary point structures on the underlying PES for the process. The activation energy of a proton "hop" to another oxygen in the anhydrous zeolite aluminum tetrahedron is 28 kcal/mol, but the presence of a single water molecule decreases this activation energy by 24 kcal/mol.[444]

Researchers have also undertaken a computational and experimental investigation of protonated water clusters in the ZSM-5 framework acidic site first using ab initio methods. The major focus so far has been on the proton transfer PES, short-time dynamics, and spectroscopic assignments at various hydration levels. Meanwhile, an MS-RMD model describing proton transfer from the ZSM-5 acidic site to water is under development because the eventual simulation of hydrated excess proton solvation and transport in the confined zeolite space will require extensive sampling over relatively long time scales to properly account for the underlying free energy surface. Due to the large computational cost, several studies have instead resorted to a statistical approach to characterize the hydrated excess proton transport mechanism in zeolites,[453] so the MS-RMD simulations will provide a more rigorous description at the molecular scale.

In general, the MS-RMD method can be applied to study the solvation and transport of the hydrated excess proton under 1-D or 2-D confinement in a wide range of material systems such as zeolites. Unlike other simulation methods, the MS-RMD method, by accurately recapitulating the proton reactivity at the acidic site, is able to sample a sufficient amount of hydrated excess proton configurations while accounting for the confinement effects explicitly. In addition, the high computational efficiency of the MS-RMD simulations allows for the investigation of correlations of hydration level and proton reactivity in these nanoporous systems. Preliminary, but more limited, DFT-MD results show that at the hydration level of eight water molecules a total of 6−7 water molecules near the zeolite framework acid site forms a hydrogen-bonded water structure, while the remaining water molecules behave somewhat like free rotors. At this hydration level, the protonated water cluster interchanges among several conformations and is less rigid compared with those that form at lower hydration levels (≤4 H_2O). In addition, the choice of DFT functional becomes important to accurately describe the structure and dynamics of both the zeolite framework and the confined protonated water cluster (Figure 17).

2.4.2. Models. We consider here the role of theory and computation in predicting the properties of aqueous interfaces, with a focus on first-principles simulations of semiconductors and oxides in aqueous media and discuss some of the challenges involved in these simulations. Oxides are particularly important. For example, metal electrodes used in electrochemical cells and in batteries are often covered by semiconducting oxide films, and oxide/water interfaces are present in many devices as a consequence of corrosion processes. As an example, it is interesting to mention recent results of first-principles simulations of WO_3 for which studies have shown the key role of the description of defects at the interface.[414,456] In particular, the average potential energy difference at the interface of pristine and defective WO_3 varies by ∼1 eV; solvation is absolutely critical to describe energy levels. An important lesson is that energy levels of aqueous interfaces cannot be inferred from those of dry interfaces. Another important development is in the key importance of using a high level of theory,[457] beyond the widely used DFT[418,458,459] and hybrid DFT[419,420,460] to carry out quantitative predictions of electronic properties. This high level of theory, based on GW calculations, has generated a better understanding that the excess charge present at defective WO_3 surfaces due to oxygen vacancies forms large two-dimensional polarons (∼10 Å radius) on the plane of the surface; the predicted charge-localization properties hint at possible formation of stable (OH^-) groups at the surface in contact with water and the fact that holes transferred to water may form a highly reactive (OH)*, a possible enabler of chemical reactions. Altogether, these calculations have identified three major factors that need to be accounted to describe aqueous interfaces with oxides: the presence of surface defects, the dynamics of excess charge at the surface brought about by defects, and finite temperature fluctuations of the surface electronic orbitals. First-principles simulations of interfaces can also be performed in the presence of electric biases[67,461,462] to study, for example, the modification of electronic properties and vibrational spectra under bias. We note that the calculation of differential spectra of interfaces (e.g., IR spectra) in the presence and absence of an external bias can then be compared with spectro-electrochemical measurements and used to identify specific reactions occurring at interfaces.

In spite of recent progress in describing a number of aqueous interfaces, including some electrified ones,[412,413] remarkable challenges remain before efficient computational protocols become available, to tackle many samples at a time. One outstanding challenge is represented by the size of systems to be simulated, together with the time scale of the simulations. An essential prerequisite to a microscopic understanding of solid/water interfaces for electrochemical applications is the determination of realistic atomistic models of systems consisting of several hundreds of atoms. In addition, long time scales (of the order of hundreds of ps) are often required for meaningful simulations of electrified interfaces. These major challenges may be addressed by developing novel algorithms and codes at the quantum level, and by coupling those with codes operating at different length- and time-scales, including classical and coarse-grained simulations[463] and advanced sampling techniques.[464,465] Once an interfacial structural model (see, e.g. Figure 18) is obtained via simulations, its validation needs to be

https://doi.org/10.1021/acs.chemrev.1c00069
Chem. Rev. 2021, 121, 9450−9501

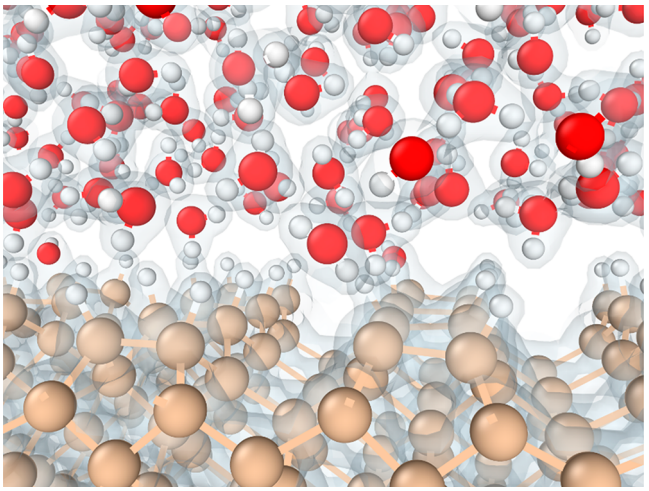

Figure 18. Atomistic configuration extracted from a first-principles molecular dynamics simulation of a hydrogenated Si-water interface. The charge density determined by density functional theory calculations is shown as transparent isosurfaces around molecules and atoms. Red, brown, and white spheres represent oxygen, silicon, and hydrogen atoms, respectively.

carefully executed, for example, by comparing computed vibrational spectra or X-ray reflectivity measurements, with experiments, when available. For example, we recently devised a quantitative validation protocol for first-principles molecular dynamics simulations of oxide-aqueous interfaces. The approach makes direct comparisons of interfacial X-ray reflectivity (XRR) signals from experimental measurements and those obtained from ab initio simulations. The protocol was demonstrated for the case of the of an $Al_2O_3(001)$/water interface, one of the simplest oxide-water interfaces, and is being further developed for more complex interfaces.[428]

Another open issue to be addressed in the study of electrified interfaces is the determination of reaction barriers for chemical reactions occurring at, or close to, a surface. These reaction barriers may in principle be determined by free-energy calculations based on advanced sampling methods[466] (e.g., metadynamics and methods based on neural networks).[467,468] However, the coupling of such methods with first-principles MD is in its infancy,[466] and their availability, together with that of related codes, will be critical to properly sample the complex energy landscape of a realistic electrified interface. We expect the realization of this coupling between sampling methods and quantum codes to be particularly demanding in the case of aqueous interfaces, as we anticipate that the use of advanced DFT methods (for example computationally demanding hybrid functionals) will be necessary to describe proper electronic charge density distributions at interfaces. In addition, to obtain rate constants and dynamical information for proton-coupled electron transfer (PCET) reactions[466] that are often central to processes occurring at electrochemical interfaces, a theoretical and computational framework needs to be built to compute rate constants in the condensed phase. Such framework will encompass simulations of nonadiabatic processes and quantum effects of the electrons and protons. Numerous inputs are required to study reaction barriers, including free-energy differences between the reactant and product states, reorganization energies, and the coupling between reactant and product vibronic states. In principle, all of these quantities can be determined from first-principles calculations by extending the approaches used for solvated molecular species to solid/liquid interfaces. Such a simulation framework for condensed phases remains to be fully developed and validated. Even further in the future is the development of simulation techniques capable of handling, in a predictive manner and from first-principles, transport processes of large ions in aqueous media. Progress has been reported on small ions.[469,470]

Perhaps the biggest challenge faced at present is that of integration. A close integration will require sharing of samples, codes, and data between various research groups in a concerted manner yet to be fully invented and experimented. Eventually, the establishment of a robust feedback loop should lead to new paradigms allowing, for example, for characterization and even modification of interfacial properties by on-the-fly coupled experimental and computational analyses.

3. TRANSPORT

3.1. Introduction/Overview

Transport phenomena share distinct similarities to adsorption and reactivity in their dependence on the movement of water and solutes along, toward, and away from water/solid interfaces. In the case of transport, interfacial environments are engineered to enhance or restrict (or combinations thereof) such movement, and depend greatly on both chemical and geometrical effects such as confinement. One of the major objectives in the design of transport materials for water-energy systems is to apply advanced fabrication, simulation, and characterization methods to investigate the transport behavior of mesoscale charged particles in hydrated porous media ranging from a few nanometers to one hundred nanometers. This section aims to introduce the transport and flow properties of charged species including ions, charged biological molecules such as proteins or viruses, and nanoparticles through porous or confined media.

To understand ion transport mechanisms through porous media, electrical double layer (EDL) effects are essential to determine its working principle. Ions undergo an electrostatic interaction with charged surfaces within the EDL. The thickness of the EDL is often expressed as the Debye length (λ_D), having a reverse relation with ion concentration. Debye length in a 10^{-3} M KCl solution, for example, is 9.6 nm at 25 °C, which is non-negligible compared with narrow nanochannel widths in confined geometries. When λ_D is much smaller than the nanochannel radius, surface charges are more effectively shielded, and Ohmic ion transport behavior will be observed as in a bulk solution. However, if λ_D is bigger than, or comparable to, the nanochannel radius, the traditional understanding of ion transport is incomplete to predict ion interactions as regulated in a nanochannel. In such cases, the relatively high surface-to-volume ratio results in new physical phenomena, such as concentration polarization[471] and ion enrichment.[135] Given the drastic phenomena shift around some critical channel diameter, fabrication of well-controlled nanochannels with pore sizes comparable to λ_D becomes essential for studying the effects on ion transport behavior. When the concentration of counterions cannot balance the surface-charge density of a nanochannel, electro-osmotic phenomena will contribute to attracting excess counterions into the nanochannels, which will increase the surface conductance.[472] Surface morphology, pore size, and charge density of the nanochannel are also important factors.

Similarly, the exact mechanisms of particle transport in confined geometries remains unclear. The gap of ionic

https://doi.org/10.1021/acs.chemrev.1c00069
Chem. Rev. 2021, 121, 9450−9501

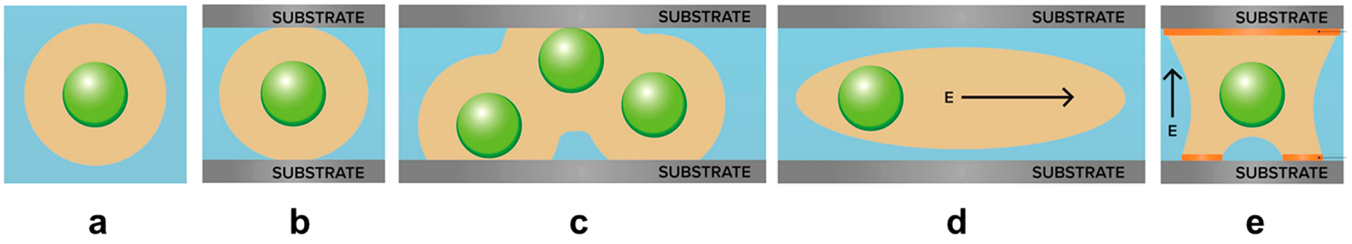

Figure 19. Schematic representation of ionic correlations (orange) around charged nanoparticles (blue) in the bulk and under mesoscale confinement with surfaces of controlled charge. (a) Bulk; (b) confined; (c) confined and concentrated; (d) confined and under the influence of an applied field; and (e) confined by a charge-patterned substrate.

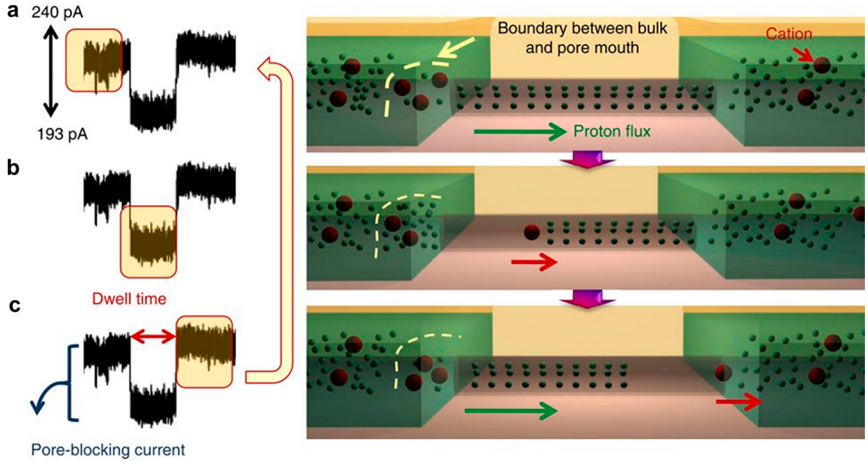

Figure 20. Schematic illustration of ion transport and pore blocking in single-walled carbon nanotubes (SWNTs). (a) Proton flux, (b) ion insertion (blocked by cations), and (c) recovery of proton flux. Reprinted with permission from ref 474. Copyright 2013 Nature Publishing Group.

correlation between a nanoscale channel and bulk solution exists regardless of the surface structure, chemical properties, or solution media (e.g., ion concentration and medium state). The generalized idea is illustrated in Figure 19, where nanoparticles with their associated ionic clouds are depicted in bulk and under extreme confinement. Interactions between such particles lead to a merging of the ionic clouds, akin to Debye screening. In the presence of confinement or applied fields (flow or voltage), such clouds become heavily distorted and anisotropic, leading to screening of a different nature from that in unconfined systems.

By introducing fields and surface patterns in one and two dimensions, researchers can directly interfere with the range of ionic correlations, manipulating structure and transport in hitherto unavailable ways. In this section, we review a series of experimental systems that can achieve this and, at the same time, help guide multiscale simulation and theory. In this way, we seek to describe experimental advances that pose well-conceived questions that would be difficult to formulate and address by trial-and-error experimentation. At the same time, modeling and simulations provide a necessary framework to help improve both experimental and theoretical transport knowledge. It is important to emphasize that such efforts find excellent correspondence in a variety of fields. As an example, a strategy based on first-principles simulations, to determine ratios of Raman scattering cross sections of aqueous species under extreme conditions, has been presented to understand mass transport in the Earth's interior.[473]

3.2. Well-Defined Material Platforms for Studying Transport in Confined Environments

In this section, we review substrates and materials based on model and applied nanochannels and some of the synthetic methods employed to generate them. As an example of confined nanochannels, single or a few channels studies have been conducted using CNTs (Figure 20).[474] Such studies provide unique examples of precisely controlled channel diameter systems while employing an approach that is supported by computational and experimental studies. In pore-blocking events, fast proton flux through the interior of a single-walled nanotube (SWNT) (Figure 20a) results in a high current level (240 pA). In Figure 20b, cations (e.g., K^+, Na^+, and Li^+) enter the SWNT and obstruct the proton flux, resulting in a low current level (193 pA). Once the cation acting as a blocker diffuses through the end of the SWNT, the high current level is rapidly restored because of the high proton concentration near the pore mouth (Figure 20c), demonstrating nonmonotonic ion transport with a diameter dependence in the 0.5−2 nm regime.

The efforts described above have helped generate a better understanding of ionic conduction through highly confined channels. However, further development of single-channel systems is required to overcome issues related to low signal-to-noise ratio and practical uses with inherent limitations of fast and mass-convective flow. Efforts to develop structure−property relationships have also been impeded by the difficulty in quantitatively characterizing structure over accurate measurement in the full range of critical characteristic dimensions. Transport through confined channels is sensitively altered by many parameters including geometry, charged state, and uniformity. To address this, substrates and model systems with identical and reliable multinanochannels will help to improve understanding with clearer signal from multiple signal sources. At the same time, higher porosity and precisely distributed pore sizes in all the channels need to be managed

https://doi.org/10.1021/acs.chemrev.1c00069
Chem. Rev. 2021, 121, 9450−9501

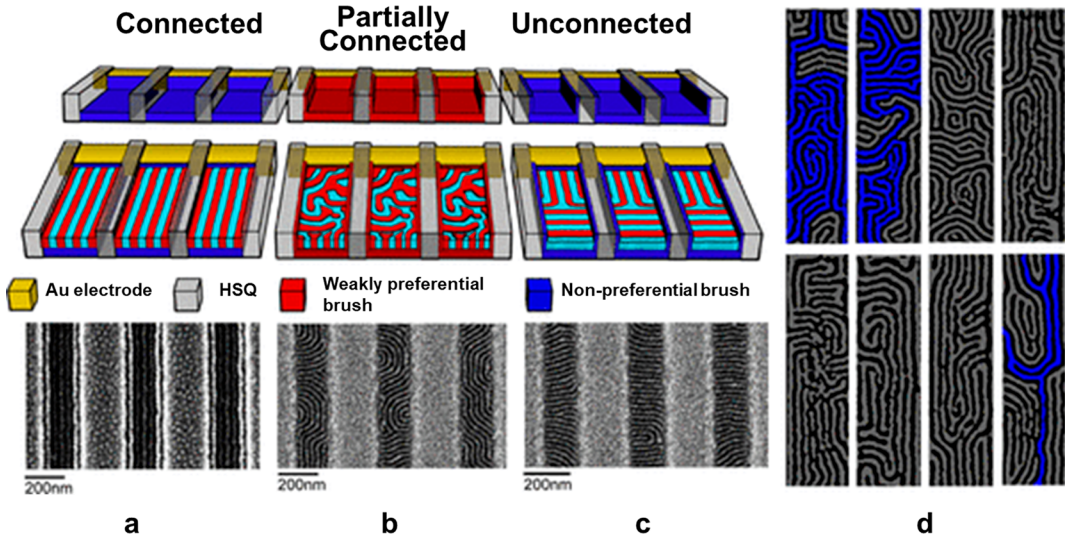

Figure 21. Orientation of the polystyrene-*block*-poly(2-vinylpyridine) (PS-*b*-P2VP) domains relative to the hydrogen silsesquioxane (HSQ) guiding stripes and the electrodes that form the individual trenches. Schematic and SEM micrograph of (a) connected, (b) partially, and (c) unconnected structures. (d) Partially connected morphology SEM micrographs after image flattening and path identification where disconnected paths are labeled gray and the connected domains are labeled blue. Reprinted with permission from ref 487. Copyright 2019 American Chemical Society.

identically to remove unexpected variations. In this way, finely tuned, small-sized, and high-density pore array fabrication and chemical treatment methods from a variety of wall chemistries are essential. As described below, block copolymer systems provide one possible route for achieving this.

Ion-conducting polymers play a central role in transport for electrochemical conversion and storage such as fuel cells,[475] electrolyzers,[476] and redox flow batteries.[477] Bulk properties of ion-conducting polymers such as Nafion have been studied extensively, yet much less is known for these materials at water/solid interfaces under confinement.[478] For example, there is a great discrepancy between bulk Nafion membranes and Nafion thin films under confinement.[478] For the commercialization of the technologies mentioned above, it is of vital importance to understand structure−property relationships for Nafion under confinement to optimize the layer structure and system design.

Polymeric membrane structures, however, have inherent challenges in the context of serving as a practical membrane. Transport through confined channels is influenced not only by the pore diameter but also the free energy cost associated with dehydrating the ion. Therefore, modification of a membrane's surface chemistry has also attracted attention to achieve an appropriate free-energy profile for optimal transport and manipulate the affinity and repulsive interactions with precision such that they can be switched or tuned for reversible adsorption. Electrostatics, hydrogen bonding, surface chemistry, and microstructure greatly influence interfacial affinity and the organization of the solution's boundary layers. Various methods have been suggested as a post-treatment after membrane fabrication. Post-treatment processes such as ALD and SIS, as described previously in this Review, are promising candidates with their uniformity, scalability, and broad options of material selection. Especially with SIS processes, based on the interaction between gas phase metallic precursors and polar groups on polymer chains, it is possible to form metallic oxide membranes from organically defined structures, and introduce engineered surface chemistry and charge to alter the environment of the nanochannels.[230,479]

At the same time, there is a general need within energy-water systems and models to adjust not only the chemical and geometrical properties of porous media but also the solutes themselves to investigate how their properties influence transport. Solute properties necessarily include a range of effects that differ in nature from that of ions, including polydispersity (variations in size) and more pronounced hard-core colloidal repulsive and entropic forces. At the same time, organic and inorganic nanoparticles are commonly observed in natural ecosystems and industrial wastewater streams, posing challenges to separation technologies and often causing fouling and degradation of filtration membranes.[480] In this way, engineered nanoparticles at the nanoscale with dimensions approaching that of porous transport media provide a powerful platform to study various aspects of the water/solid interfaces, from fundamental insights in the interfacial solvent restructuring[481] to the development of scalable water treatment technologies.[482]

3.2.1. Block Copolymers. Block copolymers (BCPs) are one of the promising material classes to fulfill both manufacturing and geometrical needs for ideal nanochannel arrays as ion- or nanoparticle-transport media. To manipulate and investigate the flow of ionic or other species in such media, a well-controlled and identical parallel transport environment is required. It is also advantageous to have a large number of channels rather than a single transport route in order to achieve higher signal-to-noise ratio, and thus analytical clarity (which make it detectable with conventional mass-flow analysis). Such systems also offer the prospect of eventual practical use in membrane applications. Membranes with these geometrical properties are called "isoporous" membranes, and researchers have developed many techniques to experimentally achieve membranes approaching isoporosity across a range of pore scales.[483,484]

BCPs are suitable materials to practically fabricate multichannel membranes with precisely controlled nanochannels that meet these requirements (Figure 21).[479,485,486] BCPs consist of two-or-more polymer blocks that are chemically immiscible with each other, but covalently bonded. Due to that structural character, various self-assembled periodic structures can form,

https://doi.org/10.1021/acs.chemrev.1c00069
Chem. Rev. 2021, 121, 9450−9501

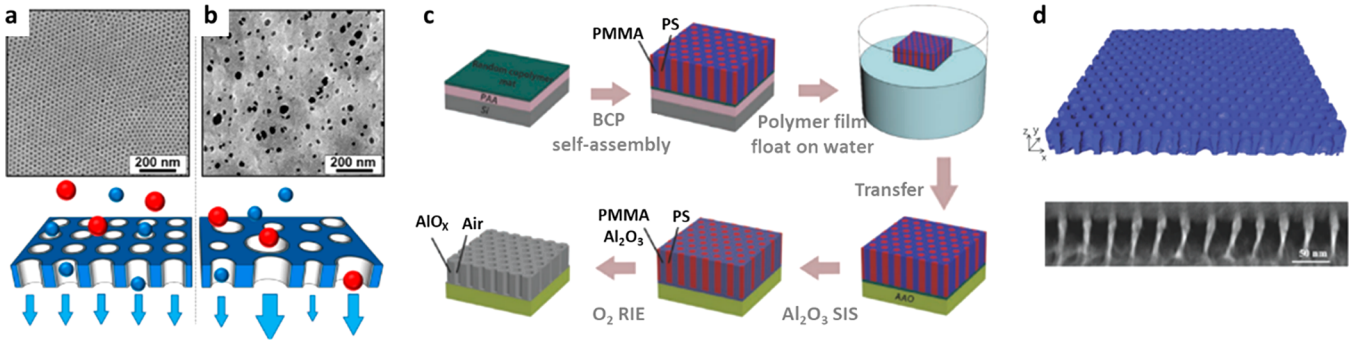

Figure 22. (a,b) Comparison of a BCP-derived isoporous membrane and a commercial membrane made using a standard phase separation process which has a broad dispersity of pore sizes. (c,d) Developed BCP-templated Al_2O_3 membrane fabrication flow and the membrane geometry determined by TEM tomography analysis. Reprinted with permission from ref 479. Copyright 2017 Wiley-VCH Publishing.

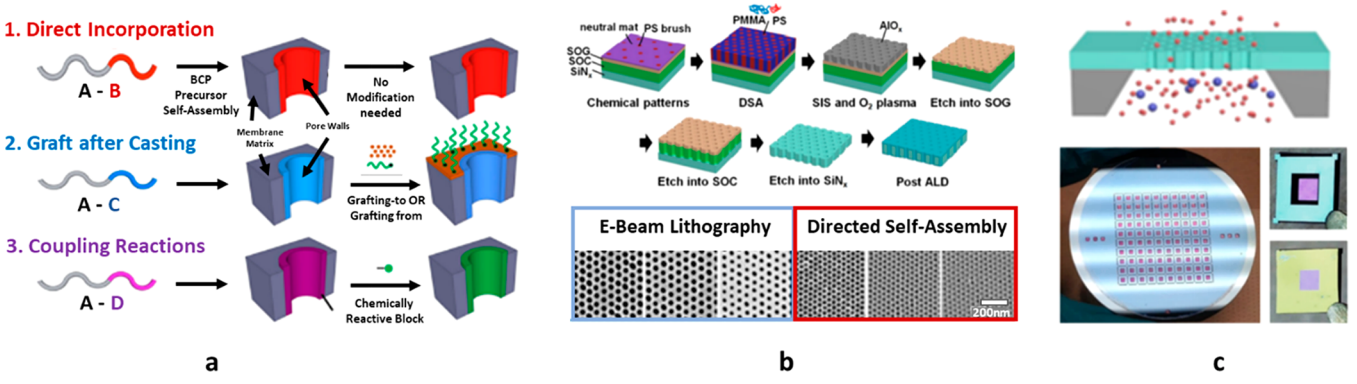

Figure 23. (a) Examples of pore-chemistry modification. (b) Proposed approach to form well-aligned and BCP-templated membranes with DSA. Continuum of confinement dimensions fabricated through a combination of electron beam lithography and DSA. (c) Wafer-scale isoporous membrane with back etch process.

commonly composed of lamellar, cylindrical, or spherical geometries with corresponding feature sizes of 5−50 nm. Based on the structural benefits of uniform and high-density pathways produced in a scalable manner, BCP materials appear suitable for several membrane applications.[487] Without further modification, BCP-derived membranes will fall into the ultrafiltration regime, separating nanoscale species. Pores in these systems can also be scaled down via conformal coating methods to reach into the loose-nanofiltration arena. A precisely tunable feature size is also reproducible since it originates simply from the polymer blocks' molecular weight. Additionally, the pore dimension can be further reduced to be comparable in the size of target molecules or to the Debye screening length for electrostatic interactions and smaller than the mean free path between molecular collisions. This feature size reduction is enabled with preservation of segregation strength χN with high-χ, and has become more achievable with recent developments in BCP design and synthesis (χ is the binary interaction parameter). Post-treatment with ALD and other methods can also tune down porous feature sizes. In addition, nanochannels can be organized to form high-density arrays by directed self-assembly (DSA), ensuring adjacent environments to generate identical and uniform flow distribution through an entire membrane.

Illustrating BCPs as a platform for ion transport, fully connected (Figure 21a), partially connected (Figure 21b), and unconnected (Figure 21c) ionic pathways of BCP with lamellar morphology were formed via DSA of BCP containing a polymer block of ionic conductor.[488] The ion-transport properties of such a block copolymer electrolyte (BCE) were quantified by forming polymer thin films on interdigitated electrodes (IDEs) with high signal-to-noise ratio in electrochemical impedance. All ionic channels contribute equally to the overall ionic conductivity of these BCEs. By forming thousands of identical conducting pathways, it is possible to deconvolute the ionic contribution from each connected pathway by analyzing electrochemical impedance.

Excitingly, BCPs fulfill most conditions of an isoporous membrane with a scalable and reproducible isoporous pore geometry, a fine pore size with narrow size distribution, high porosity, and undisrupted pathways that increase flux. In applications, geometrical arrangement of nanochannels occurs in a perpendicular direction overcoming the difficulty of manufacturing high-density and highly aligned channel arrays. From these points of view, cylinder-forming BCPs are ideal. Meanwhile, ALD and SIS processes can serve as an effective way for chemical and structural modification to precisely manipulate solute transport. As an example, BCP-templated Al_2O_3 membranes were fabricated as a simple idealized system (Figure 22). Cylinder-forming BCPs (PS-*b*-PMMA) were spin-coated and annealed on a chemically neutral surface, with BCP membranes containing perpendicular-oriented PS cylinders forming within the PMMA matrix. To identify the thermodynamically favorable boundary conditions for the perpendicular orientation, various physical parameters were considered and investigated for continuous nanochannels throughout the entire film. In a subsequent step, the SIS process was employed to change the membrane chemistry, transforming the PMMA

https://doi.org/10.1021/acs.chemrev.1c00069
Chem. Rev. 2021, 121, 9450−9501

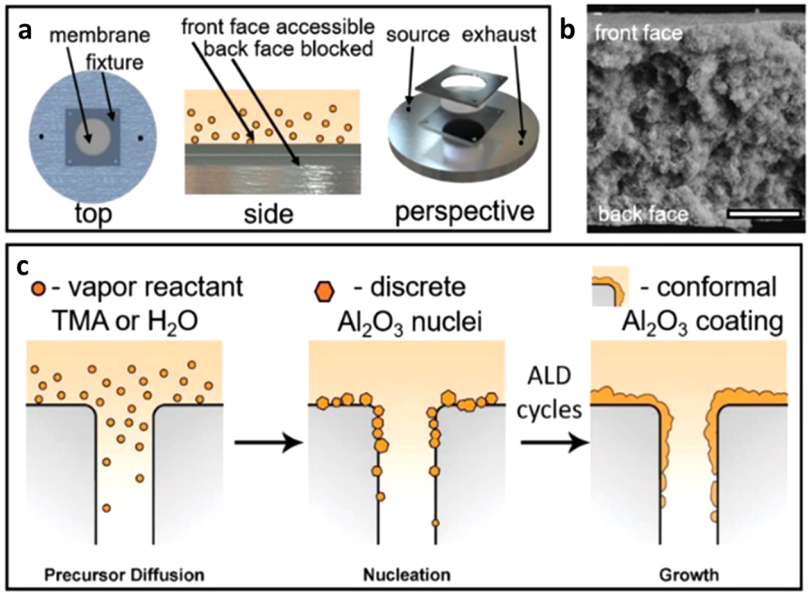

Figure 24. (a) Schematic of the physical housing of the membrane which isolates the front face for vapor diffusion. (b) Cross-sectional SEM of the poly(propylene) reveals the tortuous porosity that leads to diffusion-controlled ALD; scale bar is 80 μm. (c) Vapor diffuses through the pore volume from the front side. Nucleation occurs more quickly near the surface due to greater concentration of reactants closer to the front surface. After nucleation, growth proceeds to form a coating with decreasing coverage through the membrane. Reprinted with permission from ref 496. Copyright 2018 Wiley-VCH Publishing.

matrix architecture into an inorganic (Al_2O_3) membrane after removal of the organic phase (including the original PS cylinders, which become the pores). Meanwhile, the SIS process itself contributes to shrinking the physical pore size with repeated cycles.[479] Extensions of this study may be improved with DSA to provide an identical environment around each individual channel.

Aside from controlled channel geometry, it is also important to manipulate surface chemistry to incorporate appropriate functionalities on physically defined membranes.[489] For example, the electrical charge through Al_2O_3 nanochannels is precisely tunable relying on the pH environment; therefore, the effective pore size can be tuned to improve selectivity of hydrated solutes.[479] There are several approaches to modify membrane surfaces including incorporating the functional chemistries in BCP, or grafting or decorating the pore walls as shown Figure 23a.[230,490,491] From this approach, fundamental studies of solute transport through chemically engineered nanochannels can be elucidated. Meanwhile, ALD processes share the processing benefits of SIS, while having potential to manipulate nanochannel wall chemistries or even forming asymmetric profiles (i.e., Janus architecture) based on their gas phase precursor transport mechanism, which can be applicable to BCP-templated isoporous membranes (Figure 23b,c).

3.2.2. Janus Membranes. Janus membranes are asymmetric porous membranes with distinct chemical properties on each side, such as hydrophilic/hydrophobic functionalities on either side of the membrane.[492] Janus membranes could have impact in capturing the osmotic energy existing in seawater and brackish water as a potentially renewable and sustainable energy source,[493] improving emulsification/demulsification processes, fog harvesting, and may other applications. Ion-selective Janus membranes allow for spontaneous transport of certain ions through the membrane, converting the free energy difference to electrical energy via a net diffusion current.[494] The change of conductance originates from the originally asymmetric cation/anion distribution on each side of the individual nanopores under equilibrium conditions.[495] When an external electrical field is applied, the ion current is proportional to the original equilibrium ion concentration. The membrane efficiency can be optimized through the surface charge profile and pore geometry.

A diffusion-controlled ALD approach has been utilized to fabricate Janus membranes with control of the depth extent. In this study, hydrophobic poly(propylene) (PP) membranes were secured in a custom-machined aluminum fixture to limit exposure of the reactant vapors to one face of the membrane (Figure 24a). By precisely manipulating precursor expose time, cycle number, and precursor density, researchers demonstrated how a hydrophilic/superaerophobic Al_2O_3 layer coated on PP membranes could dramatically reduce the size of pressurized air bubbles released into a column of water in an aeration experiment.[496] Fine-bubble aeration processes can significantly reduce the energy demand of aerobic digesters in wastewater treatment plants. The cross-sectional SEM image of this membrane, shown in Figure 24b, reveals a highly polydisperse networked and tortuous pore path morphology. Figure 24c shows the diffusion and nucleation of the precursor and growth of the Al_2O_3 coating. Such studies indicate a complex chemical grafting approach that is cost-effective, fast, and controllable, and could be further implemented to fabricate large-scale Janus membranes targeting many of the applications outlined above.

3.2.3. Customized Nanoparticles as Tailored Solutes. From a fundamental point of view, the effects of water/solid interfaces are amplified in nanoparticle systems due to large surface-to-volume ratios. The properties of such interfaces have been extensively studied in the context of interparticle forces, colloidal stability, and ion adsorption.[497] At low ion concentrations, the nanoparticle/water interface can be described within classical Gouy−Chapman−Stern double layer theory.[498] However, qualitatively different behaviors emerge in concentrated electrolyte solutions where ionic correlations can extend far beyond the electrostatic Debye screening length.[499,500]

https://doi.org/10.1021/acs.chemrev.1c00069
Chem. Rev. 2021, 121, 9450−9501

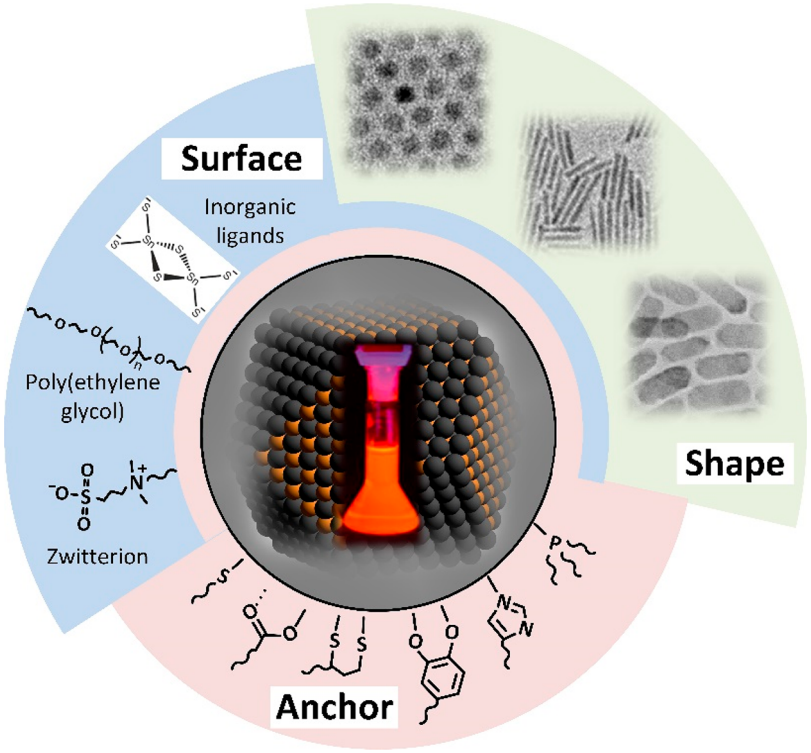

Figure 25. Engineered nanoparticles, for which the shape and capping species can be tailored, are used as tools for fundamental studies of the structure of water/solid interfaces and transport through nanoporous membranes. Nanoparticles are also used in real-world water treatment technologies.

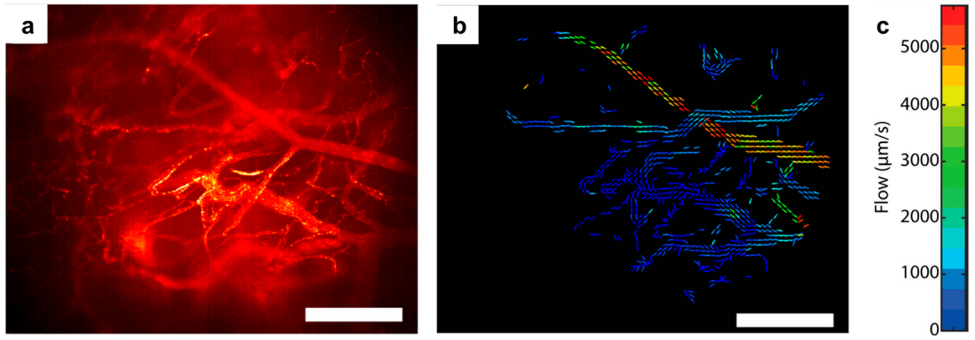

Figure 26. (a) Semiconductor quantum dots (QDs) are convenient fluorescent labels for imaging fluid flows through confined environments, in this case microvascular networks. (b,c) QD probes can be used to measure local fluid velocities and generate flow maps. The scale bars are 300 μm, and the units for velocity are μm/s. Reprinted with permission from ref 509. Copyright 2017 Nature Publishing Group.

Layering of water molecules[501] and formation of alternating layers of positive and negative ions can cause oscillatory pair potentials between nanoparticles,[499,502] not accounted by traditional double-layer approaches.[503] The fundamental understanding of water/solid interfaces at high ion concentrations represents an intriguing unsolved problem.[504]

Nanoparticles are often used to study transport of nanoscale objects in confined environments; however, the picture remains incomplete. The traditional mean-field approaches, such as Fick's laws of diffusion, fail to correctly predict transport on length scales comparable to the dimensions of a diffusing object, calling for experimental studies and further developments of theoretical and computational methods. The experimental studies of transport in nanoconfined environments require nanoscale probes with precisely engineered size, shape, and surface properties. Recent developments of nanoparticle synthesis[505] and surface chemistry[506] facilitated development of such probes for biological imaging[507] and other fields (Figure 25).

In one set of examples, nanoparticle inorganic cores can be made fluorescent, like in the case of semiconductor quantum dots (QDs). Excitation by blue photons generates emission in green, red, or infrared parts of the spectrum. QD size can be controllably varied from about two to tens of nanometers without compromising uniformity and optical properties. Moreover, specially designed nanoparticles (e.g., $NaYF_4$ nanocrystals with Yb^{3+} and Er^{3+} dopants) can efficiently up-convert photon energy generating strong anti-Stokes emission in the visible upon two-photon excitation with near-IR photons.[508] Photon upconversion improves signal-to-noise ratio for optical tracking in transport studies. In general, luminescent nanoparticles are significantly more stable against photobleaching compared with organic dyes, and positions of individual fluorescent nanoparticles can be followed in real time over

https://doi.org/10.1021/acs.chemrev.1c00069
Chem. Rev. 2021, 121, 9450−9501

extended periods of time using confocal microscopy for imaging flow maps and local fluid velocities (Figure 26).[508,509]

The nanoparticle shape can be varied as shown in Figure 25. Switching from spherical to anisotropic fluorescent probes can provide additional information because the photons emitted by nanostructures with anisotropic shape carry information about the orientation of the emitter,[510] providing information not only on the position but also on the orientation of the diffusing or drifting particles. For example, anisotropic rod-like particles spontaneously align in a direction of flow[511] and emit light linearly polarized along the long rod axis,[512] which allows using photon polarizations to reconstruct additional details of the flows patterns.

Fluorescent quantum dots represent just one example of nanoscale probes to study diffusion and transport through slits, pores, and nanofiltration membranes. Similar libraries of nanoscale probes containing high-Z elements (Pt, Au, Bi, etc.) can be used for in situ electron microscopy and X-ray tomography studies.[513] Nanoparticles with superparamagnetic cores (e.g., FePt, Fe_3O_4) are useful as the T_2 contrast agents for in situ position tracking by magnetic resonance imaging.[514]

Besides inorganic cores, the nanoparticle surfaces can be designed to control charge, zeta-potential, hydrophilic and hydrophilic interactions, as well as other characteristics imposed by experimental needs.[506] Typically, this is achieved by organic or inorganic surface ligands containing surface anchor groups covalently bound to other functional groups as shown in Figure 25.

On the applied side, scalable synthesis, engineerability, relatively low costs, and chemical stability make nanoparticles competitive for real-world water treatment technologies.[482,515] For example, titania and hydrous iron oxide nanoparticles are used in commercial products for removal of arsenic and heavy metals from drinking water.[516] The antibacterial properties of silver nanoparticles have been employed for water disinfection,[517] while the photocatalytic properties of titania nanoparticles enable efficient removal of organic pollutants.[515] Besides individual nanoparticles, nanoparticle films have been successfully explored as nearly isoporous ultrafiltration membranes with the efficient rejection cutoff based on the ion size, charge, and polarizability.[489,518]

3.3. Transport Characterization Methods

A comprehensive understanding of ionic and molecular flow through porous media is central to our understanding of transport in confined geometries. Important examples include materials for filtration and capture, selective permeation barriers and catalysis, and biological membranes. Transport studies involving macroscopic membranes are informative, yet lack the detailed multiscale information that governs molecular flux spanning atomic, nano, and meso length-scales. Such information is crucial in energy-water systems as we seek to design more energy-efficient and selective water filtration membranes, with important knowledge still needed for modeling neutral and charged molecular and particulate flow proximal to solid−water interfaces.

The characterization tools employed in transport must necessarily take into account a range of spatio- and dynamic features with sufficient resolution and accuracy. Such features include flows and transport through porous media with a proper treatment of charges, long-range electrostatic and hydrodynamic interactions, and others, particularly in the immediate vicinity of surfaces and pore walls. As described above in the case of BCPs, IDEs provide a means by which self-assembled alternating conducting and insulating domains with dimensions from 5−20 nm (or larger) can be probed over the entire area of the film and through its thickness. Placing the film on an IDE allows for characterization of transport properties by electrochemical impedance spectroscopy, which in turn can be directly compared to simulation and theory.

In nanochannels, the qualitative visualization of flow is by itself a challenging task; quantitative measurement is even more so, as it requires a thorough characterization of all parameters associated with the experiment in order that measurements and theoretical models can be validated against one another. As described below, electron microscopy is one particular tool that could be of great utility, but liquid-based studies remain in their infancy. Advancements in electron microscopy have employed a simple sandwich liquid cell configuration composed of two opposing silicon nitride (SiN_X) windows meticulously separated by a fixed spacer through which media is infused. To enable measurements, researchers much accurately know the inelastic mean free path (IMFP) of electron scattering in water. As described in a recent study, it is important to understand potential differences in the IMFP as measured in water versus crystalline solids.[519] The IMFP for water is an essential parameter for any study that uses electron scattering to study materials in water-based systems. In parallel with electron microscopy cell development, new data acquisition systems to track nanoparticle coordinates during time-resolved flow can be used to understand important time-resolution limits. Current temporal resolutions are limited to ∼30 frames/sec in low-resolution modes and ∼3 frames/sec in higher-resolution operations. These data rates are limited by the detector technology with improvements necessitated to better understand and unlock insights to highly dynamical behavior.

3.3.1. Ion Transport. Membranes innately contain a distribution of pore sizes, structural inhomogeneities, and compositions that can notably influence the emanating fluxes of species in liquid environments. Here, we describe methods for the quantitative measurements of ion transport at the level of a single pore. Building upon the development of scanning tunneling (STM) and atomic force (AFM) microscopy, we describe incisive local probe chemical tools based on scanning electrochemical microscopy, SECM,[520−522] and the powerful variant, SECM-AFM.[523,524] These methods offer unique capabilities for nondestructive quantitative measurements of transport at the level of a single pore, as well as imaging local dynamic changes to membranes under in operando conditions in solution. Critically, such measurements allow one to break the spatial averaging that occurs in more traditional macroscopic measurements where transport is examined globally through membranes sampling a wide palette of pore sizes, geometric shapes, and chemical decoration.

SECM is a scanning probe technique that provides local surface electrochemical information from monitoring reactions between a microelectrode probe and redox mediators in solution. This technique has been widely used to image transport through porous structures. However, SECM is limited by the convolution of the topographic and current signals: The microelectrode probe typically held at a fixed height above the sample surface without accounting for topographic variations in the sample; these variations are therefore reflected in the measured current. Combining SECM with AFM allows for decoupling of the topography and current signals by first acquiring an AFM topographic scan, then retracing this

https://doi.org/10.1021/acs.chemrev.1c00069
Chem. Rev. 2021, 121, 9450−9501

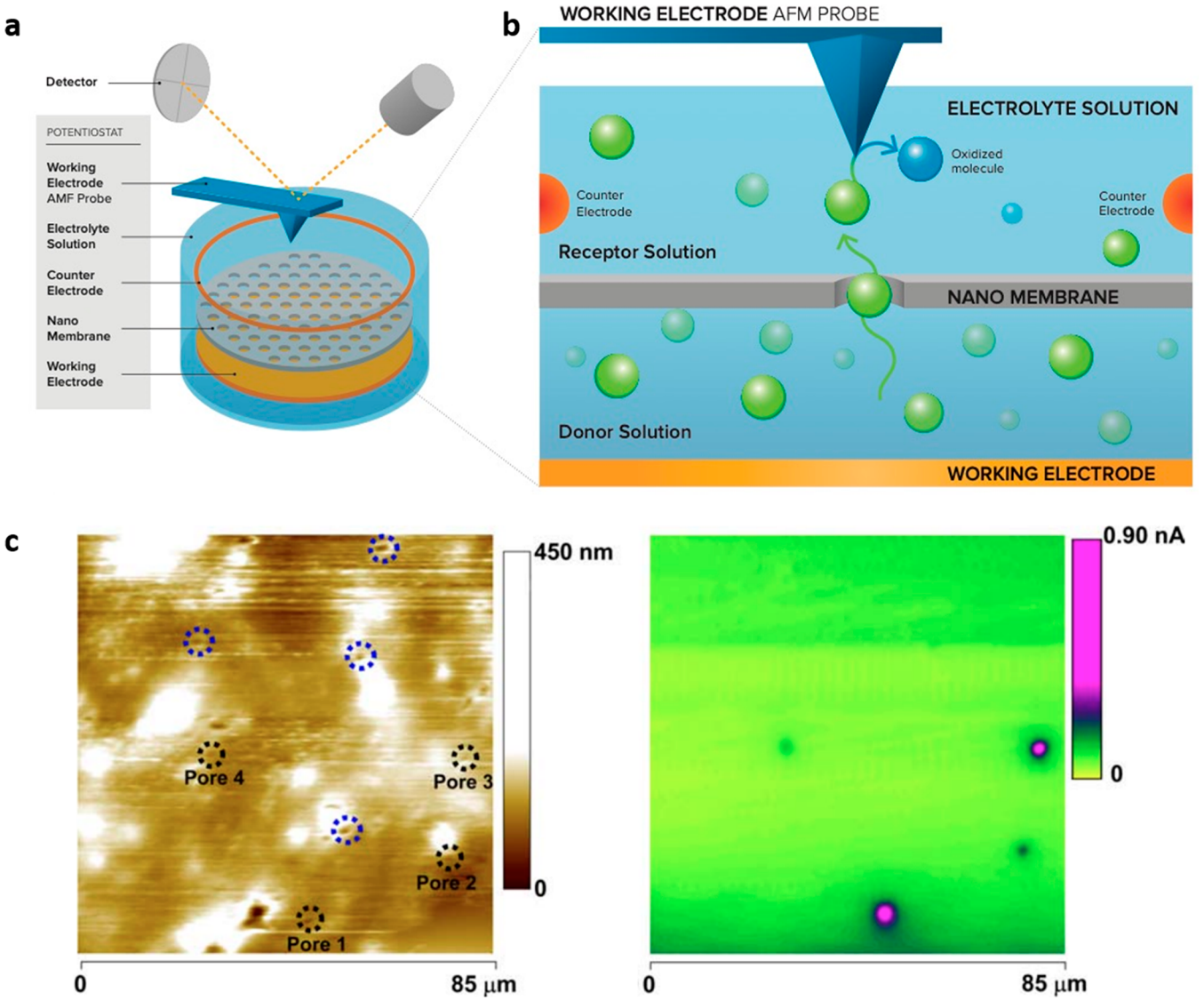

Figure 27. (a) Schematic showing the SECM-AFM: The sample and probe have integrated working electrodes, and an applied bias voltage is set with respect to the reference electrode. Dual SECM-AFM probes allow for integration with an AFM to correlate EC data with local topography. (b) Detection of transport through a single pore by SECM: A porous sample separates a receptor solution from a donor solution containing reduced redox mediators, creating a concentration gradient. Mediators are reduced at the sample working electrode (yellow) and oxidized at the probe working electrode (blue), where they are detected. (c) Topography (left) and current (right) images of redox mediator transport through a PET membrane. Of the eight pores identified in the topography image, only four (numbered and circled in black) were active to transport as shown by the current measurements. This study demonstrates the power of localized imaging acquired by SECM-AFM in characterizing transport through membranes. Reproduced with permission 523. Copyright 2005 Elsevier B.V.

topography at a constant distance above the surface while measuring the current signal. Combined SECM-AFM can thus provide current measurements that are more representative of the sample surface, enabling more complex characterization of membrane activity. Essential features of the overall electrochemical setup in SECM-AFM are shown schematically in Figure 27a, applicable to conducting as well as insulating materials. Here, we discuss a selection of literature highlighting the use of both SECM and SECM-AFM to characterize transport through porous media.

SECM studies allow for the examination of a single pore or well-characterized membrane regions,[525−529] providing information for direct comparison with theory and simulations that seek to model transport on the atomic and nanoscales, the key length-scales that govern mass transport through such media.[530] Figure 27b illustrates the ability to locate and sample fluxes emanating from a single pore. The voltage bias between the sample working electrode and probe working electrode can be adjusted to measure diffusive or iontophoretic transport. In diffusive transport, the voltage on the sample and probe working electrodes are the same magnitude but of opposite signs, allowing measurement of the diffusion of redox mediators through a pore. Iontophoretic transport is driven by an applied voltage gradient. Further extension of these methods allows one to examine, for example, nanotextured electrodes,[531] single-nanoparticle catalysis,[532] channeled transport architectures,[533] and transport through pores in biologically relevant membranes.[534−536]

In addition to providing a clear assessment of the relative contributions arising from diffusive and iontophoretic transport, SECM offers another key advantage: It offers chemical selectivity due to the ability to sweep operative electrode

https://doi.org/10.1021/acs.chemrev.1c00069
Chem. Rev. 2021, 121, 9450−9501

potentials, a capability not intrinsic to another incisive method, scanning ion-conductance microscopy (SICM).[537] There are other notable advantages that the local nature of SECM measurements provide to studies of transport that go beyond new information on flow in confinement. The local nature of SECM allows decoupling of the intrinsic effects of nanoconfinement from the redox activity due to surface geometry.[531] Additionally, utilization of this technique, and extension into combined SECM-AFM, allows for characterization of active pore densities of typical and novel filtration membranes. Membrane features that appear to be pores active to transport in AFM topography images do not necessarily correspond to active pores by SECM current measurements, as shown in an example of combined SECM-AFM images of membranes in Figure 27c.[523] Mapping active versus inactive pores on a given membrane surface provides valuable information on where synthesis methods can be improved for the development of more efficient membranes. Combined SECM-AFM is highly applicable to more broadly characterizing filtration selectivity and understanding the effect of novel film architectures designed for improvements in efficient flow while maintaining desired species rejection rates and sensitivity to fouling. In sum, SECM in concert with correlated AFM imaging provides an arguably unique information-rich probe of flows emanating from isolated pores and well-characterized local regions of membrane materials. These data on chemically and structurally specific structures allow for critical tests of our fundamental understanding of transport in nanostructures and confinement.

3.3.2. Electron Microscopy. The study of particles in liquids has involved a variety of traditional experimental protocols[538−540] over the years, the majority of these assessing macroscopic properties by measuring ensembles of particles using spatially averaging probes with dimensions in excess of 100 nm. While these techniques give insight into macro-to-mesoscopic behavior, ultimately it is the individual nanoparticle, defined by its size, shape, chemistry, and its interaction with its local environment, that controls the interactions of interest. The goals of the transport experiments described herein are to study the dynamics of diffusion and flow of precharacterized particles during controlled/restricted flow in micro-to-nano scale pores and channels at high spatial resolution and sensitivity.

Characterizing individual nanoparticles has for decades been a key strength of scanning, transmission, and analytical electron microscopy (SEM, TEM, AEM), where micro-to-nano-to-atomic scale resolution of materials is routine. Until recently, this level of resolution has only been achieved under conditions involving high vacuum due to the inherent scattering of electrons through "media," a clear impediment to studies in liquids using electrons. With the development of ultrathin (∼40−80 nm) silicon nitride windows and liquid cells for TEM, environmental studies of nanoparticles in media have been realized.[541] The SiN_x windows and correspondingly thin liquids surrounding the nanoparticles allow the electron beam to propagate with minimal scattering and enable high-resolution imaging and characterization of the particles within the enclosed environment (gaseous or liquid). This facilitates either static or dynamic studies where the nanoparticles are completely suspended or encapsulated between the windows.[542−547] An example is shown in Figure 28 where 15 nm Au particles and their motion in water are illustrated. This state-of-the-art experimental technology is challenging, because of the need for absolute characterization of the nanoparticles as well as their immediate environment.[548−553] To this end, a custom nanochannel microarray system has been developed for use in the PicoProbe AEM Instrument of Argonne National Laboratory. These SiN_x window nanochannel arrays (Figure 29) are lithographically engineered into silicon wafers[554] and can have configurations that consist of linear, nonlinear, and/or intersecting chambers (1−5 μm wide ×300 μm long × (30−200) nm high). Selected nanomaterials and media can be flowed or mixed in these channels through the judicious use of external feed lines. In contrast to the two-chip sandwich style in situ holders or graphene liquid cell systems, the nanochannel system is fully characterized and allows one to elicit quantitative measures of Brownian motion, flow, diffusion, and interactions and aggregation of the selected nanoparticle systems. A further enhancement that is implementable is the coating of the walls of the nanochannels using ALD, thus enabling the study nanoparticle/interface chemical interactions. Through the use of the advanced analytical detectors on the PicoProbe, one can monitor elemental redistributions that may (intentionally or otherwise) occur during extended investigations.[548,553]

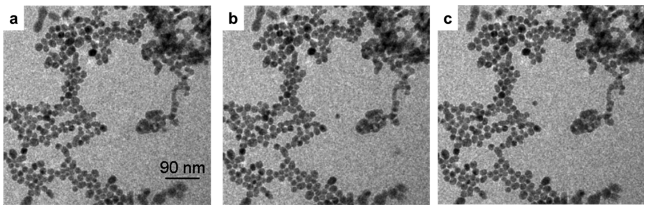

Figure 28. Time sequence of TEM images of 15 nm Au particles in liquid water. In this three-frame sequence, the majority of the Au nanoparticles are static as they have become tethered to the silicon nitride window. In the center (b) and right (c) sequence of two consecutive frames, an isolated Au particle is tracked moving across the field of view under the influence of a generated liquid pressure wave at a rate of ∼2.5 μm/s.

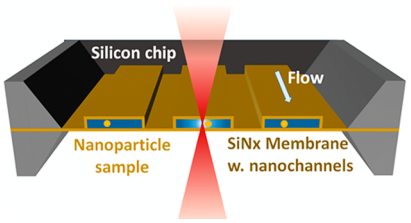

Figure 29. Schematic cross-section of nanochannel silicon chip. Nanochannels are shown in blue (filled with water), silicon nitride in brown, silicon in gray, and the electron beam in red. Dimensions and configurations of the nanochannel are lithographically defined and range from 1 to 5 μm wide, 100−300 μm long, 30−200 nm high.

In preliminary studies, the mean inner potential of liquid water ($V_{o,1}$ = +4.48 ± 0.19 V) was measured,[555] as well as the inelastic mean free path of electrons in water ($E_{m,water}$ = 7.5 ± 0.2 eV @ E_0 = 300 keV).[519] Flow and diffusion measurements on spherical and complex structured nanoparticles are ongoing, with indications of interactions with the nanochannel walls being important. Such measurements provide critical baseline data that feed into theory and modeling operations of confined geometric transport, as well as the in situ liquid cell EM community worldwide.

3.4. Simulations of Transport in Confined Environments

To date, predictive models are not able to explain the entire range of flow and transport phenomena that arise in porous

https://doi.org/10.1021/acs.chemrev.1c00069
Chem. Rev. 2021, 121, 9450−9501

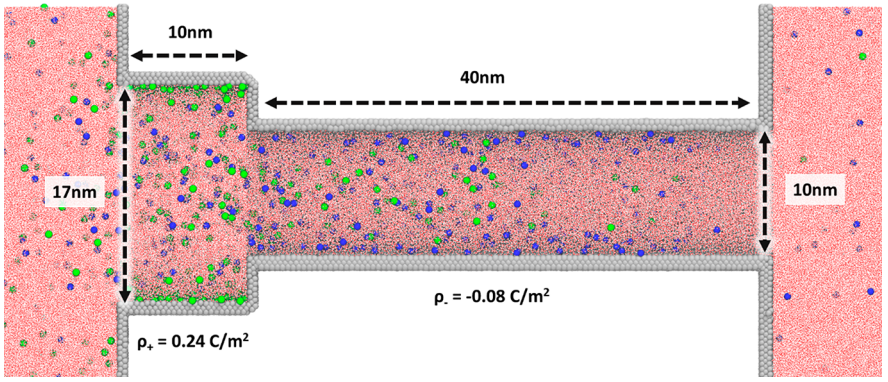

Figure 30. Representative configuration of an aqueous electrolyte solution flowing through the pore of a Janus membrane. Ions sizes in green and blue are exaggerated to enhance visibility, explicit water molecules are rendered in red.

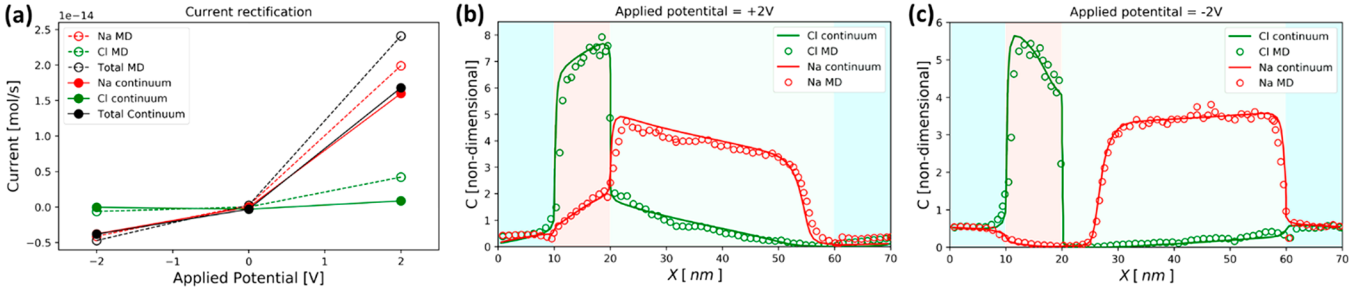

Figure 31. Comparison between MD and continuum calculations. a) Ionic current rectification, full lines/markers represent Poisson−Nernst−Planck coupled with Navier−Stokes, while empty markers/dashed lines are MD results. Ionic concentration profile for the active (b) and inactive version of the pore (c), normalized by the concentration in the reservoir. Here lines correspond to the continuum model and empty circles to MD. The light-blue background depicts the reservoir of the system, while the pink and green correspond to the positively and negatively charged walls regions, respectively.

media, particularly when charges play a significant role. Efforts to develop structure−property relationships have also been severely impeded by the difficulty in quantitatively characterizing structure over (1) macroscopic sample volumes over which transport properties may be measured, (2) the full range of critical characteristic dimensions within that volume that span the molecular to nanometer to micron to millimeter length scales, and (3) the challenges associated with sampling the relatively small flow rates that are routinely accessed in experiments. Statistical or averaged structural descriptions of porous media are inadequate to capture the essential roles played by pore connectivity, defects, topology, roughness, chemistry, and charge distribution at all the relevant length scales.

Fueled by recent advances in sampling techniques, numerical methods, and computer power, it is now possible to address some of the questions outlined in this Review at the level of atomistic and coarse-grained molecular dynamic simulations (MD). As an example, Figure 30 shows a representative configuration of an aqueous electrolyte solution flowing through the pore of a Janus membrane. The implementation of MD simulations in the context of the transport phenomena reviewed in this section have been proven to be beneficial, as exemplified below, to scrutinize and improve mean-field theoretical approaches or to resolve transport mechanisms that are able to explain experimental observations.

3.4.1. Atomistic and Mean-Field Simulations. As discussed earlier, the application of a voltage across Janus membranes such as the one illustrated in Figure 30 can be used to extract energy relying on the flows and inhomogeneities that arise in such a system. At the length scales of interest, the aqueous solvent can no longer be represented as a hydrodynamic continuum. The hydrogen-bonding network of the solution is disrupted not only by the ions, which adopt distinct, inhomogeneous profiles, but also by the presence of the confining charged walls. However, because of the large design space for ion-rectifying Janus membranes (pore geometry, surface charge density, charge gradient shape, etc.), it is still impractical to rely exclusively on full MD simulations to explore the entire range of possibilities. Under these conditions, MD simulations could be used as a benchmark for the validation of mean-field simulations which can, in turn, be applied to a more systematical exploration of the design space.

As summarized in Figure 31, mean-field simulations applied to the study of Janus membranes like the one illustrated in Figure 30, provide a qualitative level of agreement with simulations at the atomic level. Specifically, the agreement is almost quantitative for the static distribution of charges in the system as well as for the current rectification and ion selectivity capabilities. Solving Poisson−Nernst−Planck (PNP) alone, without considering the convection effect introduced by the asymmetrical ion mobility, fails to accurately describe the "active" version of the rectifying membrane. Comparison between MD and continuum simulations has also shown that even when the coincidence is greatly improved if PNP is coupled with Navier−Stokes equations, there are still some potentially important discrete effects that are not captured in the continuum model. Remarkably, most of the ionic conduction seen in the MD simulation occurs near the walls of the pore, but that is precisely the region that is most poorly depicted by the continuum model. Molecularly, ionic conduction is strongly directed by the influence of the preferential solvent structuring

https://doi.org/10.1021/acs.chemrev.1c00069
Chem. Rev. 2021, 121, 9450−9501

and orientation imposed by the surface, and the effect of the finite size and correlations between the particles of the walls, the solvent, and the ions. On the other hand, in the continuum, not only is the molecular description missing, but the enforced boundary conditions might not be entirely appropriate. In the case study of nanometric Janus membranes, the apparent exceedingly good agreement between MD and mean-field simulations is partially due to a cancelation of errors where the continuum overestimates ion concentration near the walls but at the same time enforces zero velocity at the boundary.

3.4.2. Ion-Conducting Polymers. All-atoms molecular dynamic simulations have proven to be extremely valuable for elucidating the mechanisms of ionic transport, which ultimately leads to elements for rational design of materials. As mentioned along the corpus of this Review, ionic transport properties are very sensitive to the local environment of the charges. This is especially important, but extremely challenging to model in systems of strongly confining, heterogeneous settings like the ones we find in self-assembled polymeric matrices.

A beautiful example of how experimental and simulation techniques complement one another is provided by the disambiguation of the underlying mechanism for the ionic mobility enhancement in poly(2-vinylpyridine)(P2VP) functionalized with *N*-methylpyridinium iodide (NMP+I−)—a system of particular interest due to its amenability in applications involving directed self-assembly[556] (Figure 32).

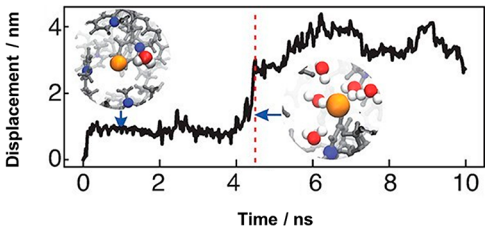

Figure 32. Ion displacement vs time. The red dashed line indicates the switch in the dominating interaction between the ion in the surroundings from ion-polymer backbone (left) to ion−water (right). Reprinted with permission from ref 556. Copyright 2020 American Chemical Society.

Experimental evidence has shown that functionalized P2VP matrices exhibit improved ionic conduction when the water content of the sample is increased from 0 to around 25%. Interestingly, under the same conditions of the experiment, the glass transition temperature of the sample is shown to concomitantly decrease with the water content. In such circumstances, one can arguably attribute the increment of ionic conduction simply to the enhanced polymer dynamic due to the plasticizing effect of the water addition. The MD simulations, however, revealed that, even though water indeed lubricates the contact between the polymer chains and reduces the glass transition temperature of the polymer, ionic conduction is actually improved due to the reduced interaction time between the diffusing ions and the polymer, as a consequence of a more abundant ion−water interaction in the swollen sample.[556]

4. CONCLUSION

This Review has highlighted the importance of interfaces, and specifically interfacial interactions, in water-energy systems, and how by controlling these interactions, one can influence three important areas of fundamental and applied significance: (i) adsorption, (ii) reactivity, and (iii) transport. Such phenomena are central to a broad array of scientific and technological processes in disciplines as varied as heterogeneous catalysis and electrochemistry, life sciences and biomedical applications, environmental and geosciences. While researchers continue to make important progress in advancing our understanding of such phenomena, driving new technological developments in Advanced Materials for Energy-Water Systems, much remains to be learned. Numerous fundamental questions remain unanswered despite decades of study into the central role of water/solid interfaces. From molecular-scale questions involving the nuances of water's hydrogen bonding at interfaces with electrolyte solutions, to the interfacial transfer of energy in the form of protons and electrons, to the adsorption and chemical reactivity of solutes at structured and confined interfaces, and many other particulars connected to water, the solid−water interface is undoubtedly complex. As this Review has illustrated, unraveling these complexities in their entirety is only possible when synthesis, characterization, and simulation/theory are combined synergistically.

Further advances that improve our understanding and efficient use of water and energy will remain of critical importance, and developing a deeper understanding of the molecular- and mesoscale phenomena at water/solid interfaces is an essential activity for driving future innovation and addressing grand challenges in supplying sufficient fit-for-purpose water in the future. As noted by Leonardo da Vinci, "water is the driving force of all nature."[557] In this Review, we have focused on interfaces as a central governing principle and how much of the unique behavior of water and aqueous systems stems from what happens at interfaces. With the emergence of newfound capabilities to experimentally probe and computationally model these complex systems, the chemistry, physics, and materials science of aqueous solution/solid interfaces has become one of the most exciting fields in science.

AUTHOR INFORMATION

Corresponding Author

Seth B. Darling − *Advanced Materials for Energy-Water Systems (AMEWS) Energy Frontier Research Center (EFRC), Center for Molecular Engineering, and Chemical Sciences and Engineering Division, Argonne National Laboratory, Lemont, Illinois 60439, United States; Pritzker School of Molecular Engineering, University of Chicago, Chicago, Illinois 60637, United States;* orcid.org/0000-0002-5461-6965; Email: darling@anl.gov

Authors

Edward Barry − *Advanced Materials for Energy-Water Systems (AMEWS) Energy Frontier Research Center (EFRC), Applied Materials Division, and Center for Molecular Engineering, Argonne National Laboratory, Lemont, Illinois 60439, United States*

Raelyn Burns − *Advanced Materials for Energy-Water Systems (AMEWS) Energy Frontier Research Center (EFRC) and Applied Materials Division, Argonne National Laboratory, Lemont, Illinois 60439, United States*

Wei Chen − *Advanced Materials for Energy-Water Systems (AMEWS) Energy Frontier Research Center (EFRC), Materials Science Division, and Center for Molecular Engineering, Argonne National Laboratory, Lemont, Illinois 60439, United States; Pritzker School of Molecular*

https://doi.org/10.1021/acs.chemrev.1c00069
Chem. Rev. 2021, 121, 9450−9501

Engineering, University of Chicago, Chicago, Illinois 60637, United States; orcid.org/0000-0001-8906-4278

Guilhem X. De Hoe − *Advanced Materials for Energy-Water Systems (AMEWS) Energy Frontier Research Center (EFRC), Materials Science Division, and Center for Molecular Engineering, Argonne National Laboratory, Lemont, Illinois 60439, United States; Pritzker School of Molecular Engineering, University of Chicago, Chicago, Illinois 60637, United States;* orcid.org/0000-0002-0996-7491

Joan Manuel Montes De Oca − *Advanced Materials for Energy-Water Systems (AMEWS) Energy Frontier Research Center (EFRC), Argonne National Laboratory, Lemont, Illinois 60439, United States; Pritzker School of Molecular Engineering, University of Chicago, Chicago, Illinois 60637, United States;* orcid.org/0000-0002-3744-5287

Juan J. de Pablo − *Advanced Materials for Energy-Water Systems (AMEWS) Energy Frontier Research Center (EFRC) and Materials Science Division, Argonne National Laboratory, Lemont, Illinois 60439, United States; Pritzker School of Molecular Engineering, University of Chicago, Chicago, Illinois 60637, United States;* orcid.org/0000-0002-3526-516X

James Dombrowski − *Advanced Materials for Energy-Water Systems (AMEWS) Energy Frontier Research Center (EFRC), Argonne National Laboratory, Lemont, Illinois 60439, United States; Department of Chemical and Biological Engineering, Northwestern University, Evanston, Illinois 60208, United States*

Jeffrey W. Elam − *Advanced Materials for Energy-Water Systems (AMEWS) Energy Frontier Research Center (EFRC), Applied Materials Division, and Center for Molecular Engineering, Argonne National Laboratory, Lemont, Illinois 60439, United States;* orcid.org/0000-0002-5861-2996

Alanna M. Felts − *Advanced Materials for Energy-Water Systems (AMEWS) Energy Frontier Research Center (EFRC), Argonne National Laboratory, Lemont, Illinois 60439, United States; Department of Chemistry, Northwestern University, Evanston, Illinois 60208, United States*

Giulia Galli − *Advanced Materials for Energy-Water Systems (AMEWS) Energy Frontier Research Center (EFRC) and Materials Science Division, Argonne National Laboratory, Lemont, Illinois 60439, United States; Pritzker School of Molecular Engineering, University of Chicago, Chicago, Illinois 60637, United States;* orcid.org/0000-0002-8001-5290

John Hack − *Advanced Materials for Energy-Water Systems (AMEWS) Energy Frontier Research Center (EFRC), Argonne National Laboratory, Lemont, Illinois 60439, United States; Department of Chemistry, University of Chicago, Chicago, Illinois 60637, United States;* orcid.org/0000-0003-0042-0921

Qiming He − *Advanced Materials for Energy-Water Systems (AMEWS) Energy Frontier Research Center (EFRC), Materials Science Division, and Center for Molecular Engineering, Argonne National Laboratory, Lemont, Illinois 60439, United States; Pritzker School of Molecular Engineering, University of Chicago, Chicago, Illinois 60637, United States;* orcid.org/0000-0002-2652-3200

Xiang He − *Advanced Materials for Energy-Water Systems (AMEWS) Energy Frontier Research Center (EFRC) and Chemical Sciences and Engineering Division, Argonne National Laboratory, Lemont, Illinois 60439, United States;* orcid.org/0000-0002-2427-9048

Eli Hoenig − *Advanced Materials for Energy-Water Systems (AMEWS) Energy Frontier Research Center (EFRC), Argonne National Laboratory, Lemont, Illinois 60439, United States; Pritzker School of Molecular Engineering, University of Chicago, Chicago, Illinois 60637, United States*

Aysenur Iscen − *Advanced Materials for Energy-Water Systems (AMEWS) Energy Frontier Research Center (EFRC), Argonne National Laboratory, Lemont, Illinois 60439, United States; Department of Chemical and Biological Engineering, Northwestern University, Evanston, Illinois 60208, United States;* orcid.org/0000-0002-9609-4552

Benjamin Kash − *Pritzker School of Molecular Engineering, University of Chicago, Chicago, Illinois 60637, United States*

Harold H. Kung − *Advanced Materials for Energy-Water Systems (AMEWS) Energy Frontier Research Center (EFRC), Argonne National Laboratory, Lemont, Illinois 60439, United States; Department of Chemical and Biological Engineering, Northwestern University, Evanston, Illinois 60208, United States;* orcid.org/0000-0001-9599-0155

Nicholas H. C. Lewis − *Advanced Materials for Energy-Water Systems (AMEWS) Energy Frontier Research Center (EFRC), Argonne National Laboratory, Lemont, Illinois 60439, United States; Department of Chemistry, University of Chicago, Chicago, Illinois 60637, United States;* orcid.org/0000-0002-2554-0199

Chong Liu − *Advanced Materials for Energy-Water Systems (AMEWS) Energy Frontier Research Center (EFRC), Argonne National Laboratory, Lemont, Illinois 60439, United States; Pritzker School of Molecular Engineering, University of Chicago, Chicago, Illinois 60637, United States;* orcid.org/0000-0003-4851-7888

Xinyou Ma − *Advanced Materials for Energy-Water Systems (AMEWS) Energy Frontier Research Center (EFRC), Argonne National Laboratory, Lemont, Illinois 60439, United States; Department of Chemistry, University of Chicago, Chicago, Illinois 60637, United States;* orcid.org/0000-0002-0923-8758

Anil Mane − *Advanced Materials for Energy-Water Systems (AMEWS) Energy Frontier Research Center (EFRC) and Applied Materials Division, Argonne National Laboratory, Lemont, Illinois 60439, United States*

Alex B. F. Martinson − *Advanced Materials for Energy-Water Systems (AMEWS) Energy Frontier Research Center (EFRC), Materials Science Division, and Center for Molecular Engineering, Argonne National Laboratory, Lemont, Illinois 60439, United States;* orcid.org/0000-0003-3916-1672

Karen L. Mulfort − *Advanced Materials for Energy-Water Systems (AMEWS) Energy Frontier Research Center (EFRC) and Chemical Sciences and Engineering Division, Argonne National Laboratory, Lemont, Illinois 60439, United States;* orcid.org/0000-0002-3132-1179

Julia Murphy − *Advanced Materials for Energy-Water Systems (AMEWS) Energy Frontier Research Center (EFRC), Argonne National Laboratory, Lemont, Illinois 60439, United States; Department of Chemistry, University of Chicago, Chicago, Illinois 60637, United States*

Kristian Mølhave − *Advanced Materials for Energy-Water Systems (AMEWS) Energy Frontier Research Center (EFRC), Argonne National Laboratory, Lemont, Illinois 60439, United States; Technical University of Denmark, Lyngby, Hovedstaden 2800, DK Denmark;* orcid.org/0000-0002-6493-2750

Paul Nealey − *Advanced Materials for Energy-Water Systems (AMEWS) Energy Frontier Research Center (EFRC) and Materials Science Division, Argonne National Laboratory,*

https://doi.org/10.1021/acs.chemrev.1c00069
Chem. Rev. 2021, 121, 9450−9501

Lemont, Illinois 60439, United States; Pritzker School of Molecular Engineering, University of Chicago, Chicago, Illinois 60637, United States; orcid.org/0000-0003-3889-142X

Yijun Qiao − *Advanced Materials for Energy-Water Systems (AMEWS) Energy Frontier Research Center (EFRC), Materials Science Division, and Center for Molecular Engineering, Argonne National Laboratory, Lemont, Illinois 60439, United States*

Vepa Rozyyev − *Advanced Materials for Energy-Water Systems (AMEWS) Energy Frontier Research Center (EFRC) and Applied Materials Division, Argonne National Laboratory, Lemont, Illinois 60439, United States*

George C. Schatz − *Advanced Materials for Energy-Water Systems (AMEWS) Energy Frontier Research Center (EFRC), Argonne National Laboratory, Lemont, Illinois 60439, United States; Department of Chemistry, Northwestern University, Evanston, Illinois 60208, United States;* orcid.org/0000-0001-5837-4740

Steven J. Sibener − *Advanced Materials for Energy-Water Systems (AMEWS) Energy Frontier Research Center (EFRC), Argonne National Laboratory, Lemont, Illinois 60439, United States; Department of Chemistry, University of Chicago, Chicago, Illinois 60637, United States;* orcid.org/0000-0002-5298-5484

Dmitri Talapin − *Advanced Materials for Energy-Water Systems (AMEWS) Energy Frontier Research Center (EFRC), Argonne National Laboratory, Lemont, Illinois 60439, United States; Department of Chemistry, University of Chicago, Chicago, Illinois 60637, United States;* orcid.org/0000-0002-6414-8587

David M. Tiede − *Advanced Materials for Energy-Water Systems (AMEWS) Energy Frontier Research Center (EFRC) and Chemical Sciences and Engineering Division, Argonne National Laboratory, Lemont, Illinois 60439, United States;* orcid.org/0000-0002-2784-4954

Matthew V. Tirrell − *Advanced Materials for Energy-Water Systems (AMEWS) Energy Frontier Research Center (EFRC), Materials Science Division, and Center for Molecular Engineering, Argonne National Laboratory, Lemont, Illinois 60439, United States; Pritzker School of Molecular Engineering, University of Chicago, Chicago, Illinois 60637, United States;* orcid.org/0000-0001-6185-119X

Andrei Tokmakoff − *Advanced Materials for Energy-Water Systems (AMEWS) Energy Frontier Research Center (EFRC), Argonne National Laboratory, Lemont, Illinois 60439, United States; Department of Chemistry, University of Chicago, Chicago, Illinois 60637, United States;* orcid.org/0000-0002-2434-8744

Gregory A. Voth − *Advanced Materials for Energy-Water Systems (AMEWS) Energy Frontier Research Center (EFRC), Argonne National Laboratory, Lemont, Illinois 60439, United States; Department of Chemistry, University of Chicago, Chicago, Illinois 60637, United States;* orcid.org/0000-0002-3267-6748

Zhongyang Wang − *Advanced Materials for Energy-Water Systems (AMEWS) Energy Frontier Research Center (EFRC), Argonne National Laboratory, Lemont, Illinois 60439, United States; Pritzker School of Molecular Engineering, University of Chicago, Chicago, Illinois 60637, United States*

Zifan Ye − *Advanced Materials for Energy-Water Systems (AMEWS) Energy Frontier Research Center (EFRC), Argonne National Laboratory, Lemont, Illinois 60439, United States; Pritzker School of Molecular Engineering, University of Chicago, Chicago, Illinois 60637, United States*

Murat Yesibolati − *Advanced Materials for Energy-Water Systems (AMEWS) Energy Frontier Research Center (EFRC), Argonne National Laboratory, Lemont, Illinois 60439, United States; Technical University of Denmark, Lyngby, Hovedstaden 2800, DK Denmark;* orcid.org/0000-0002-0053-4147

Nestor J. Zaluzec − *Advanced Materials for Energy-Water Systems (AMEWS) Energy Frontier Research Center (EFRC) and Photon Sciences Directorate, Argonne National Laboratory, Lemont, Illinois 60439, United States*

Complete contact information is available at: https://pubs.acs.org/10.1021/acs.chemrev.1c00069

Notes

The authors declare no competing financial interest.

Biographies

Edward Barry is a scientist at Argonne National Laboratory and a fellow of the University of Chicago Consortium for Advanced Science and Engineering (CASE). Edward received his undergraduate degree from Fordham University and his doctorate from Brandeis University. His group's research focuses on general classes of materials design and assembly, with a recent emphasis on sorbents and membranes, and new technology development for pollutant treatment in water. Following postdoctoral studies at the University of Chicago, Edward began his work at Argonne National Laboratory as Named Fellow in the Center for Nanoscale Materials (CNM). Barry is a former recipient of the 2010 Cozzarelli Prize from the *Proceedings of the National Academy of Sciences*, and 2017 R&D 100 Awards.

Raelyn Burns is a recent physics graduate with a focus in materials science and manufacturing at Jackson State University. As a summer research intern, Raelyn completed work with the Advanced Materials for Energy-Water Systems (AMEWS) EFRC during the summer of 2020. Her interests span laboratory research, having completed a number of different projects in different capacities including water purification, and photoconductivity, as well as programs geared towards education and STEM.

Wei Chen is a chemist in the Center for Molecular Engineering and the Materials Science Division at Argonne National Laboratory. His group's research is focused on the structural and dynamic characterization of ionic polymers with well-defined microstructure and architecture through neutron and X-ray scattering techniques for achieving antifouling water treatment. He has published over 100 scientific articles.

Guilhem started his research career working with Prof. Philip Costanzo at California Polytechnic State University in San Luis Obispo, CA. After earning his B.S. in Chemistry, he went on to get his Ph.D. in Chemistry at the University of Minnesota and worked on sustainable plastics with Prof. Marc Hillmyer. Guilhem then moved to Chicago to work as a postdoctoral researcher on zwitterionic polymers with Prof. Matthew Tirrell, splitting his time between Argonne National Laboratory and the University of Chicago. He is now a research fellow at the University of Manchester working with Prof. Michael Shaver.

Joan Manuel Montes de Oca is a Postdoctoral Researcher at the Pritzker School of Molecular Engineering at University of Chicago. He received his Ph.D. in Chemistry at the Universidad Nacional del Sur, in Buenos Aires, Argentina. Joan's dissertation focused on water structure and dynamics at the nanoscale, in contexts ranging from supercooled and glassy regimes, to strong biological or inorganic confinement. His

current research interests are primarily centered on the molecular mechanisms underlying ionic transport in membranes and pores, with special emphasis on the explicit role of water.

Juan de Pablo is a Liew Family Professor in Molecular Engineering at the University of Chicago, Vice President for National Laboratories, Science Strategy, Innovation, and Global Initiatives and holds a Senior Scientist position at Argonne National Laboratory. His research focuses on polymers, biological macromolecules, and liquid crystals, a diverse class of materials widely used in many fields of engineering. Juan is a leader in developing molecular models, computer simulations of complex processes over wide ranges of length and time scales, and artificial-intelligence-enhanced methods to design advanced materials systems. He has coauthored over 600 papers, a textbook, and over 20 patents.

James P. Dombrowski is a postdoctoral researcher at Worcester Polytechnic Institute with Prof. Pratap M. Rao and former postdoctoral researcher at Northwestern University with Prof. Harold H. Kung. His research focuses on synthesis of materials with an emphasis on molecular precursor methodologies and air-free manipulations. He completed his doctoral studies under the guidance of Profs. T. Don Tilley and Alexis T. Bell at the University of California−Berkeley on thermolytic molecular precursors as models and precursors to metal silicate materials. He has published six technical journal articles.

Jeffrey W. Elam is a Senior Chemist and Group Leader in the Applied Materials Division at Argonne National Laboratory and a Thrust Leader in the Advanced Materials for Energy-Water Systems (AMEWS) Energy Frontier Research Center (EFRC). His research focuses on the science and technology of atomically precise films, developing new synthetic methods for functionalizing surfaces, and applying these methods to challenging problems such as water treatment. Jeff has published over 300 manuscripts, holds 46 US patents in thin-film coating technology, and has won five R&D100 Awards for his inventions.

Alanna Felts is a third-year Ph.D. candidate in the Schatz group at Northwestern University. Her research focuses on the behavior of ions and hydrogen bonding in electrolytic solution at various interfaces. She obtained her bachelor's degree at the University of California, Irvine, where she worked with Professor Apkarian on plasmon driven chemistry in gold nanosphere assemblies.

Giulia Galli is the Liew Family Professor of Electronic Structure and Simulations in the Pritzker School of Molecular Engineering and Professor of Chemistry at the University of Chicago. She also holds a Senior Scientist position at Argonne National Laboratory, where she is the director of the Midwest Integrated Center for Computational Materials. Her research activity is focused on the development and use of theoretical and computational methods to understand and predict the properties and behavior of materials (solids, liquids, and nanostructures) from first principles.

John Hack received his B.S. in Physics in 2017 from the University of Virginia. He is currently a Ph.D. student in the laboratory of Andrei Tokmakoff at the University of Chicago. His research interests include studying the hydrogen-bonding structure and dynamics of water under confinement.

Qiming He is a research professional at the Pritzker School of Molecular Engineering, the University of Chicago. He is also a member of the Advanced Materials for Energy-Water Systems (AMEWS) Energy Frontier Research Center (EFRC). His research focuses on tailoring of surface chemistry on topologically complex substrates to understand adsorption in aqueous systems using zwitterionic polymers.

Xiang He is a Postdoctoral Appointee at the Advanced Materials for Energy-Water Systems (AMEWS) Energy Frontier Research Center (EFRC). His current research interests include (1) using high-energy X-ray scattering with pair distribution function to decipher the structures of functional materials as well as solvation structures, and (2) applying surface-bound molecular catalysts for the electrochemical water remediation. He earned his Ph.D. degree from Virginia Commonwealth University by investigating the structural design and environmental applications of metal−organic frameworks.

Eli Hoenig is a doctoral student in the Pritzker School of Molecular Engineering at the University of Chicago. Advised by Professor Chong Liu, he studies the behavior of ions and water molecules under nanometer-scale confinement. Using two-dimensional materials as building blocks, he also engineers ion-selective channels and membranes. His publications to date have covered topics such as precision spectroscopy, ultrafast lasers, and nanofluidics.

Aysenur Iscen completed her Ph.D. in Chemical and Biological Engineering under supervision of Prof. George C. Schatz at Northwestern University in 2019, where she worked on computational methods to develop bioinspired materials through her involvement in collaborative research centers. She earned her B.S. degree in Chemical Engineering from Yeditepe University in Istanbul, Turkey. She is currently working as a postdoctoral researcher with Prof. Kurt Kremer at the Max Planck Institute for Polymer Research in Mainz, Germany.

Benjamin Kash is an undergraduate at the University of Chicago studying chemistry and molecular engineering. He currently works in the Amanchukwu Lab with projects focusing on the electrocatalytic reduction of carbon dioxide. Following graduation, Ben intends to pursue a Ph.D. to further explore his interests in renewable energy and the energy-water nexus. He has published in *Inorganica Chimica Acta* and the *New Journal of Chemistry*.

Harold H. Kung is Walter P. Murphy Professor of Chemical and Biological Engineering at Northwestern University. His group's research focuses on improving efficiencies of chemical transformations for sustainability, reducing emissions and utilization of natural resources through the discovery and development of new catalyst, energy storage materials, catalytic processes. Harold has published 300 scientific articles, one monograph, and holds 10 patents.

Nicholas H.C. Lewis is a Postdoctoral Scholar in the James Franck Institute at the University of Chicago. He works in the group of Andrei Tokmakoff and his research primarily involves using ultrafast spectroscopy techniques to study water and solvation.

Chong Liu is the Neubauer Family Assistant Professor of Pritzker School of Molecular Engineering at University of Chicago. Her group works on materials design for chemical and electrochemical separation of critical elements and water purification. She has published more than 40 papers and filed seven patents.

Xinyou Ma received his B.S. in applied chemistry from Beijing University of Chemical Technology in 2012 and his Ph.D. in Chemistry from Texas Tech University in 2018 under the supervision of William L. Hase. In 2018, he joined Professor Gregory A. Voth's research group and the Advanced Materials for Energy-Water Systems (AMEWS) Energy Frontier Research Center (EFRC) as a postdoctoral research scholar, where he studies the confinement effect of proton solvation and transport in a variety of nanoporous systems, including carbon nanotube and zeolite.

Anil Mane is a principal material science engineer in Argonne's Applied Materials Division (AMD). He has extensive research and development experience in the field of thin film nanostructure materials growth by ALD, CVD, PVD, and MBE methods, characterization, and integration

https://doi.org/10.1021/acs.chemrev.1c00069
Chem. Rev. 2021, 121, 9450−9501

into nanodevices. Mane has >125 peer-reviewed publications, >40 patents, and 4 R&D100 awards. His current research interests are next-generation technologically feasible nanostructure materials design, creation and engineering, especially by ALD/CVD techniques. Identification of new nanotechnology-based products, development from concept research to scale-up and technology commercialization. At present, he is working on materials for photodetectors, membranes, nanocomposites, functional coatings, and energy storage.

Alex B. F. Martinson is a Chemist in the Materials Science Division at Argonne National Laboratory. He also serves as the Deputy Director of Science for the Advanced Materials for Energy-Water Systems (AMEWS) Energy Frontier Research Center (EFRC). His group's research includes selective surface synthesis, photoelectrochemistry, and precision cluster catalysis in order to reveal the shortcomings of our control over energy and matter. Alex has published over 100 scientific articles and holds more than 10 patents in the fields of precision surface synthesis, solar energy conversion, water-energy systems, and catalysis.

Karen L. Mulfort is a Chemist in the Solar Energy Conversion Group of the Chemical Sciences & Engineering Division at Argonne National Laboratory. She earned her Ph.D. at Northwestern University and was a Director's Postdoctoral Fellow at Argonne. Her research program focuses on the investigation of molecular architectures in electro- and photocatalytic systems relevant to solar fuels generation and water remediation. Karen and her work have been recognized with the Rising Star Award from the Women Chemists Committee of the American Chemical Society and an Early Career Research Program from the U.S. Department of Energy.

Julia Murphy is currently a Ph.D. student at the University of Chicago under the supervision of Prof. Steven Sibener. Her research focuses on utilizing atomic force microscopy to understand the self-assembly and surface dynamics of polymer thin films, as well as using scanning electrochemical microscopy to characterize transport through porous media.

Kristian Speranza Mølhave is Professor in Nanotechnology Systems for In situ Electron Microscopy Applications at DTU Nanolab at the Technical University of Denmark (DTU). He leads the Molecular Windows research group, developing novel microchip-based microscopy methods for high-resolution imaging especially for electron microscopes in order to provide new insights into physical, chemical, and biological processes on the nanoscale.

Paul F. Nealey is currently the Brady W. Dougan Family Professor in the Pritzker School of Molecular Engineering at the University of Chicago, and a Senior Scientist at Argonne National Laboratory. His research interests include nanofabrication techniques based on advanced lithography and directed self-assembly, dimension dependent material properties of nanoscopic macromolecular systems, quantitative three-dimensional characterization of the structure and dynamics of soft materials, and transport in nanostructured materials. He is a member of the National Academy of Engineering and a fellow of the American Physical Society.

Yijun Qiao obtained his bachelor degree in 2015 from Huazhong University of Science and Technology. After that, he was a Ph.D. student at State Key Laboratory of Tribology of Tsinghua University. Yijun joined Wei Chen's research group in 2019 at Argonne National Laboratory as a visiting research student. His research interests include lubrication mechanisms and solid−liquid interfacial structure.

Vepa Rozyyev completed his bachelor's degree in Chemistry in 2016 and master's degree in Energy and Environmental Engineering in 2018 at Korea Advanced Institute of Science and Technology (KAIST) in South Korea. He is currently Ph.D. candidate at Pritzker School of Molecular Engineering at the University of Chicago (United States) under the supervision of Jeffrey W. Elam. His Ph.D. work is focused on investigating adsorbent materials prepared by atomic layer deposition.

George C. Schatz is Charles E. and Emma H. Morrison Professor of Chemistry at Northwestern University. He received his undergraduate degree in chemistry at Clarkson University and a Ph.D at Caltech; he was a postdoc at MIT, and has been at Northwestern since 1976. Schatz is a theoretician who studies the optical, structural and dynamical properties of nanomaterials and interfaces, including plasmonic nanoparticles, plasmonic metamaterials, DNA and peptide nanostructures, and carbon-based materials. Schatz is a member of the National Academy of Sciences, and the American Academy of Arts and Sciences.

Steven J. Sibener is the Carl William Eisendrath Distinguished Service Professor in the Department of Chemistry and The James Franck Institute of the University of Chicago. He received his doctorate at Berkeley, and was a postdoctoral researcher at Bell Laboratories. He has research interests that focus on the interfacial behavior of materials including polymers, semiconductors, metals, superconductors, water, and ice. Such systems are examined using scanning probe methods, gas-surface neutral particle scattering, and MD simulations.

Dmitri V. Talapin is Ernest DeWitt Burton Distinguished Service Professor in the Department of Chemistry, James Franck Institute, and Pritzker School of Molecular Engineering at the University of Chicago. His group's research interests focus on inorganic nanomaterials, from synthetic methodology to self-assembly to charge transport and optoelectronic devices. His recognitions include ACS Inorganic Nanoscience Award, Materials Research Society Outstanding Young Investigator Award, David and Lucile Packard Fellowship in Science and Engineering, and others. He was elected a Fellow of the Royal Society of Chemistry in 2014.

David M. Tiede is Group Leader for the Solar Conversion Program and a Distinguished Argonne Fellow in the Chemical Sciences & Engineering Division at Argonne National Laboratory and is a Fellow of the American Association for the Advancement of Science (AAAS). His research interests include investigation of fundamental mechanisms for solar energy conversion in natural and artificial photosynthesis, with a particular focus on the tracking of structure and structural dynamics associated with solar fuels catalysis using X-ray spectroscopy and scattering at synchrotron light sources. He has over 180 widely cited publications.

Matthew Tirrell is the dean of the Pritzker School of Molecular Engineering at the University of Chicago, with a joint appointment as a senior scientist at Argonne National Laboratory. He serves on the Board of Directors of Current, an organization advancing the Chicago region's water industry to leverage its strengths for greater economic impact. Tirrell has coauthored about 400 papers, one book, has six U.S. patents, and has supervised about 100 Ph.D. students and 50 postdocs in areas of polymer phase behavior, interfacial phenomena, self-assembly, and nanomedicine.

Andrei Tokmakoff is the Henry G. Gale Distinguished Service Professor and Chair of the Department of Chemistry at the University of Chicago. His research group uses ultrafast vibrational spectroscopy to investigate the molecular dynamics of water and electrolytes, and the structural dynamics of proteins and DNA. He has received many awards, including the Earle K. Plyler Prize for Molecular Spectroscopy & Dynamics from the APS, the Ellis R. Lippincott Award from the OSA, and the Ahmed Zewail Award in Ultrafast Science and Technology from the ACS.

Gregory A. Voth is the Haig P. Papazian Distinguished Service Professor of Chemistry at The University of Chicago. He received a

https://doi.org/10.1021/acs.chemrev.1c00069
Chem. Rev. 2021, 121, 9450−9501

Ph.D. in Theoretical Chemistry from the California Institute of Technology in 1987. He has received a number of awards and other forms of recognition for his work, including most recently the Innovation Award from the Biophysical Society, the Joel Henry Hildebrand National American Chemical Society Award in the Theoretical and Experimental Chemistry of Liquids, the Royal Society of Chemistry S.F. Boys-A. Rahman Award for Outstanding Innovative Research in Computational Chemistry, and the American Chemical Society Division of Physical Chemistry Award in Theoretical Chemistry. Voth specializes in the development and application of theoretical and computational methods to study problems involving the structure and dynamics of complex condensed phase systems, including proteins, membranes, liquids, and materials.

Zhongyang Wang earned his doctorate degree from Energy, Environmental and Chemical Engineering department at Washington University in Saint Louis in 2019. In his Ph.D research, he focused on understanding and improving the alkaline stability of anion exchange membranes with applications in flow batteries, alkaline membrane fuel cells and direct borohydride fuel cells. Zhongyang joined Pritzker School of Molecular Engineering at the University of Chicago in 2019 under the supervision of Professor Paul Nealey. He is now investigating phase behavior and mixed ionic/electronic transport in semicrystalline conjugated polymers.

Zifan Ye is a Ph.D. candidate in the Prof. Giulia Galli's group at The University of Chicago, Pritzker School of Molecular Engineering. She received her B.Eng degree in Materials Science from Imperial College London in 2017. Her research involves using first-principles simulations to study electronic structures and electrochemical properties of Si-based materials and water interfaces.

Murat N. Yesibolati is a postdoc researcher at Technical University of Denmark (DTU), Denmark. Murat defended his Ph.D. thesis titled "Electron holography and particle dynamics in liquid phase transmission electron microscopy" at DTU in 06.2018 under supervision of prof. Kristian Mølhave. He has been developing liquid-phase electron microscopy platforms. Currently, he is focusing on developing nanochannel liquid cell and exploring mass transport in nanochannels using advanced transmission electron microscopy with a postdoc funding support from the Advanced Materials for Energy-Water Systems (AMEWS) Energy Frontier Research Center (EFRC).

Nestor J. Zaluzec is a senior scientist in the Photon Sciences Directorate of Argonne National Laboratory. He is an experimentalist who designs, builds, and implements state-of-the-art electron optical instrumentation and their associated requisite methodology for subnanoscale characterization and analysis of hard and soft matter.

Seth B. Darling is the Director of the Center for Molecular Engineering and a Senior Scientist in the Chemical Sciences & Engineering Division at Argonne National Laboratory. He also serves as the Director of the Advanced Materials for Energy-Water Systems (AMEWS) Energy Frontier Research Center (EFRC). His group's research centers around molecular engineering with a current emphasis on advanced materials for cleaning water. He has published over 140 scientific articles, holds over a dozen patents, is a coauthor of popular books on water and on debunking climate skeptic myths, and lectures widely on topics related to energy, water, and climate.

ACKNOWLEDGMENTS

This work was funded by the Advanced Materials for Energy-Water Systems (AMEWS) Center, an Energy Frontier Research Center funded by the U.S. Department of Energy, Office of Science, Basic Energy Sciences.

REFERENCES

(1) United Nations *Sustainable Development Goal 6 - Synthesis Report 2018 on Water and Sanitation*; June 28, 2018. See the following: https://www.unwater.org/publications/sdg-6-synthesis-report-2018-on-water-and-sanitation/.
(2) Food and Agriculture Organization of the United Nations (FAO), **2018**.
(3) Dalin, C.; Wada, Y.; Kastner, T.; Puma, M. J. Groundwater Depletion Embedded in International Food Trade. *Nature* **2017**, *543*, 700−704.
(4) Ewing, G. E. Ambient Thin Film Water on Insulator Surfaces. *Chem. Rev.* **2006**, *106*, 1511−1526.
(5) Verdaguer, A.; Sacha, G.; Bluhm, H.; Salmeron, M. Molecular Structure of Water at Interfaces: Wetting at the Nanometer Scale. *Chem. Rev.* **2006**, *106*, 1478−1510.
(6) Björneholm, O.; Hansen, M. H.; Hodgson, A.; Liu, L.-M.; Limmer, D. T.; Michaelides, A.; Pedevilla, P.; Rossmeisl, J.; Shen, H.; Tocci, G.; et al. Water at Interfaces. *Chem. Rev.* **2016**, *116*, 7698−7726.
(7) Carrasco, J.; Hodgson, A.; Michaelides, A. A Molecular Perspective of Water at Metal Interfaces. *Nat. Mater.* **2012**, *11*, 667−674.
(8) Darling, S. B. Perspective: Interfacial Materials at the Interface of Energy and Water. *J. Appl. Phys.* **2018**, *124*, 030901.
(9) U. S. Department of Energy Office of Basic Energy Sciences. *Basic Research Needs for Energy and Water*; Presented at BES workshop on Basic Research Needs for Energy and Water, January 4−6, 2017.
(10) Fu, F. L.; Wang, Q. Removal of Heavy Metal Ions from Wastewaters: A Review. *J. Environ. Manage.* **2011**, *92*, 407−418.
(11) Ho, Y. S.; Ng, J. C. Y.; McKay, G. Kinetics of Pollutant Sorption by Biosorbents: Review. *Sep. Purif. Methods* **2000**, *29*, 189−232.
(12) Netz, R. R.; Andelman, D. Neutral and Charged Polymers at Interfaces. *Phys. Rep.* **2003**, *380*, 1−95.
(13) Zhang, R. N.; Liu, Y. N.; He, M. R.; Su, Y. L.; Zhao, X. T.; Elimelech, M.; Jiang, Z. Y. Antifouling Membranes for Sustainable Water Purification: Strategies and Mechanisms. *Chem. Soc. Rev.* **2016**, *45*, 5888−5924.
(14) Dau, H.; Limberg, C.; Reier, T.; Risch, M.; Roggan, S.; Strasser, P. The Mechanism of Water Oxidation: From Electrolysis Via Homogeneous to Biological Catalysis. *ChemCatChem* **2010**, *2*, 724−761.
(15) Hoffmann, M. R.; Martin, S. T.; Choi, W. Y.; Bahnemann, D. W. Environmental Applications of Semiconductor Photocatalysis. *Chem. Rev.* **1995**, *95*, 69−96.
(16) Vogler, E. A. Structure and Reactivity of Water at Biomaterial Surfaces. *Adv. Colloid Interface Sci.* **1998**, *74*, 69−117.
(17) Pirkanniemi, K.; Sillanpaa, M. Heterogeneous Water Phase Catalysis as an Environmental Application. *Chemosphere* **2002**, *48*, 1047−1060.
(18) Fatt, I. The Network Model of Porous Media I. Capillary Pressure Characteristics. *Trans. Soc. Pet. Eng.* **1956**, *207*, 144−159.
(19) Wilkinson, D.; Willemsen, J. F. Invasion Percolation: A New Form of Percolation Theory. *J. Phys. A: Math. Gen.* **1983**, *16*, 3365−3370.
(20) Blunt, M. J. Flow in Porous Media - Pore-Network Models and Multiphase Flow. *Curr. Opin. Colloid Interface Sci.* **2001**, *6*, 197−207.
(21) Berkowitz, B. Characterizing Flow and Transport in Fractured Geological Media: A Review. *Adv. Water Resour.* **2002**, *25*, 861−884.
(22) Bird, R. B.; Stewart, W. E.; Lightfoot, E. N. *Transport Phenomena, Revised 2nd ed.*; John Wiley & Sons, 2007.
(23) Lee, A.; Elam, J. W.; Darling, S. B. Membrane Materials for Water Purification: Design, Development, and Application. *Environ. Sci.: Water Res. Technol.* **2016**, *2*, 17−42.
(24) Tsuru, T.; Nakao, S.-I.; Kimura, S. Calculation of Ion Rejection by Extended Nernst-Planck Equation with Charged Reverse Osmosis Membranes for Single and Mixed Electrolyte Solutions. *J. Chem. Eng. Jpn.* **1991**, *24*, 511−517.
(25) Bowen, W. R.; Mohammad, A. W.; Hilal, N. Characterisation of Nanofiltration Membranes for Predictive Purposes - Use of Salts,

https://doi.org/10.1021/acs.chemrev.1c00069
Chem. Rev. 2021, 121, 9450−9501

Uncharged Solutes and Atomic Force Microscopy. *J. Membr. Sci.* **1997**, *126*, 91−105.
(26) Ebro, H.; Kim, Y. M.; Kim, J. H. Molecular Dynamics Simulations in Membrane-Based Water Treatment Processes: A Systematic Overview. *J. Membr. Sci.* **2013**, *438*, 112−125.
(27) Ben-Naim, A. *Molecular Theory of Solutions*; Oxford University Press, 2006.
(28) Keating, J. J., IV; Imbrogno, J.; Belfort, G. Polymer Brushes for Membrane Separations: A Review. *ACS Appl. Mater. Interfaces* **2016**, *8*, 28383−28399.
(29) Ye, Q.; Zhou, F. in *Antifouling Surfaces and Materials*; Springer, 2015, 55−81.
(30) Maan, A. M.; Hofman, A. H.; de Vos, W. M.; Kamperman, M. Recent Developments and Practical Feasibility of Polymer-Based Antifouling Coatings. *Adv. Funct. Mater.* **2020**, *30*, 2000936.
(31) Goh, P.; Ismail, A. Chemically Functionalized Polyamide Thin Film Composite Membranes: The Art of Chemistry. *Desalination* **2020**, *495*, 114655.
(32) Lu, J.; Elam, J. W.; Stair, P. C. Atomic Layer Deposition—Sequential Self-Limiting Surface Reactions for Advanced Catalyst "Bottom-up" Synthesis. *Surf. Sci. Rep.* **2016**, *71*, 410−472.
(33) George, S. M. Atomic Layer Deposition: An Overview. *Chem. Rev.* **2010**, *110*, 111−131.
(34) Dasgupta, N. P.; Li, L.; Sun, X. Atomic Layer Deposition for Energy and Environmental Applications. *Adv. Mater. Interfaces* **2016**, *3*, 1600914.
(35) Yang, H.-C.; Waldman, R. Z.; Chen, Z.; Darling, S. B. Atomic Layer Deposition for Membrane Interface Engineering. *Nanoscale* **2018**, *10*, 20505−20513.
(36) Li, Y.; Chen, L.; Wooding, J. P.; Zhang, F.; Lively, R. P.; Ramprasad, R.; Losego, M. D. Controlling Wettability, Wet Strength, and Fluid Transport Selectivity of Nanopaper with Atomic Layer Deposited (Ald) Sub-Nanometer Metal Oxide Coatings. *Nanoscale Advances* **2020**, *2*, 356−367.
(37) Xiong, G.; Elam, J. W.; Feng, H.; Han, C. Y.; Wang, H.-H.; Iton, L. E.; Curtiss, L. A.; Pellin, M. J.; Kung, M.; Kung, H.; Stair, P. C. Effect of Atomic Layer Deposition Coatings on the Surface Structure of Anodic Aluminum Oxide Membranes. *J. Phys. Chem. B* **2005**, *109*, 14059−14063.
(38) Elam, J.; Routkevitch, D.; Mardilovich, P.; George, S. Conformal Coating on Ultrahigh-Aspect-Ratio Nanopores of Anodic Alumina by Atomic Layer Deposition. *Chem. Mater.* **2003**, *15*, 3507−3517.
(39) Romero, V.; Vega, V.; García, J.; Zierold, R.; Nielsch, K.; Prida, V. M.; Hernando, B.; Benavente, J. Changes in Morphology and Ionic Transport Induced by Ald Sio2 Coating of Nanoporous Alumina Membranes. *ACS Appl. Mater. Interfaces* **2013**, *5*, 3556−3564.
(40) Yang, H.-C.; Xie, Y.; Chan, H.; Narayanan, B.; Chen, L.; Waldman, R. Z.; Sankaranarayanan, S. K.; Elam, J. W.; Darling, S. B. Crude-Oil-Repellent Membranes by Atomic Layer Deposition: Oxide Interface Engineering. *ACS Nano* **2018**, *12*, 8678−8685.
(41) Zhang, H.; Mane, A. U.; Yang, X.; Xia, Z.; Barry, E. F.; Luo, J.; Wan, Y.; Elam, J. W.; Darling, S. B. Visible-Light-Activated Photocatalytic Films toward Self-Cleaning Membranes. *Adv. Funct. Mater.* **2020**, *30*, 2002847.
(42) Xiong, S.; Kong, L.; Huang, J.; Chen, X.; Wang, Y. Atomic-Layer-Deposition-Enabled Nonwoven Membranes with Hierarchical Zno Nanostructures for Switchable Water/Oil Separations. *J. Membr. Sci.* **2015**, *493*, 478−485.
(43) Barry, E.; Mane, A. U.; Libera, J. A.; Elam, J. W.; Darling, S. B. Advanced Oil Sorbents Using Sequential Infiltration Synthesis. *J. Mater. Chem. A* **2017**, *5*, 2929−2935.
(44) Yang, X.; Sun, P.; Zhang, H.; Xia, Z.; Waldman, R. Z.; Mane, A. U.; Elam, J. W.; Shao, L.; Darling, S. B. Polyphenol-Sensitized Atomic Layer Deposition for Membrane Interface Hydrophilization. *Adv. Funct. Mater.* **2020**, *30*, 1910062.
(45) Wu, S.-L.; Liu, F.; Yang, H.-C.; Darling, S. B. Recent Progress in Molecular Engineering to Tailor Organic-Inorganic Interfaces in Composite Membranes. *Molecular Systems Design & Engineering* **2020**, *5*, 433−444.
(46) Sundberg, P.; Karppinen, M. Organic and Inorganic-Organic Thin Film Structures by Molecular Layer Deposition: A Review. *Beilstein J. Nanotechnol.* **2014**, *5*, 1104−1136.
(47) Bonaccorso, F.; Colombo, L.; Yu, G.; Stoller, M.; Tozzini, V.; Ferrari, A. C.; Ruoff, R. S.; Pellegrini, V. Graphene, Related Two-Dimensional Crystals, and Hybrid Systems for Energy Conversion and Storage. *Science* **2015**, *347*, 1246501.
(48) Montes-Navajas, P.; Asenjo, N. G.; Santamaría, R.; Menendez, R.; Corma, A.; García, H. Surface Area Measurement of Graphene Oxide in Aqueous Solutions. *Langmuir* **2013**, *29*, 13443−13448.
(49) Zhang, H. Ultrathin Two-Dimensional Nanomaterials. *ACS Nano* **2015**, *9*, 9451−9469.
(50) Zhang, Y.; Xu, L.; Walker, W. R.; Tittle, C. M.; Backhouse, C. J.; Pope, M. A. Langmuir Films and Uniform, Large Area, Transparent Coatings of Chemically Exfoliated Mos 2 Single Layers. *J. Mater. Chem. C* **2017**, *5*, 11275−11287.
(51) Brodie, B. C. XIII. On the Atomic Weight of Graphite. *Philos. Trans. R. Soc. London* **1859**, 249−259.
(52) Hofmann, U.; König, E. Untersuchungen Über Graphitoxyd. *Z. Anorg. Allg. Chem.* **1937**, *234*, 311−336.
(53) Hummers, W. S.; Offeman, R. E. Preparation of Graphitic Oxide. *J. Am. Chem. Soc.* **1958**, *80*, 1339−1339.
(54) Marcano, D. C.; Kosynkin, D. V.; Berlin, J. M.; Sinitskii, A.; Sun, Z.; Slesarev, A.; Alemany, L. B.; Lu, W.; Tour, J. M. Improved Synthesis of Graphene Oxide. *ACS Nano* **2010**, *4*, 4806−4814.
(55) Eda, G.; Yamaguchi, H.; Voiry, D.; Fujita, T.; Chen, M.; Chhowalla, M. Photoluminescence from Chemically Exfoliated Mos2. *Nano Lett.* **2011**, *11*, 5111−5116.
(56) Chhowalla, M.; Shin, H. S.; Eda, G.; Li, L.-J.; Loh, K. P.; Zhang, H. The Chemistry of Two-Dimensional Layered Transition Metal Dichalcogenide Nanosheets. *Nat. Chem.* **2013**, *5*, 263−275.
(57) Lei, W.; Mochalin, V. N.; Liu, D.; Qin, S.; Gogotsi, Y.; Chen, Y. Boron Nitride Colloidal Solutions, Ultralight Aerogels and Free-standing Membranes through One-Step Exfoliation and Functionalization. *Nat. Commun.* **2015**, *6*, 1−8.
(58) Naguib, M.; Kurtoglu, M.; Presser, V.; Lu, J.; Niu, J.; Heon, M.; Hultman, L.; Gogotsi, Y.; Barsoum, M. W. Two-Dimensional Nanocrystals Produced by Exfoliation of Ti3alc2. *Adv. Mater.* **2011**, *23*, 4248−4253.
(59) Anasori, B.; Lukatskaya, M. R.; Gogotsi, Y. 2d Metal Carbides and Nitrides (Mxenes) for Energy Storage. *Nature Reviews Materials* **2017**, *2*, 1−17.
(60) Coleman, J. N.; Lotya, M.; O'Neill, A.; Bergin, S. D.; King, P. J.; Khan, U.; Young, K.; Gaucher, A.; De, S.; Smith, R. J.; et al. Two-Dimensional Nanosheets Produced by Liquid Exfoliation of Layered Materials. *Science* **2011**, *331*, 568−571.
(61) Nicolosi, V.; Chhowalla, M.; Kanatzidis, M. G.; Strano, M. S.; Coleman, J. N. Liquid Exfoliation of Layered Materials. *Science* **2013**, *340*, 1226419.
(62) Coleman, J. N. Liquid Exfoliation of Defect-Free Graphene. *Acc. Chem. Res.* **2013**, *46*, 14−22.
(63) Kim, J.; Kwon, S.; Cho, D.-H.; Kang, B.; Kwon, H.; Kim, Y.; Park, S. O.; Jung, G. Y.; Shin, E.; Kim, W.-G. Direct Exfoliation and Dispersion of Two-Dimensional Materials in Pure Water Via Temperature Control. *Nat. Commun.* **2015**, *6*, 8294.
(64) Luo, W.; Wang, Y.; Hitz, E.; Lin, Y.; Yang, B.; Hu, L. Solution Processed Boron Nitride Nanosheets: Synthesis, Assemblies and Emerging Applications. *Adv. Funct. Mater.* **2017**, *27*, 1701450.
(65) Zeng, Z.; Yin, Z.; Huang, X.; Li, H.; He, Q.; Lu, G.; Boey, F.; Zhang, H. Single-Layer Semiconducting Nanosheets: High-Yield Preparation and Device Fabrication. *Angew. Chem., Int. Ed.* **2011**, *50*, 11093−11097.
(66) Su, C.-Y.; Lu, A.-Y.; Xu, Y.; Chen, F.-R.; Khlobystov, A. N.; Li, L.-J. High-Quality Thin Graphene Films from Fast Electrochemical Exfoliation. *ACS Nano* **2011**, *5*, 2332−2339.
(67) Parvez, K.; Li, R.; Puniredd, S. R.; Hernandez, Y.; Hinkel, F.; Wang, S.; Feng, X.; Müllen, K. Electrochemically Exfoliated Graphene as Solution-Processable, Highly Conductive Electrodes for Organic Electronics. *ACS Nano* **2013**, *7*, 3598−3606.

https://doi.org/10.1021/acs.chemrev.1c00069
Chem. Rev. 2021, 121, 9450−9501

(68) Rangappa, D.; Sone, K.; Wang, M.; Gautam, U. K.; Golberg, D.; Itoh, H.; Ichihara, M.; Honma, I. Rapid and Direct Conversion of Graphite Crystals into High-Yielding, Good-Quality Graphene by Supercritical Fluid Exfoliation. *Chem. - Eur. J.* **2010**, *16*, 6488−6494.
(69) Pu, N.-W.; Wang, C.-A.; Sung, Y.; Liu, Y.-M.; Ger, M.-D. Production of Few-Layer Graphene by Supercritical Co2 Exfoliation of Graphite. *Mater. Lett.* **2009**, *63*, 1987−1989.
(70) Hou, S.; Su, S.; Kasner, M. L.; Shah, P.; Patel, K.; Madarang, C. J. Formation of Highly Stable Dispersions of Silane-Functionalized Reduced Graphene Oxide. *Chem. Phys. Lett.* **2010**, *501*, 68−74.
(71) Xu, Z.; Zhang, J.; Shan, M.; Li, Y.; Li, B.; Niu, J.; Zhou, B.; Qian, X. Organosilane-Functionalized Graphene Oxide for Enhanced Antifouling and Mechanical Properties of Polyvinylidene Fluoride Ultrafiltration Membranes. *J. Membr. Sci.* **2014**, *458*, 1−13.
(72) Wan, Y.-J.; Gong, L.-X.; Tang, L.-C.; Wu, L.-B.; Jiang, J.-X. Mechanical Properties of Epoxy Composites Filled with Silane-Functionalized Graphene Oxide. *Composites, Part A* **2014**, *64*, 79−89.
(73) Eng, A. Y. S.; Chua, C. K.; Pumera, M. Refinements to the Structure of Graphite Oxide: Absolute Quantification of Functional Groups Via Selective Labelling. *Nanoscale* **2015**, *7*, 20256−20266.
(74) Igbinigun, E.; Fennell, Y.; Malaisamy, R.; Jones, K. L.; Morris, V. Graphene Oxide Functionalized Polyethersulfone Membrane to Reduce Organic Fouling. *J. Membr. Sci.* **2016**, *514*, 518−526.
(75) Li, J.; Vergne, M. J.; Mowles, E. D.; Zhong, W.-H.; Hercules, D. M.; Lukehart, C. M. Surface Functionalization and Characterization of Graphitic Carbon Nanofibers (Gcnfs). *Carbon* **2005**, *43*, 2883−2893.
(76) Shen, L.; Xiong, S.; Wang, Y. Graphene Oxide Incorporated Thin-Film Composite Membranes for Forward Osmosis Applications. *Chem. Eng. Sci.* **2016**, *143*, 194−205.
(77) Chen, D.; Feng, H.; Li, J. Graphene Oxide: Preparation, Functionalization, and Electrochemical Applications. *Chem. Rev.* **2012**, *112*, 6027−6053.
(78) Chou, S. S.; De, M.; Kim, J.; Byun, S.; Dykstra, C.; Yu, J.; Huang, J.; Dravid, V. P. Ligand Conjugation of Chemically Exfoliated Mos2. *J. Am. Chem. Soc.* **2013**, *135*, 4584−4587.
(79) Kim, J.-S.; Yoo, H.-W.; Choi, H. O.; Jung, H.-T. Tunable Volatile Organic Compounds Sensor by Using Thiolated Ligand Conjugation on Mos2. *Nano Lett.* **2014**, *14*, 5941−5947.
(80) Sim, D. M.; Kim, M.; Yim, S.; Choi, M.-J.; Choi, J.; Yoo, S.; Jung, Y. S. Controlled Doping of Vacancy-Containing Few-Layer Mos2 Via Highly Stable Thiol-Based Molecular Chemisorption. *ACS Nano* **2015**, *9*, 12115−12123.
(81) Nguyen, E. P.; Carey, B. J.; Ou, J. Z.; van Embden, J.; Gaspera, E. D.; Chrimes, A. F.; Spencer, M. J.; Zhuiykov, S.; Kalantar-Zadeh, K.; Daeneke, T. Electronic Tuning of 2d Mos2 through Surface Functionalization. *Adv. Mater.* **2015**, *27*, 6225−6229.
(82) Ding, Q.; Czech, K. J.; Zhao, Y.; Zhai, J.; Hamers, R. J.; Wright, J. C.; Jin, S. Basal-Plane Ligand Functionalization on Semiconducting 2h-Mos2Monolayers. *ACS Appl. Mater. Interfaces* **2017**, *9*, 12734−12742.
(83) Knirsch, K. C.; Berner, N. C.; Nerl, H. C.; Cucinotta, C. S.; Gholamvand, Z.; McEvoy, N.; Wang, Z.; Abramovic, I.; Vecera, P.; Halik, M.; et al. Basal-Plane Functionalization of Chemically Exfoliated Molybdenum Disulfide by Diazonium Salts. *ACS Nano* **2015**, *9*, 6018−6030.
(84) Voiry, D.; Goswami, A.; Kappera, R.; e Silva, C. D. C. C.; Kaplan, D.; Fujita, T.; Chen, M.; Asefa, T.; Chhowalla, M. Covalent Functionalization of Monolayered Transition Metal Dichalcogenides by Phase Engineering. *Nat. Chem.* **2015**, *7*, 45−49.
(85) Sainsbury, T.; Satti, A.; May, P.; Wang, Z.; McGovern, I.; Gun'ko, Y. K.; Coleman, J. Oxygen Radical Functionalization of Boron Nitride Nanosheets. *J. Am. Chem. Soc.* **2012**, *134*, 18758−18771.
(86) Sainsbury, T.; O'Neill, A.; Passarelli, M. K.; Seraffon, M.; Gohil, D.; Gnaniah, S.; Spencer, S. J.; Rae, A.; Coleman, J. N. Dibromocarbene Functionalization of Boron Nitride Nanosheets: Toward Band Gap Manipulation and Nanocomposite Applications. *Chem. Mater.* **2014**, *26*, 7039−7050.
(87) Sainsbury, T.; Satti, A.; May, P.; O'Neill, A.; Nicolosi, V.; Gun'ko, Y. K.; Coleman, J. N. Covalently Functionalized Hexagonal Boron Nitride Nanosheets by Nitrene Addition. *Chem. - Eur. J.* **2012**, *18*, 10808−10812.
(88) Ji, J.; Zhao, L.; Shen, Y.; Liu, S.; Zhang, Y. Covalent Stabilization and Functionalization of Mxene Via Silylation Reactions with Improved Surface Properties. *FlatChem.* **2019**, *17*, 100128.
(89) Sen, R.; Gahtory, D.; Carvalho, R. R.; Albada, B.; van Delft, F. L.; Zuilhof, H. Ultrathin Covalently Bound Organic Layers on Mica: Formation of Atomically Flat Biofunctionalizable Surfaces. *Angew. Chem., Int. Ed.* **2017**, *56*, 4130−4134.
(90) Park, A. Y.; Kwon, H.; Woo, A. J.; Kim, S. J. Layered Double Hydroxide Surface Modified with (3-Aminopropyl) Triethoxysilane by Covalent Bonding. *Adv. Mater.* **2005**, *17*, 106−109.
(91) Kalali, E. N.; Wang, X.; Wang, D.-Y. Functionalized Layered Double Hydroxide-Based Epoxy Nanocomposites with Improved Flame Retardancy and Mechanical Properties. *J. Mater. Chem. A* **2015**, *3*, 6819−6826.
(92) Sitko, R.; Turek, E.; Zawisza, B.; Malicka, E.; Talik, E.; Heimann, J.; Gagor, A.; Feist, B.; Wrzalik, R. Adsorption of Divalent Metal Ions from Aqueous Solutions Using Graphene Oxide. *Dalton Transactions* **2013**, *42*, 5682−5689.
(93) Cui, L.; Wang, Y.; Gao, L.; Hu, L.; Yan, L.; Wei, Q.; Du, B. Edta Functionalized Magnetic Graphene Oxide for Removal of Pb (Ii), Hg (Ii) and Cu (Ii) in Water Treatment: Adsorption Mechanism and Separation Property. *Chem. Eng. J.* **2015**, *281*, 1−10.
(94) Gao, Y.; Li, Y.; Zhang, L.; Huang, H.; Hu, J.; Shah, S. M.; Su, X. Adsorption and Removal of Tetracycline Antibiotics from Aqueous Solution by Graphene Oxide. *J. Colloid Interface Sci.* **2012**, *368*, 540−546.
(95) Wang, H.; Yuan, X.; Wu, Y.; Huang, H.; Zeng, G.; Liu, Y.; Wang, X.; Lin, N.; Qi, Y. Adsorption Characteristics and Behaviors of Graphene Oxide for Zn (Ii) Removal from Aqueous Solution. *Appl. Surf. Sci.* **2013**, *279*, 432−440.
(96) Pan, N.; Li, L.; Ding, J.; Li, S.; Wang, R.; Jin, Y.; Wang, X.; Xia, C. Preparation of Graphene Oxide-Manganese Dioxide for Highly Efficient Adsorption and Separation of Th (Iv)/U (Vi). *J. Hazard. Mater.* **2016**, *309*, 107−115.
(97) Zhou, Y.; Zhou, L.; Zhang, X.; Chen, Y. Preparation of Zeolitic Imidazolate Framework-8/Graphene Oxide Composites with Enhanced Vocs Adsorption Capacity. *Microporous Mesoporous Mater.* **2016**, *225*, 488−493.
(98) Du, Q.; Sun, J.; Li, Y.; Yang, X.; Wang, X.; Wang, Z.; Xia, L. Highly Enhanced Adsorption of Congo Red onto Graphene Oxide/Chitosan Fibers by Wet-Chemical Etching Off Silica Nanoparticles. *Chem. Eng. J.* **2014**, *245*, 99−106.
(99) Wang, H.; Yuan, X.; Wu, Y.; Chen, X.; Leng, L.; Wang, H.; Li, H.; Zeng, G. Facile Synthesis of Polypyrrole Decorated Reduced Graphene Oxide-Fe3o4Magnetic Composites and Its Application for the Cr (Vi) Removal. *Chem. Eng. J.* **2015**, *262*, 597−606.
(100) Liu, C.; Wu, T.; Hsu, P.-C.; Xie, J.; Zhao, J.; Liu, K.; Sun, J.; Xu, J.; Tang, J.; Ye, Z.; et al. Direct/Alternating Current Electrochemical Method for Removing and Recovering Heavy Metal from Water Using Graphene Oxide Electrode. *ACS Nano* **2019**, *13*, 6431−6437.
(101) Liu, X.; Li, J.; Wang, X.; Chen, C.; Wang, X. High Performance of Phosphate-Functionalized Graphene Oxide for the Selective Adsorption of U (Vi) from Acidic Solution. *J. Nucl. Mater.* **2015**, *466*, 56−64.
(102) Shao, D.; Hou, G.; Li, J.; Wen, T.; Ren, X.; Wang, X. Pani/Go as a Super Adsorbent for the Selective Adsorption of Uranium (Vi). *Chem. Eng. J.* **2014**, *255*, 604−612.
(103) Sitko, R.; Janik, P.; Feist, B.; Talik, E.; Gagor, A. Suspended Aminosilanized Graphene Oxide Nanosheets for Selective Preconcentration of Lead Ions and Ultrasensitive Determination by Electrothermal Atomic Absorption Spectrometry. *ACS Appl. Mater. Interfaces* **2014**, *6*, 20144−20153.
(104) Li, H.; Pan, L.; Nie, C.; Liu, Y.; Sun, Z. Reduced Graphene Oxide and Activated Carbon Composites for Capacitive Deionization. *J. Mater. Chem.* **2012**, *22*, 15556−15561.

https://doi.org/10.1021/acs.chemrev.1c00069
Chem. Rev. 2021, 121, 9450−9501

(105) Wimalasiri, Y.; Zou, L. Carbon Nanotube/Graphene Composite for Enhanced Capacitive Deionization Performance. *Carbon* **2013**, *59*, 464−471.
(106) Li, H.; Zou, L.; Pan, L.; Sun, Z. Novel Graphene-Like Electrodes for Capacitive Deionization. *Environ. Sci. Technol.* **2010**, *44*, 8692−8697.
(107) Yin, H.; Zhao, S.; Wan, J.; Tang, H.; Chang, L.; He, L.; Zhao, H.; Gao, Y.; Tang, Z. Three-Dimensional Graphene/Metal Oxide Nanoparticle Hybrids for High-Performance Capacitive Deionization of Saline Water. *Adv. Mater.* **2013**, *25*, 6270−6276.
(108) Xing, F.; Li, T.; Li, J.; Zhu, H.; Wang, N.; Cao, X. Chemically Exfoliated Mos2 for Capacitive Deionization of Saline Water. *Nano Energy* **2017**, *31*, 590−595.
(109) Tian, S.; Zhang, X.; Zhang, Z. Capacitive Deionization with Mos2/G-C3n4 Electrodes. *Desalination* **2020**, *479*, 114348.
(110) Wang, S.; Wang, G.; Wu, T.; Zhang, Y.; Zhan, F.; Wang, Y.; Wang, J.; Fu, Y.; Qiu, J. Bcn Nanosheets Templated by Gc 3 N 4 for High Performance Capacitive Deionization. *J. Mater. Chem. A* **2018**, *6*, 14644−14650.
(111) Srimuk, P.; Kaasik, F.; Krüner, B.; Tolosa, A.; Fleischmann, S.; Jäckel, N.; Tekeli, M. C.; Aslan, M.; Suss, M. E.; Presser, V. Mxene as a Novel Intercalation-Type Pseudocapacitive Cathode and Anode for Capacitive Deionization. *J. Mater. Chem. A* **2016**, *4*, 18265−18271.
(112) Bao, W.; Tang, X.; Guo, X.; Choi, S.; Wang, C.; Gogotsi, Y.; Wang, G. Porous Cryo-Dried Mxene for Efficient Capacitive Deionization. *Joule* **2018**, *2*, 778−787.
(113) Amiri, A.; Chen, Y.; Teng, C. B.; Naraghi, M. Porous Nitrogen-Doped Mxene-Based Electrodes for Capacitive Deionization. *Energy Storage Materials* **2020**, *25*, 731−739.
(114) Nair, R.; Wu, H.; Jayaram, P.; Grigorieva, I.; Geim, A. Unimpeded Permeation of Water through Helium-Leak-Tight Graphene-Based Membranes. *Science* **2012**, *335*, 442−444.
(115) Neek-Amal, M.; Peeters, F. M.; Grigorieva, I. V.; Geim, A. K. Commensurability Effects in Viscosity of Nanoconfined Water. *ACS Nano* **2016**, *10*, 3685−3692.
(116) Fumagalli, L.; Esfandiar, A.; Fabregas, R.; Hu, S.; Ares, P.; Janardanan, A.; Yang, Q.; Radha, B.; Taniguchi, T.; Watanabe, K.; et al. Anomalously Low Dielectric Constant of Confined Water. *Science* **2018**, *360*, 1339−1342.
(117) Jalali, H.; Ghorbanfekr, H.; Hamid, I.; Neek-Amal, M.; Rashidi, R.; Peeters, F. Out-of-Plane Permittivity of Confined Water. *Phys. Rev. E: Stat. Phys., Plasmas, Fluids, Relat. Interdiscip. Top.* **2020**, *102*, 022803.
(118) Zhang, C.; Gygi, F. O.; Galli, G. Strongly Anisotropic Dielectric Relaxation of Water at the Nanoscale. *J. Phys. Chem. Lett.* **2013**, *4*, 2477−2481.
(119) Hoenig, E.; Strong, S. E.; Wang, M.; Radhakrishnan, J. M.; Zaluzec, N. J.; Skinner, J.; Liu, C. Controlling the Structure of Mos2Membranes Via Covalent Functionalization with Molecular Spacers. *Nano Lett.* **2020**, *20*, 7844−7851.
(120) Hoenig, E.; Strong, S. E.; Wang, M.; Radhakrishnan, J. M.; Zaluzec, N. J.; Skinner, J.; Liu, C. Controlling the Structure of Mos2Membranes Via Covalent Functionalization with Molecular Spacers. *Nano Lett.* **2020**,.*20*7844
(121) Radha, B.; Esfandiar, A.; Wang, F.; Rooney, A.; Gopinadhan, K.; Keerthi, A.; Mishchenko, A.; Janardanan, A.; Blake, P.; Fumagalli, L.; et al. Molecular Transport through Capillaries Made with Atomic-Scale Precision. *Nature* **2016**, *538*, 222−225.
(122) Xie, Q.; Alibakhshi, M. A.; Jiao, S.; Xu, Z.; Hempel, M.; Kong, J.; Park, H. G.; Duan, C. Fast Water Transport in Graphene Nanofluidic Channels. *Nat. Nanotechnol.* **2018**, *13*, 238−245.
(123) Esfandiar, A.; Radha, B.; Wang, F.; Yang, Q.; Hu, S.; Garaj, S.; Nair, R.; Geim, A.; Gopinadhan, K. Size Effect in Ion Transport through Angstrom-Scale Slits. *Science* **2017**, *358*, 511−513.
(124) Siria, A.; Bocquet, M.-L.; Bocquet, L. New Avenues for the Large-Scale Harvesting of Blue Energy. *Nature Reviews Chemistry* **2017**, *1*, 0091.
(125) Xiao, K.; Jiang, L.; Antonietti, M. Ion Transport in Nanofluidic Devices for Energy Harvesting. *Joule* **2019**,.32364
(126) Guo, W.; Cheng, C.; Wu, Y.; Jiang, Y.; Gao, J.; Li, D.; Jiang, L. Bio-Inspired Two-Dimensional Nanofluidic Generators Based on a Layered Graphene Hydrogel Membrane. *Adv. Mater.* **2013**, *25*, 6064−6068.
(127) Cheng, H.; Zhou, Y.; Feng, Y.; Geng, W.; Liu, Q.; Guo, W.; Jiang, L. Electrokinetic Energy Conversion in Self-Assembled 2d Nanofluidic Channels with Janus Nanobuilding Blocks. *Adv. Mater.* **2017**, *29*, 1700177.
(128) Zhang, Z.; Yang, S.; Zhang, P.; Zhang, J.; Chen, G.; Feng, X. Mechanically Strong Mxene/Kevlar Nanofiber Composite Membranes as High-Performance Nanofluidic Osmotic Power Generators. *Nat. Commun.* **2019**, *10*, 2920.
(129) Ji, J.; Kang, Q.; Zhou, Y.; Feng, Y.; Chen, X.; Yuan, J.; Guo, W.; Wei, Y.; Jiang, L. Osmotic Power Generation with Positively and Negatively Charged 2d Nanofluidic Membrane Pairs. *Adv. Funct. Mater.* **2017**, *27*, 1603623.
(130) Ladd, J.; Zhang, Z.; Chen, S.; Hower, J. C.; Jiang, S. Zwitterionic Polymers Exhibiting High Resistance to Nonspecific Protein Adsorption from Human Serum and Plasma. *Biomacromolecules* **2008**, *9*, 1357−1361.
(131) Zoppe, J. O.; Ataman, N. C.; Mocny, P.; Wang, J.; Moraes, J.; Klok, H.-A. Surface-Initiated Controlled Radical Polymerization: State-of-the-Art, Opportunities, and Challenges in Surface and Interface Engineering with Polymer Brushes. *Chem. Rev.* **2017**, *117*, 1105−1318.
(132) Chen, S.; Li, L.; Zhao, C.; Zheng, J. Surface Hydration: Principles and Applications toward Low-Fouling/Nonfouling Biomaterials. *Polymer* **2010**, *51*, 5283−5293.
(133) Yang, W. J.; Neoh, K.-G.; Kang, E.-T.; Teo, S. L.-M.; Rittschof, D. Polymer Brush Coatings for Combating Marine Biofouling. *Prog. Polym. Sci.* **2014**, *39*, 1017−1042.
(134) Schlenoff, J. B. Zwitteration: Coating Surfaces with Zwitterionic Functionality to Reduce Nonspecific Adsorption. *Langmuir* **2014**, *30*, 9625−9636.
(135) He, Q.; Qiao, Y.; Mandia, D. J.; Gan, S.; Zhang, H.; Zhou, H.; Elam, J. W.; Darling, S. B.; Tirrell, M. V.; Chen, W. Enrichment and Distribution of Pb2+ Ions in Zwitterionic Poly (Cysteine Methacrylate) Brushes at the Solid-Liquid Interface. *Langmuir* **2019**, *35*, 17082−17089.
(136) Baggerman, J.; Smulders, M. M.; Zuilhof, H. Romantic Surfaces: A Systematic Overview of Stable, Biospecific, and Antifouling Zwitterionic Surfaces. *Langmuir* **2019**, *35*, 1072−1084.
(137) Yameen, B.; Ali, M.; Neumann, R.; Ensinger, W.; Knoll, W.; Azzaroni, O. Single Conical Nanopores Displaying Ph-Tunable Rectifying Characteristics. Manipulating Ionic Transport with Zwitterionic Polymer Brushes. *J. Am. Chem. Soc.* **2009**, *131*, 2070−2071.
(138) Silies, L.; Andrieu-Brunsen, A. Programming Ionic Pore Accessibility in Zwitterionic Polymer Modified Nanopores. *Langmuir* **2018**, *34*, 807−816.
(139) Zeng, Z.; Yeh, L.-H.; Zhang, M.; Qian, S. Ion Transport and Selectivity in Biomimetic Nanopores with Ph-Tunable Zwitterionic Polyelectrolyte Brushes. *Nanoscale* **2015**, *7*, 17020−17029.
(140) Liu, T.-Y.; Yuan, H.-G.; Li, Q.; Tang, Y.-H.; Zhang, Q.; Qian, W.; Van der Bruggen, B.; Wang, X. Ion-Responsive Channels of Zwitterion-Carbon Nanotube Membrane for Rapid Water Permeation and Ultrahigh Mono-/Multivalent Ion Selectivity. *ACS Nano* **2015**, *9*, 7488−7496.
(141) Guo, Y.-S.; Mi, Y.-F.; Ji, Y.-L.; An, Q.-F.; Gao, C.-J. One-Step Surface Grafting Method for Preparing Zwitterionic Nanofiltation Membrane Via in Situ Introduction of Initiator in Interfacial Polymerization. *ACS Appl. Poly. Mater.* **2019**, *1*, 1022−1033.
(142) Guo, Y.-S.; Ji, Y.-L.; Wu, B.; Wang, N.-X.; Yin, M.-J.; An, Q.-F.; Gao, C.-J. High-Flux Zwitterionic Nanofiltration Membrane Constructed by in-Situ Introduction Method for Monovalent Salt/Antibiotics Separation. *J. Membr. Sci.* **2020**, *593*, 117441.
(143) Tang, F.; Ohto, T.; Sun, S.; Rouxel, J. R.; Imoto, S.; Backus, E. H.; Mukamel, S.; Bonn, M.; Nagata, Y. Molecular Structure and Modeling of Water-Air and Ice-Air Interfaces Monitored by Sum-Frequency Generation. *Chem. Rev.* **2020**, *120*, 3633−3667.

https://doi.org/10.1021/acs.chemrev.1c00069
Chem. Rev. 2021, 121, 9450−9501

(144) Nihonyanagi, S.; Mondal, J. A.; Yamaguchi, S.; Tahara, T. Structure and Dynamics of Interfacial Water Studied by Heterodyne-Detected Vibrational Sum-Frequency Generation. *Annu. Rev. Phys. Chem.* **2013**, *64*, 579−603.
(145) Geissler, P. L. Water Interfaces, Solvation, and Spectroscopy. *Annu. Rev. Phys. Chem.* **2013**, *64*, 317−337.
(146) Shen, Y. R.; Ostroverkhov, V. Sum-Frequency Vibrational Spectroscopy on Water Interfaces: Polar Orientation of Water Molecules at Interfaces. *Chem. Rev.* **2006**, *106*, 1140−1154.
(147) Perakis, F.; De Marco, L.; Shalit, A.; Tang, F.; Kann, Z. R.; Kühne, T. D.; Torre, R.; Bonn, M.; Nagata, Y. Vibrational Spectroscopy and Dynamics of Water. *Chem. Rev.* **2016**, *116*, 7590−7607.
(148) Fujiwara, H. *Spectroscopic Ellipsometry: Principles and Applications*; John Wiley & Sons, 2007.
(149) Kroning, A.; Furchner, A.; Aulich, D.; Bittrich, E.; Rauch, S.; Uhlmann, P.; Eichhorn, K.-J.; Seeber, M.; Luzinov, I.; Kilbey, S. M.; et al. In Situ Infrared Ellipsometry for Protein Adsorption Studies on Ultrathin Smart Polymer Brushes in Aqueous Environment. *ACS Appl. Mater. Interfaces* **2015**, *7*, 12430−12439.
(150) VanHove, M. A.; Weinberg, W. H.; Chan, C.-M. *Low-Energy Electron Diffraction: Experiment, Theory and Surface Structure Determination*; Springer Science & Business Media, 2012.
(151) Lied, A.; Dosch, H.; Bilgram, J. Surface Melting of Ice I H Single Crystals Revealed by Glancing Angle X-Ray Scattering. *Phys. Rev. Lett.* **1994**, *72*, 3554.
(152) Als-Nielsen, J.; Jacquemain, D.; Kjaer, K.; Leveiller, F.; Lahav, M.; Leiserowitz, L. Principles and Applications of Grazing Incidence X-Ray and Neutron Scattering from Ordered Molecular Monolayers at the Air-Water Interface. *Phys. Rep.* **1994**, *246*, 251.
(153) Russell, T. X-Ray and Neutron Reflectivity for the Investigation of Polymers. *Mater. Sci. Rep.* **1990**, *5*, 171−271.
(154) Kulik, H. J.; Marzari, N.; Correa, A. A.; Prendergast, D.; Schwegler, E.; Galli, G. Local Effects in the X-Ray Absorption Spectrum of Salt Water. *J. Phys. Chem. B* **2010**, *114*, 9594−9601.
(155) Oura, K.; Lifshits, V.; Saranin, A.; Zotov, A.; Katayama, M. *Surface Science: An Introduction. 2003*; Springer: Berlin, 2003.
(156) Wandelt, K.; Thurgate, S. *Solid-Liquid Interfaces: Macroscopic Phenomena—Microscopic Understanding*; Springer Science & Business Media, 2002.
(157) Lang, P. R.; Liu, Y. *Soft Matter at Aqueous Interfaces*; Springer, 2016.
(158) Sztucki, M.; Di Cola, E.; Narayanan, T. Anomalous Small-Angle X-Ray Scattering from Charged Soft Matter. *Eur. Phys. J.: Spec. Top.* **2012**, *208*, 319−331.
(159) Fenter, P. A. X-Ray Reflectivity as a Probe of Mineral-Fluid Interfaces: A User Guide. *Rev. Mineral. Geochem.* **2002**, *49*, 149−221.
(160) Park, C.; Fenter, P. A. Phasing of Resonant Anomalous X-Ray Reflectivity Spectra and Direct Fourier Synthesis of Element-Specific Partial Structures at Buried Interfaces. *J. Appl. Crystallogr.* **2007**, *40*, 290−301.
(161) Fenter, P.; Park, C.; Nagy, K. L.; Sturchio, N. C. Resonant Anomalous X-Ray Reflectivity as a Probe of Ion Adsorption at Solid-Liquid Interfaces. *Thin Solid Films* **2007**, *515*, 5654−5659.
(162) Chu, Y.; You, H.; Tanzer, J.; Lister, T.; Nagy, Z. Surface Resonance X-Ray Scattering Observation of Core-Electron Binding-Energy Shifts of Pt (111)-Surface Atoms During Electrochemical Oxidation. *Phys. Rev. Lett.* **1999**, *83*, 552−555.
(163) Park, C.; Fenter, P. A.; Sturchio, N. C.; Regalbuto, J. R. Probing Outer-Sphere Adsorption of Aqueous Metal Complexes at the Oxide-Water Interface with Resonant Anomalous X-Ray Reflectivity. *Phys. Rev. Lett.* **2005**, *94*, 076104.
(164) Fenter, P.; Lee, S. S. Hydration Layer Structure at Solid-Water Interfaces. *MRS Bull.* **2014**, *39*, 1056−1061.
(165) Kohli, V.; Zhang, Z.; Park, C.; Fenter, P. Rb+ and Sr2+ Adsorption at the Tio2 (110)- Electrolyte Interface Observed with Resonant Anomalous X-Ray Reflectivity. *Langmuir* **2010**, *26*, 950−958.
(166) Bellucci, F.; Lee, S. S.; Kubicki, J. D.; Bandura, A.; Zhang, Z.; Wesolowski, D. J.; Fenter, P. Rb+ Adsorption at the Quartz (101)-Aqueous Interface: Comparison of Resonant Anomalous X-Ray Reflectivity with Ab Initio Calculations. *J. Phys. Chem. C* **2015**, *119*, 4778−4788.
(167) De Hoe, G. X.; Mao, J.; Jiang, Z.; Darling, S. B.; Tirrell, M. V.; Chen, W. Probing Diffuse Polymer Brush Interfaces Using Resonant Soft X-Ray Scattering. *Synchrotron Radiation News* **2020**, *33*, 24−30.
(168) Halperin, A.; Tirrell, M.; Lodge, T. *Macromolecules: Synthesis, Order and Advanced Properties*; Springer, 1992; pp 31−71.
(169) Milner, S. T.; Witten, T. A.; Cates, M. E. Theory of the Grafted Polymer Brush. *Macromolecules* **1988**, *21*, 2610−2619.
(170) Murat, M.; Grest, G. S. Interaction between Grafted Polymeric Brushes: A Molecular-Dynamics Study. *Phys. Rev. Lett.* **1989**, *63*, 1074−1077.
(171) Binder, K.; Milchev, A. Polymer Brushes on Flat and Curved Surfaces: How Computer Simulations Can Help to Test Theories and to Interpret Experiments. *J. Polym. Sci., Part B: Polym. Phys.* **2012**, *50*, 1515−1555.
(172) Kato, K.; Uchida, E.; Kang, E.-T.; Uyama, Y.; Ikada, Y. Polymer Surface with Graft Chains. *Prog. Polym. Sci.* **2003**, *28*, 209−259.
(173) Kelley, T. W.; Schorr, P. A.; Johnson, K. D.; Tirrell, M.; Frisbie, C. D. Direct Force Measurements at Polymer Brush Surfaces by Atomic Force Microscopy. *Macromolecules* **1998**, *31*, 4297−4300.
(174) Yu, J.; Mao, J.; Yuan, G.; Satija, S.; Jiang, Z.; Chen, W.; Tirrell, M. Structure of Polyelectrolyte Brushes in the Presence of Multivalent Counterions. *Macromolecules* **2016**, *49*, 5609−5617.
(175) Yu, J.; Jackson, N.; Xu, X.; Morgenstern, Y.; Kaufman, Y.; Ruths, M.; De Pablo, J.; Tirrell, M. Multivalent Counterions Diminish the Lubricity of Polyelectrolyte Brushes. *Science* **2018**, *360*, 1434−1438.
(176) Yu, J.; Jackson, N. E.; Xu, X.; Brettmann, B. K.; Ruths, M.; de Pablo, J. J.; Tirrell, M. Multivalent Ions Induce Lateral Structural Inhomogeneities in Polyelectrolyte Brushes. *Science Advances* **2017**, *3*, No. eaao1497.
(177) Chen, T.; Ferris, R.; Zhang, J.; Ducker, R.; Zauscher, S. Stimulus-Responsive Polymer Brushes on Surfaces: Transduction Mechanisms and Applications. *Prog. Polym. Sci.* **2010**, *35*, 94−112.
(178) Minko, S.; Responsive Polymer Brushes*J. Macromol. Sci., Polym. Rev.*, **2006**.*46*397
(179) Yang, J.; Chen, H.; Xiao, S.; Shen, M.; Chen, F.; Fan, P.; Zhong, M.; Zheng, J. Salt-Responsive Zwitterionic Polymer Brushes with Tunable Friction and Antifouling Properties. *Langmuir* **2015**, *31*, 9125−9133.
(180) Barrat, J. L. A Possible Mechanism for Swelling of Polymer Brushes under Shear. *Macromolecules* **1992**, *25*, 832−834.
(181) Kumaran, V. Hydrodynamic Interactions in Flow Past Grafted Polymers. *Macromolecules* **1993**, *26*, 2464−2469.
(182) Doyle, P. S.; Shaqfeh, E. S.; Gast, A. P. Rheology of "Wet" Polymer Brushes Via Brownian Dynamics Simulation: Steady Vs Oscillatory Shear. *Phys. Rev. Lett.* **1997**, *78*, 1182−1186.
(183) Saphiannikova, M. G.; Pryamitsyn, V. A.; Cosgrove, T. Self-Consistent Brownian Dynamics Simulation of Polymer Brushes under Shear. *Macromolecules* **1998**, *31*, 6662−6668.
(184) Deng, M.; Li, X.; Liang, H.; Caswell, B.; Karniadakis, G. E. Simulation and Modelling of Slip Flow over Surfaces Grafted with Polymer Brushes and Glycocalyx Fibres. *J. Fluid Mech.* **2012**, *711*, 192−211.
(185) Qiao, Y.; Zhou, H.; Jiang, Z.; He, Q.; Gan, S.; Wang, H.; Wen, S.; de Pablo, J.; Liu, Y.; Tirrell, M. V.; et al. An in Situ Shearing X-Ray Measurement System for Exploring Structures and Dynamics at the Solid-Liquid Interface. *Rev. Sci. Instrum.* **2020**, *91*, 013908.
(186) Fried, S. D.; Boxer, S. G. Measuring Electric Fields and Noncovalent Interactions Using the Vibrational Stark Effect. *Acc. Chem. Res.* **2015**, *48*, 998−1006.
(187) Kim, H.; Cho, M. Infrared Probes for Studying the Structure and Dynamics of Biomolecules. *Chem. Rev.* **2013**, *113*, 5817−5847.
(188) Ganim, Z.; Tokmakoff, A.; Vaziri, A. Vibrational Excitons in Ionophores: Experimental Probes for Quantum Coherence-Assisted Ion Transport and Selectivity in Ion Channels. *New J. Phys.* **2011**, *13*, 113030.
(189) Edington, S. C.; Gonzalez, A.; Middendorf, T. R.; Halling, D. B.; Aldrich, R. W.; Baiz, C. R. Coordination to Lanthanide Ions Distorts

https://doi.org/10.1021/acs.chemrev.1c00069
Chem. Rev. 2021, 121, 9450−9501

Binding Site Conformation in Calmodulin. *Proc. Natl. Acad. Sci. U. S. A.* **2018**, *115*, E3126−E3134.
(190) Kratochvil, H. T.; Carr, J. K.; Matulef, K.; Annen, A. W.; Li, H.; Maj, M.; Ostmeyer, J.; Serrano, A. L.; Raghuraman, H.; Moran, S. D.; et al. Instantaneous Ion Configurations in the K+ Ion Channel Selectivity Filter Revealed by 2d Ir Spectroscopy. *Science* **2016**, *353*, 1040−1044.
(191) Piontek, S. M.; Tuladhar, A.; Marshall, T.; Borguet, E. Monovalent and Divalent Cations at the A-Al2o3 (0001)/Water Interface: How Cation Identity Affects Interfacial Ordering and Vibrational Dynamics. *J. Phys. Chem. C* **2019**, *123*, 18315−18324.
(192) Sayama, A.; Nihonyanagi, S.; Ohshima, Y.; Tahara, T. In Situ Observation of the Potential-Dependent Structure of an Electrolyte/Electrode Interface by Heterodyne-Detected Vibrational Sum Frequency Generation. *Phys. Chem. Chem. Phys.* **2020**, *22*, 2580−2589.
(193) Sorenson, S. A.; Patrow, J. G.; Dawlaty, J. M. Solvation Reaction Field at the Interface Measured by Vibrational Sum Frequency Generation Spectroscopy. *J. Am. Chem. Soc.* **2017**, *139*, 2369−2378.
(194) Patrow, J. G.; Sorenson, S. A.; Dawlaty, J. M. Direct Spectroscopic Measurement of Interfacial Electric Fields near an Electrode under Polarizing or Current-Carrying Conditions. *J. Phys. Chem. C* **2017**, *121*, 11585−11592.
(195) Goldsmith, Z. K.; Secor, M.; Hammes-Schiffer, S. Inhomogeneity of Interfacial Electric Fields at Vibrational Probes on Electrode Surfaces. *ACS Cent. Sci.* **2020**, *6*, 304−311.
(196) Kwak, K.; Park, S.; Finkelstein, I. J.; Fayer, M. D. Frequency-Frequency Correlation Functions and Apodization in Two-Dimensional Infrared Vibrational Echo Spectroscopy: A New Approach. *J. Chem. Phys.* **2007**, *127*, 124503.
(197) Yan, C.; Thomaz, J. E.; Wang, Y.-L.; Nishida, J.; Yuan, R.; Breen, J. P.; Fayer, M. D. Ultrafast to Ultraslow Dynamics of a Langmuir Monolayer at the Air/Water Interface Observed with Reflection Enhanced 2d Ir Spectroscopy. *J. Am. Chem. Soc.* **2017**, *139*, 16518−16527.
(198) Kraack, J. P.; Hamm, P. Surface-Sensitive and Surface-Specific Ultrafast Two-Dimensional Vibrational Spectroscopy. *Chem. Rev.* **2017**, *117*, 10623−10664.
(199) Kraack, J. P.; Kaech, A.; Hamm, P. Surface Enhancement in Ultrafast 2d Atr Ir Spectroscopy at the Metal-Liquid Interface. *J. Phys. Chem. C* **2016**, *120*, 3350−3359.
(200) Kraack, J. P.; Hamm, P. Solvent-Controlled Morphology of Catalytic Monolayers at Solid-Liquid Interfaces. *J. Phys. Chem. C* **2018**, *122*, 2259−2267.
(201) Yamada, S. A.; Hung, S. T.; Shin, J. Y.; Fayer, M. D. Complex Formation and Dissociation Dynamics on Amorphous Silica Surfaces. *J. Phys. Chem. B* **2021**, *125*, 4566−4581.
(202) Lewis, N. H.; Iscen, A.; Felts, A.; Dereka, B.; Schatz, G. C.; Tokmakoff, A. Vibrational Probe of Aqueous Electrolytes: The Field Is Not Enough. *J. Phys. Chem. B* **2020**, *124*, 7013−7026.
(203) Verde, A. V.; Beltramo, P. J.; Maranas, J. K. Adsorption of Homopolypeptides on Gold Investigated Using Atomistic Molecular Dynamics. *Langmuir* **2011**, *27*, 5918−5926.
(204) Heinz, H.; Farmer, B. L.; Pandey, R. B.; Slocik, J. M.; Patnaik, S. S.; Pachter, R.; Naik, R. R. Nature of Molecular Interactions of Peptides with Gold, Palladium, and Pd-Au Bimetal Surfaces in Aqueous Solution. *J. Am. Chem. Soc.* **2009**, *131*, 9704−9714.
(205) Verde, A. V.; Acres, J. M.; Maranas, J. K. Investigating the Specificity of Peptide Adsorption on Gold Using Molecular Dynamics Simulations. *Biomacromolecules* **2009**, *10*, 2118−2128.
(206) Hoefling, M.; Iori, F.; Corni, S.; Gottschalk, K. E. Interaction of Amino Acids with the Au(111) Surface: Adsorption Free Energies from Molecular Dynamics Simulations. *Langmuir* **2010**, *26*, 8347−8351.
(207) Feng, J.; Pandey, R. B.; Berry, R. J.; Farmer, B. L.; Naik, R. R.; Heinz, H. Adsorption Mechanism of Single Amino Acid and Surfactant Molecules to Au \ 111 \ Surfaces in Aqueous Solution: Design Rules for Metal-Binding Molecules. *Soft Matter* **2011**, *7*, 2113−2120.
(208) Kislenko, S. A.; Nikitina, V. A.; Nazmutdinov, R. R. A Molecular Dynamics Study of the Ionic and Molecular Permeability of Alkanethiol Monolayers on the Gold Electrode Surface. *High Energy Chem.* **2015**, *49*, 341−346.
(209) Lin, W.; Wu, W.; Weitz, E.; Schatz, G. C. Molecular-Level Insight into the Hydroxylated Monomeric Vo X/Θ-Al2o3 (010) and Its Adsorption of Methanol. *J. Phys. Chem. C* **2019**, *123*, 27704−27711.
(210) Quezada, G. R.; Rozas, R. E.; Toledo, P. G. Molecular Dynamics Simulations of Quartz (101)-Water and Corundum (001)-Water Interfaces: Effect of Surface Charge and Ions on Cation Adsorption, Water Orientation, and Surface Charge Reversal. *J. Phys. Chem. C* **2017**, *121*, 25271−25282.
(211) Coasne, B.; Galarneau, A.; Pellenq, R. J. M.; Di Renzo, F. Adsorption, Intrusion and Freezing in Porous Silica: The View from the Nanoscale. *Chem. Soc. Rev.* **2013**, *42*, 4141−4171.
(212) Wright, L. B.; Walsh, T. R. First-Principles Molecular Dynamics Simulations of Nh 4+ and Ch3coo- Adsorption at the Aqueous Quartz Interface. *J. Chem. Phys.* **2012**, *137*, 224702.
(213) Konatham, D.; Yu, J.; Ho, T. A.; Striolo, A. Simulation Insights for Graphene-Based Water Desalination Membranes. *Langmuir* **2013**, *29*, 11884−11897.
(214) Gai, J. G.; Gong, X. L.; Wang, W. W.; Zhang, X.; Kang, W. L. An Ultrafast Water Transport Forward Osmosis Membrane: Porous Graphene. *J. Mater. Chem. A* **2014**, *2*, 4023−4028.
(215) Cohen-Tanugi, D.; Grossman, J. C. Water Desalination across Nanoporous Graphene. *Nano Lett.* **2012**, *12*, 3602−3608.
(216) Shahbabaei, M.; Kim, D. Molecular Dynamics Simulation of Water Transport Mechanisms through Nanoporous Boron Nitride and Graphene Multilayers. *J. Phys. Chem. B* **2017**, *121*, 4137−4144.
(217) Suk, M. E.; Aluru, N. R. Water Transport through Ultrathin Graphene. *J. Phys. Chem. Lett.* **2010**, *1*, 1590−1594.
(218) Wei, N.; Peng, X.; Xu, Z. Breakdown of Fast Water Transport in Graphene Oxides. *Phys. Rev. E* **2014**, *89*, 012113.
(219) Fang, C.; Yu, Z.; Qiao, R. Impact of Surface Ionization on Water Transport and Salt Leakage through Graphene Oxide Membranes. *J. Phys. Chem. C* **2017**, *121*, 13412−13420.
(220) Azamat, J.; Khataee, A.; Joo, S. W. Molecular Dynamics Simulation of Trihalomethanes Separation from Water by Functionalized Nanoporous Graphene under Induced Pressure. *Chem. Eng. Sci.* **2015**, *127*, 285−292.
(221) Zhu, Y.; Ruan, Y.; Zhang, Y.; Chen, Y.; Lu, X.; Lu, L. Mg2+-Channel-Inspired Nanopores for Mg2+/Li+ Separation: The Effect of Coordination on the Ionic Hydration Microstructures. *Langmuir* **2017**, *33*, 9201−9210.
(222) Sabatier, P. Hydrogénations Et Déshydrogénations Par Catalyse. *Ber. Dtsch. Chem. Ges.* **1911**, *44*, 1984−2001.
(223) Bligaard, T.; Nørskov, J. K.; Dahl, S.; Matthiesen, J.; Christensen, C. H.; Sehested, J. The Brønsted-Evans-Polanyi Relation and the Volcano Curve in Heterogeneous Catalysis. *J. Catal.* **2004**, *224*, 206−217.
(224) Nørskov, J. K.; Rossmeisl, J.; Logadottir, A.; Lindqvist, L.; Kitchin, J. R.; Bligaard, T.; Jonsson, H. Origin of the Overpotential for Oxygen Reduction at a Fuel-Cell Cathode. *J. Phys. Chem. B* **2004**, *108*, 17886−17892.
(225) Zagal, J. H.; Koper, M. T. Reactivity Descriptors for the Activity of Molecular Mn4 Catalysts for the Oxygen Reduction Reaction. *Angew. Chem., Int. Ed.* **2016**, *55*, 14510−14521.
(226) Ye, J.; Dombrowski, J. P.; Hu, X.; Whitney-Warner, J.; Guo, S.; Kung, M. C.; Kung, H. H. Production of H_2o_2 During Au/C Catalyzed Aerobic Oxidation of 1,2-Propanediol. *Appl. Catal., A* **2020**, *599*, 117616.
(227) Ketchie, W. C.; Murayama, M.; Davis, R. J. Promotional Effect of Hydroxyl on the Aqueous Phase Oxidation of Carbon Monoxide and Glycerol over Supported Au Catalysts. *Top. Catal.* **2007**, *44*, 307−317.
(228) Liu, M.; Pang, Y.; Zhang, B.; De Luna, P.; Voznyy, O.; Xu, J.; Zheng, X.; Dinh, C. T.; Fan, F.; Cao, C.; et al. Enhanced Electrocatalytic Co 2 Reduction Via Field-Induced Reagent Concentration. *Nature* **2016**, *537*, 382−386.
(229) Waldman, R. Z.; Jeon, N.; Mandia, D. J.; Heinonen, O.; Darling, S. B.; Martinson, A. B. Sequential Infiltration Synthesis of Electronic

https://doi.org/10.1021/acs.chemrev.1c00069
Chem. Rev. 2021, 121, 9450−9501

Materials: Group 13 Oxides Via Metal Alkyl Precursors. *Chem. Mater.* **2019**, *31*, 5274−5285.
(230) Waldman, R. Z.; Mandia, D. J.; Yanguas-Gil, A.; Martinson, A. B. F.; Elam, J. W.; Darling, S. B. The Chemical Physics of Sequential Infiltration Synthesis - a Thermodynamic and Kinetic Perspective. *J. Chem. Phys.* **2019**, *151*, 190901.
(231) Wilson, C.; Grubbs, R.; George, S. Nucleation and Growth During Al2o3 Atomic Layer Deposition on Polymers. *Chem. Mater.* **2005**, *17*, 5625−5634.
(232) Gong, B.; Peng, Q.; Jur, J. S.; Devine, C. K.; Lee, K.; Parsons, G. N. Sequential Vapor Infiltration of Metal Oxides into Sacrificial Polyester Fibers: Shape Replication and Controlled Porosity of Microporous/Mesoporous Oxide Monoliths. *Chem. Mater.* **2011**, *23*, 3476−3485.
(233) Ingram, W. F.; Jur, J. S. Properties and Applications of Vapor Infiltration into Polymeric Substrates. *JOM* **2019**, *71*, 238−245.
(234) Han, E.; Stuen, K. O.; La, Y.-H.; Nealey, P. F.; Gopalan, P. Effect of Composition of Substrate-Modifying Random Copolymers on the Orientation of Symmetric and Asymmetric Diblock Copolymer Domains. *Macromolecules* **2008**, *41*, 9090−9097.
(235) Tanabe, K.; Hölderich, W. F. Industrial Application of Solid Acid-Base Catalysts. *Appl. Catal., A* **1999**, *181*, 399−434.
(236) Li, G.; Wang, B.; Resasco, D. E. Water-Mediated Heterogeneously Catalyzed Reactions. *ACS Catal.* **2020**, *10*, 1294−1309.
(237) Resasco, D. E.; Wang, B.; Crossley, S. Zeolite-Catalysed C-C Bond Forming Reactions for Biomass Conversion to Fuels and Chemicals. *Catal. Sci. Technol.* **2016**, *6*, 2543−2559.
(238) Chen, K.; Kelsey, J.; White, J. L.; Zhang, L.; Resasco, D. Water Interactions in Zeolite Catalysts and Their Hydrophobically Modified Analogues. *ACS Catal.* **2015**, *5*, 7480−7487.
(239) Galadima, A.; Muraza, O. Stability Improvement of Zeolite Catalysts under Hydrothermal Conditions for Their Potential Applications in Biomass Valorization and Crude Oil Upgrading. *Microporous Mesoporous Mater.* **2017**, *249*, 42−54.
(240) Zhi, Y.; Shi, H.; Mu, L.; Liu, Y.; Mei, D.; Camaioni, D. M.; Lercher, J. A. Dehydration Pathways of 1-Propanol on Hzsm-5 in the Presence and Absence of Water. *J. Am. Chem. Soc.* **2015**, *137*, 15781−15794.
(241) Wang, H.; Hou, Y.; Sun, W.; Hu, Q.; Xiong, H.; Wang, T.; Yan, B.; Qian, W. Insight into the Effects of Water on the Ethene to Aromatics Reaction with Hzsm-5. *ACS Catal.* **2020**, *10*, 5288−5298.
(242) Liu, Y.; Vjunov, A.; Shi, H.; Eckstein, S.; Camaioni, D. M.; Mei, D.; Baráth, E.; Lercher, J. A. Enhancing the Catalytic Activity of Hydronium Ions through Constrained Environments. *Nat. Commun.* **2017**, *8*, 14113.
(243) Chen, K.; Damron, J.; Pearson, C.; Resasco, D.; Zhang, L.; White, J. L. Zeolite Catalysis: Water Can Dramatically Increase or Suppress Alkane C-H Bond Activation. *ACS Catal.* **2014**, *4*, 3039−3044.
(244) Chen, K.; Gumidyala, A.; Abdolrhamani, M.; Villines, C.; Crossley, S.; White, J. L. Trace Water Amounts Can Increase Benzene H/D Exchange Rates in an Acidic Zeolite. *J. Catal.* **2017**, *351*, 130−135.
(245) Jentys, A.; Warecka, G.; Derewinski, M.; Lercher, J. A. Adsorption of Water on Zsm 5 Zeolites. *J. Phys. Chem.* **1989**, *93*, 4837−4843.
(246) Hunger, B.; Heuchel, M.; Matysik, S.; Beck, K.; Einicke, W. Adsorption of Water on Zsm-5 Zeolites. *Thermochim. Acta* **1995**, *269*, 599−611.
(247) Sárkány, J. Effects of Water and Ion-Exchanged Counterion on the Ftir Spectra of Zsm-5. I. Nah-Zsm-5:: H-Bonding with Oh Groups of Zeolite and Formation of H+ (H2o) N. *Appl. Catal., A* **1999**, *188*, 369−379.
(248) Wakabayashi, F.; Kondo, J. N.; Domen, K.; Hirose, C. Ft-Ir Study of H218o Adsorption on H-Zsm-5: Direct Evidence for the Hydrogen-Bonded Adsorption of Water. *J. Phys. Chem.* **1996**, *100*, 1442−1444.
(249) Kondo, J. N.; Iizuka, M.; Domen, K.; Wakabayashi, F. Ir Study of H2o Adsorbed on H-Zsm-5. *Langmuir* **1997**, *13*, 747−750.
(250) Losch, P.; Joshi, H. R.; Vozniuk, O.; Grünert, A.; Ochoa-Hernández, C.; Jabraoui, H.; Badawi, M.; Schmidt, W. Proton Mobility, Intrinsic Acid Strength, and Acid Site Location in Zeolites Revealed by Varying Temperature Infrared Spectroscopy and Density Functional Theory Studies. *J. Am. Chem. Soc.* **2018**, *140*, 17790−17799.
(251) Vjunov, A.; Wang, M.; Govind, N.; Huthwelker, T.; Shi, H.; Mei, D.; Fulton, J. L.; Lercher, J. A. Tracking the Chemical Transformations at the Brønsted Acid Site Upon Water-Induced Deprotonation in a Zeolite Pore. *Chem. Mater.* **2017**, *29*, 9030−9042.
(252) Pelmenschikov, A.; Van Wolput, J.; Jänchen, J.; Van Santen, R. (a, B, C) Triplet of Infrared Oh Bands of Zeolitic H-Complexes. *J. Phys. Chem.* **1995**, *99*, 3612−3617.
(253) Pelmenschikov, A.; Van Santen, R. Water Adsorption on Zeolites: Ab-Initio Interpretation of Ir Data. *J. Phys. Chem.* **1993**, *97*, 10678−10680.
(254) Sazama, P.; Tvarůžková, Z.; Jirglová, H.; Sobalík, Z. Water adsorption on high silica zeolites. Formation of hydroxonium ions and hydrogen-bonded adducts. *Stud. Surf. Sci. Catal.* **2008**, *174*, 821−824.
(255) Krossner, M.; Sauer, J. Interaction of Water with Brønsted Acidic Sites of Zeolite Catalysts. Ab Initio Study of 1:1 and 2:1 Surface Complexes. *J. Phys. Chem.* **1996**, *100*, 6199−6211.
(256) Olson, D.; Zygmunt, S.; Erhardt, M.; Curtiss, L.; Iton, L. Evidence for Dimeric and Tetrameric Water Clusters in Hzsm-5. *Zeolites* **1997**, *18*, 347−349.
(257) Zygmunt, S. A.; Curtiss, L. A.; Iton, L. E. Protonation of an H2o Dimer by a Zeolitic Brønsted Acid Site. *J. Phys. Chem. B* **2001**, *105*, 3034−3038.
(258) Jungsuttiwong, S.; Limtrakul, J.; Truong, T. N. Theoretical Study of Modes of Adsorption of Water Dimer on H-Zsm-5 and H-Faujasite Zeolites. *J. Phys. Chem. B* **2005**, *109*, 13342−13351.
(259) Eckstein, S.; Hintermeier, P. H.; Zhao, R.; Baráth, E.; Shi, H.; Liu, Y.; Lercher, J. A. Influence of Hydronium Ions in Zeolites on Sorption. *Angew. Chem., Int. Ed.* **2019**, *58*, 3450−3455.
(260) Zhan, C.-G.; Dixon, D. A. Absolute Hydration Free Energy of the Proton from First-Principles Electronic Structure Calculations. *J. Phys. Chem. A* **2001**, *105*, 11534−11540.
(261) Lee, E.; Dyke, J. An Ab Initio Molecular Orbital Study of Protonated Water Clusters, H (H2o) N+ N= 1 to 5, at the Scf and Mp2 Levels. *Mol. Phys.* **1991**, *73*, 375−405.
(262) Camaioni, D. M.; Schwerdtfeger, C. A. Comment on "Accurate Experimental Values for the Free Energies of Hydration of H+, Oh-, and H3o+. *J. Phys. Chem. A* **2005**, *109*, 10795−10797.
(263) McIntosh, B. J.; Adams, N. G.; Smith, D. Determination of the Proton Affinities of H2o and Cs2 Relative to C2h4. *Chem. Phys. Lett.* **1988**, *148*, 142−148.
(264) Hunter, E. P.; Lias, S. G. Evaluated Gas Phase Basicities and Proton Affinities of Molecules: An Update. *J. Phys. Chem. Ref. Data* **1998**, *27*, 413−656.
(265) Peterson, K. A.; Xantheas, S. S.; Dixon, D. A.; Dunning, T. H. Predicting the Proton Affinities of H2o and Nh3. *J. Phys. Chem. A* **1998**, *102*, 2449−2454.
(266) Chong, S. L.; Myers, R. A., Jr; Franklin, J. Proton Affinity of Water. *J. Chem. Phys.* **1972**, *56*, 2427−2430.
(267) Collyer, S.; McMahon, T. Proton Affinity of Water. A Scale of Gas-Phase Basicities Including Ethylene and Water from Ion Cyclotron Resonance Proton Transfer Equilibrium Measurements. *J. Phys. Chem.* **1983**, *87*, 909−911.
(268) Kawai, Y.; Yamaguchi, S.; Okada, Y.; Takeuchi, K.; Yamauchi, Y.; Ozawa, S.; Nakai, H. Reactions of Protonated Water Clusters H+ (H2o) N (N= 1−6) with Dimethylsulfoxide in a Guided Ion Beam Apparatus. *Chem. Phys. Lett.* **2003**, *377*, 69−73.
(269) Kebarle, P.; Searles, S. K.; Zolla, A.; Scarborough, J.; Arshadi, M. Solvation of the Hydrogen Ion by Water Molecules in the Gas Phase. Heats and Entropies of Solvation of Individual Reactions. H+ (H2o) N-1+ H2o. Fwdarw. H+ (H2o) N. *J. Am. Chem. Soc.* **1967**, *89*, 6393−6399.
(270) Kletnieks, P.; Ehresmann, J.; Nicholas, J.; Haw, J. Adsorbate Clustering and Proton Transfer in Zeolites: Nmr Spectroscopy and Theory. *ChemPhysChem* **2006**, *7*, 114−116.

https://doi.org/10.1021/acs.chemrev.1c00069
Chem. Rev. 2021, 121, 9450−9501

(271) Cheng, H.-P. Water Clusters: Fascinating Hydrogen-Bonding Networks, Solvation Shell Structures, and Proton Motion. *J. Phys. Chem. A* **1998**, *102*, 6201−6204.
(272) Wròblewski, T.; Ziemczonek, L.; Karwasz, G. Proton Transfer Reactions for Ionized Water Clusters. *Czech. J. Phys.* **2004**, *54*, C747−C752.
(273) Kelly, C. P.; Cramer, C. J.; Truhlar, D. G. Aqueous Solvation Free Energies of Ions and Ion- Water Clusters Based on an Accurate Value for the Absolute Aqueous Solvation Free Energy of the Proton. *J. Phys. Chem. B* **2006**, *110*, 16066−16081.
(274) Tissandier, M. D.; Cowen, K. A.; Feng, W. Y.; Gundlach, E.; Cohen, M. H.; Earhart, A. D.; Coe, J. V.; Tuttle, T. R. The Proton's Absolute Aqueous Enthalpy and Gibbs Free Energy of Solvation from Cluster-Ion Solvation Data. *J. Phys. Chem. A* **1998**, *102*, 7787−7794.
(275) Gonzales, N. O.; Bell, A. T.; Chakraborty, A. K. Density Functional Theory Calculations of the Effects of Local Composition and Defect Structure on the Proton Affinity of H- Zsm-5. *J. Phys. Chem. B* **1997**, *101*, 10058−10064.
(276) Kramer, G.; Van Santen, R. Theoretical Determination of Proton Affinity Differences in Zeolites. *J. Am. Chem. Soc.* **1993**, *115*, 2887−2897.
(277) Kramer, G.; Van Santen, R.; Emeis, C.; Nowak, A. Understanding the Acid Behaviour of Zeolites from Theory and Experiment. *Nature* **1993**, *363*, 529−531.
(278) Chandra, A.; Goursot, A.; Fajula, F. Proton Affinity Differences in Zeolite: A Dft Study. *J. Mol. Catal. A: Chem.* **1997**, *119*, 45−50.
(279) Bolis, V.; Barbaglia, A.; Broyer, M.; Busco, C.; Civalleri, B.; Ugliengo, P. Entrapping Molecules in Zeolites Nanocavities: A Thermodynamic and Ab-Initio Study. *Origins Life Evol. Biospheres* **2004**, *34*, 69−77.
(280) Bolis, V.; Broyer, M.; Barbaglia, A.; Busco, C.; Foddanu, G.; Ugliengo, P. Van Der Waals Interactions on Acidic Centres Localized in Zeolites Nanocavities: A Calorimetric and Computer Modeling Study. *J. Mol. Catal. A: Chem.* **2003**, *204*, 561−569.
(281) Busco, C.; Barbaglia, A.; Broyer, M.; Bolis, V.; Foddanu, G.; Ugliengo, P. Characterisation of Lewis and Brønsted Acidic Sites in H-Mfi and H-Bea Zeolites: A Thermodynamic and Ab Initio Study. *Thermochim. Acta* **2004**, *418*, 3−9.
(282) Rice, M. J.; Chakraborty, A. K.; Bell, A. T. A Density Functional Theory Study of the Interactions of H2o with H- Zsm-5, Cu- Zsm-5, and Co- Zsm-5. *J. Phys. Chem. A* **1998**, *102*, 7498−7504.
(283) Ison, A.; Gorte, R. J. The Adsorption of Methanol and Water on H-Zsm-5. *J. Catal.* **1984**, *89*, 150−158.
(284) Zeets, M.; Resasco, D. E.; Wang, B. Enhanced Chemical Activity and Wettability at Adjacent Brønsted Acid Sites in Hzsm-5. *Catal. Today* **2018**, *312*, 44−50.
(285) Bolis, V.; Busco, C.; Ugliengo, P. Thermodynamic Study of Water Adsorption in High-Silica Zeolites. *J. Phys. Chem. B* **2006**, *110*, 14849−14859.
(286) Olson, D.; Haag, W.; Borghard, W. Use of Water as a Probe of Zeolitic Properties: Interaction of Water with Hzsm-5. *Microporous Mesoporous Mater.* **2000**, *35*, 435−446.
(287) Fournier, J. A.; Wolke, C. T.; Johnson, M. A.; Odbadrakh, T. T.; Jordan, K. D.; Kathmann, S. M.; Xantheas, S. S. Snapshots of Proton Accommodation at a Microscopic Water Surface: Understanding the Vibrational Spectral Signatures of the Charge Defect in Cryogenically Cooled H+ (H2o) N= 2−28 Clusters. *J. Phys. Chem. A* **2015**, *119*, 9425−9440.
(288) Domen, K.; Fujino, T.; Wada, A.; Hirose, C.; Kano, S. Direct Observation of Short-Lived Unstable Surface Species by Tunable Picosecond Infrared Pulses. *Appl. Surf. Sci.* **1997**, *121*, 484−487.
(289) Fujino, T.; Kashitani, M.; Onda, K.; Wada, A.; Domen, K.; Hirose, C.; Ishida, M.; Goto, F.; Kano, S. Picosecond Infrared Pump-Probe Spectrum of D 2 O Adsorbed at Acid Od Group of Zeolite. *J. Chem. Phys.* **1998**, *109*, 2460−2466.
(290) Domen, K.; Fujino, T.; Wada, A.; Hirose, C.; Kano, S. Picosecond Vibrational Dynamics of Adsorbed D2o on Brønsted Acid Od Group in a Zeolite. *Surf. Sci.* **1997**, *386*, 78−81.
(291) Fujino, T.; Kashitani, M.; Fukuyama, K.; Kubota, J.; Kondo, J.; Wada, A.; Domen, K.; Hirose, C.; Wakabayashi, F.; Kano, S. Population Lifetimes of the Oh Stretching Band of Water Molecules on Zeolite Surfaces. *Chem. Phys. Lett.* **1996**, *261*, 534−538.
(292) Fujino, T.; Furuki, M.; Kashitani, M.; Onda, K.; Kubota, J.; Kondo, J.; Wada, A.; Domen, K.; Hirose, C.; Wakabayashi, F.; et al. The Effect of Adsorbed Noble Gas Atoms on Vibrational Relaxation of Hydroxyl Group in Zeolite. *J. Chem. Phys.* **1996**, *105*, 279−288.
(293) Domen, K.; Fujino, T.; Wada, A.; Hirose, C.; Kano, S. Vibrational Dynamics of Adsorbed D2o on Brønsted Hydroxyl Group in a Zeolite. *Microporous Mesoporous Mater.* **1998**, *21*, 673−678.
(294) Bonn, M.; Bakker, H. J.; Domen, K.; Hirose, C.; Kleyn, A. W.; Van Santen, R. A. Dynamical Studies of Zeolitic Protons and Adsorbates by Picosecond Infrared Spectroscopy. *Catal. Rev.: Sci. Eng.* **1998**, *40*, 127−173.
(295) Bonn, M.; Brugmans, M. J.; Kleyn, A. W.; van Santen, R. A. Fast Energy Delocalization Upon Vibrational Relaxation of a Deuterated Zeolite Surface Hydroxyl. *J. Chem. Phys.* **1995**, *102*, 2181−2186.
(296) Bonn, M.; van Santen, R. A.; Lercher, J. A.; Kleyn, A. W.; Bakker, H. J. Picosecond Infrared Activation of Methanol in Acid Zeolites. *Chem. Phys. Lett.* **1997**, *278*, 213−219.
(297) De Marco, L.; Fournier, J. A.; Thämer, M.; Carpenter, W.; Tokmakoff, A. Anharmonic Exciton Dynamics and Energy Dissipation in Liquid Water from Two-Dimensional Infrared Spectroscopy. *J. Chem. Phys.* **2016**, *145*, 094501.
(298) Ramasesha, K.; De Marco, L.; Mandal, A.; Tokmakoff, A. Water Vibrations Have Strongly Mixed Intra-and Intermolecular Character. *Nat. Chem.* **2013**, *5*, 935−940.
(299) Ge, A.; Rudshteyn, B.; Videla, P. E.; Miller, C. J.; Kubiak, C. P.; Batista, V. S.; Lian, T. Heterogenized Molecular Catalysts: Vibrational Sum-Frequency Spectroscopic, Electrochemical, and Theoretical Investigations. *Acc. Chem. Res.* **2019**, *52*, 1289−1300.
(300) Bullock, R. M.; Das, A. K.; Appel, A. M. Surface Immobilization of Molecular Electrocatalysts for Energy Conversion. *Chem. - Eur. J.* **2017**, *23*, 7626−7641.
(301) Cao, Z.; Zacate, S. B.; Sun, X.; Liu, J.; Hale, E. M.; Carson, W. P.; Tyndall, S. B.; Xu, J.; Liu, X.; Liu, X.; et al. Tuning Gold Nanoparticles with Chelating Ligands for Highly Efficient Electrocatalytic Co2 Reduction. *Angew. Chem.* **2018**, *130*, 12857−12861.
(302) Lauinger, S. M.; Sumliner, J. M.; Yin, Q.; Xu, Z.; Liang, G.; Glass, E. N.; Lian, T.; Hill, C. L. High Stability of Immobilized Polyoxometalates on Tio2 Nanoparticles and Nanoporous Films for Robust, Light-Induced Water Oxidation. *Chem. Mater.* **2015**, *27*, 5886−5891.
(303) Vannucci, A. K.; Alibabaei, L.; Losego, M. D.; Concepcion, J. J.; Kalanyan, B.; Parsons, G. N.; Meyer, T. J. Crossing the Divide between Homogeneous and Heterogeneous Catalysis in Water Oxidation. *Proc. Natl. Acad. Sci. U. S. A.* **2013**, *110*, 20918−20922.
(304) Rosser, T. E.; Windle, C. D.; Reisner, E. Electrocatalytic and Solar-Driven Co2 Reduction to Co with a Molecular Manganese Catalyst Immobilized on Mesoporous Tio2. *Angew. Chem.* **2016**, *128*, 7514−7518.
(305) Sheehan, S. W.; Thomsen, J. M.; Hintermair, U.; Crabtree, R. H.; Brudvig, G. W.; Schmuttenmaer, C. A. A Molecular Catalyst for Water Oxidation That Binds to Metal Oxide Surfaces. *Nat. Commun.* **2015**, *6*, 6469.
(306) Kohmoto, M.; Ozawa, H.; Yang, L.; Hagio, T.; Matsunaga, M.; Haga, M.-A. Controlling the Adsorption of Ruthenium Complexes on Carbon Surfaces through Noncovalent Bonding with Pyrene Anchors: An Electrochemical Study. *Langmuir* **2016**, *32*, 4141−4152.
(307) Blakemore, J. D.; Gupta, A.; Warren, J. J.; Brunschwig, B. S.; Gray, H. B. Noncovalent Immobilization of Electrocatalysts on Carbon Electrodes for Fuel Production. *J. Am. Chem. Soc.* **2013**, *135*, 18288−18291.
(308) Rao, P. M.; Wolfson, A.; Kababya, S.; Vega, S.; Landau, M. Immobilization of Molecular H3pw12o40 Heteropolyacid Catalyst in Alumina-Grafted Silica-Gel and Mesostructured Sba-15 Silica Matrices. *J. Catal.* **2005**, *232*, 210−225.

https://doi.org/10.1021/acs.chemrev.1c00069
Chem. Rev. 2021, 121, 9450−9501

(309) Nakazawa, J.; Smith, B. J.; Stack, T. D. P. Discrete Complexes Immobilized onto Click-Sba-15 Silica: Controllable Loadings and the Impact of Surface Coverage on Catalysis. *J. Am. Chem. Soc.* **2012**, *134*, 2750−2759.
(310) Chołuj, A.; Krzesiński, P.; Ruszczyńska, A.; Bulska, E.; Kajetanowicz, A.; Grela, K. Noncovalent Immobilization of Cationic Ruthenium Complex in a Metal-Organic Framework by Ion Exchange Leading to a Heterogeneous Olefin Metathesis Catalyst for Use in Green Solvents. *Organometallics* **2019**, *38*, 3397−3405.
(311) Wu, C. D.; Zhao, M. Incorporation of Molecular Catalysts in Metal-Organic Frameworks for Highly Efficient Heterogeneous Catalysis. *Adv. Mater.* **2017**, *29*, 1605446.
(312) Brennaman, M. K.; Dillon, R. J.; Alibabaei, L.; Gish, M. K.; Dares, C. J.; Ashford, D. L.; House, R. L.; Meyer, G. J.; Papanikolas, J. M.; Meyer, T. J. Finding the Way to Solar Fuels with Dye-Sensitized Photoelectrosynthesis Cells. *J. Am. Chem. Soc.* **2016**, *138*, 13085−13102.
(313) Youngblood, W. J.; Lee, S.-H. A.; Kobayashi, Y.; Hernandez-Pagan, E. A.; Hoertz, P. G.; Moore, T. A.; Moore, A. L.; Gust, D.; Mallouk, T. E. Photoassisted Overall Water Splitting in a Visible Light-Absorbing Dye-Sensitized Photoelectrochemical Cell. *J. Am. Chem. Soc.* **2009**, *131*, 926−927.
(314) Hamann, T. W.; Jensen, R. A.; Martinson, A. B. F.; Van Ryswyk, H.; Hupp, J. T. Advancing Beyond Current Generation Dye-Sensitized Solar Cells. *Energy Environ. Sci.* **2008**, *1*, 66−78.
(315) Hagfeldt, A.; Boschloo, G.; Sun, L.; Kloo, L.; Pettersson, H. Dye-Sensitized Solar Cells. *Chem. Rev.* **2010**, *110*, 6595−6663.
(316) Materna, K. L.; Crabtree, R. H.; Brudvig, G. W. Anchoring Groups for Photocatalytic Water Oxidation on Metal Oxide Surfaces. *Chem. Soc. Rev.* **2017**, *46*, 6099−6110.
(317) McNamara, W. R.; Snoeberger, R. C., III; Li, G.; Richter, C.; Allen, L. J.; Milot, R. L.; Schmuttenmaer, C. A.; Crabtree, R. H.; Brudvig, G. W.; Batista, V. S. Hydroxamate Anchors for Water-Stable Attachment to Tio2 Nanoparticles. *Energy Environ. Sci.* **2009**, *2*, 1173−1175.
(318) He, H.; Gurung, A.; Si, L. 8-Hydroxylquinoline as a Strong Alternative Anchoring Group for Porphyrin-Sensitized Solar Cells. *Chem. Commun.* **2012**, *48*, 5910−5912.
(319) Materna, K. L.; Jiang, J.; Crabtree, R. H.; Brudvig, G. W. Silatrane Anchors for Metal Oxide Surfaces: Optimization for Potential Photocatalytic and Electrocatalytic Applications. *ACS Appl. Mater. Interfaces* **2019**, *11*, 5602−5609.
(320) Bangle, R.; Sampaio, R. N.; Troian-Gautier, L.; Meyer, G. J. Surface Grafting of Ru(Ii) Diazonium-Based Sensitizers on Metal Oxides Enhances Alkaline Stability for Solar Energy Conversion. *ACS Appl. Mater. Interfaces* **2018**, *10*, 3121−3132.
(321) Son, H.-J.; Prasittichai, C.; Mondloch, J. E.; Luo, L.; Wu, J.; Kim, D. W.; Farha, O. K.; Hupp, J. T. Dye Stabilization and Enhanced Photoelectrode Wettability in Water-Based Dye-Sensitized Solar Cells through Post-Assembly Atomic Layer Deposition of Tio2. *J. Am. Chem. Soc.* **2013**, *135*, 11529−11532.
(322) Lapides, A. M.; Sherman, B. D.; Brennaman, M. K.; Dares, C. J.; Skinner, K. R.; Templeton, J. L.; Meyer, T. J. Synthesis, Characterization, and Water Oxidation by a Molecular Chromophore-Catalyst Assembly Prepared by Atomic Layer Deposition. The "Mummy" Strategy. *Chemical Science* **2015**, *6*, 6398−6406.
(323) Hoffeditz, W. L.; Son, H.-J.; Pellin, M. J.; Farha, O. K.; Hupp, J. T. Engendering Long-Term Air and Light Stability of a Tio2-Supported Porphyrinic Dye Via Atomic Layer Deposition. *ACS Appl. Mater. Interfaces* **2016**, *8*, 34863−34869.
(324) Son, H.-J.; Kim, C. H.; Kim, D. W.; Jeong, N. C.; Prasittichai, C.; Luo, L.; Wu, J.; Farha, O. K.; Wasielewski, M. R.; Hupp, J. T. Post-Assembly Atomic Layer Deposition of Ultrathin Metal-Oxide Coatings Enhances the Performance of an Organic Dye-Sensitized Solar Cell by Suppressing Dye Aggregation. *ACS Appl. Mater. Interfaces* **2015**, *7*, 5150−5159.
(325) Kung, M. C.; Ye, J.; Kung, H. H. 110th Anniversary: A Perspective on Catalytic Oxidative Processes for Sustainable Water Remediation. *Ind. Eng. Chem. Res.* **2019**, *58*, 17325−17337.
(326) Collins, T. J. Taml Oxidant Activators: A New Approach to the Activation of Hydrogen Peroxide for Environmentally Significant Problems. *Acc. Chem. Res.* **2002**, *35*, 782−790.
(327) Collins, T. J.; Ryabov, A. D. Targeting of High-Valent Iron-Taml Activators at Hydrocarbons and Beyond. *Chem. Rev.* **2017**, *117*, 9140−9162.
(328) de Sousa, D. P.; Miller, C. J.; Chang, Y.; Waite, T. D.; McKenzie, C. J. Electrochemically Generated Cis-Carboxylato-Coordinated Iron-(Iv) Oxo Acid-Base Congeners as Promiscuous Oxidants of Water Pollutants. *Inorg. Chem.* **2017**, *56*, 14936−14947.
(329) Warner, G. R.; Somasundar, Y.; Jansen, K. C.; Kaaret, E. Z.; Weng, C.; Burton, A. E.; Mills, M. R.; Shen, L. Q.; Ryabov, A. D.; Pros, G.; et al. Bioinspired, Multidisciplinary, Iterative Catalyst Design Creates the Highest Performance Peroxidase Mimics and the Field of Sustainable Ultradilute Oxidation Catalysis (Sudoc). *ACS Catal.* **2019**, *9*, 7023−7037.
(330) Demeter, E. L.; Hilburg, S. L.; Washburn, N. R.; Collins, T. J.; Kitchin, J. R. Electrocatalytic Oxygen Evolution with an Immobilized Taml Activator. *J. Am. Chem. Soc.* **2014**, *136*, 5603−5606.
(331) Shimakoshi, H.; Hisaeda, Y. A Hybrid Catalyst for Light-Driven Green Molecular Transformations. *ChemPlusChem* **2017**, *82*, 18−29.
(332) Liang, X.; Huang, T.; Li, M.; Mack, J.; Wildervanck, M.; Nyokong, T.; Zhu, W. Highly Efficient Ccl Bond Cleavage and Unprecedented Cc Bond Cleavage of Environmentally Toxic Ddt through Molecular Electrochemical Catalysis. *Appl. Catal., A* **2017**, *545*, 44−53.
(333) Pizarro, S.; Araya, M.; Delgadillo, A. Hexachloroethane Reduction Catalyzed by Cobaloximes. Effect of the Substituents on the Equatorial Ligands. *Polyhedron* **2018**, *141*, 94−99.
(334) Pizarro, S.; Gallardo, M.; Gajardo, F.; Delgadillo, A. Electrochemical Reduction of Lindane Using a Cobaloxime Containing Electron-Withdrawing Groups. *Inorg. Chem. Commun.* **2019**, *99*, 164−166.
(335) Obare, S. O.; Ito, T.; Meyer, G. J. Multi-Electron Transfer from Heme-Functionalized Nanocrystalline Tio2 to Organohalide Pollutants. *J. Am. Chem. Soc.* **2006**, *128*, 712−713.
(336) Stromberg, J. R.; Wnuk, J. D.; Pinlac, R. A. F.; Meyer, G. J. Multielectron Transfer at Heme-Functionalized Nanocrystalline Tio2: Reductive Dechlorination of Ddt and Ccl4 Forms Stable Carbene Compounds. *Nano Lett.* **2006**, *6*, 1284−1286.
(337) Obare, S. O.; Ito, T.; Meyer, G. J. Controlling Reduction Potentials of Semiconductor-Supported Molecular Catalysts for Environmental Remediation of Organohalide Pollutants. *Environ. Sci. Technol.* **2005**, *39*, 6266−6272.
(338) Blakemore, J. D.; Crabtree, R. H.; Brudvig, G. W. Molecular Catalysts for Water Oxidation. *Chem. Rev.* **2015**, *115*, 12974−13005.
(339) Vannucci, A. K.; Hull, J. F.; Chen, Z.; Binstead, R. A.; Concepcion, J. J.; Meyer, T. J. Water Oxidation Intermediates Applied to Catalysis: Benzyl Alcohol Oxidation. *J. Am. Chem. Soc.* **2012**, *134*, 3972−3975.
(340) Michaelos, T. K.; Shopov, D. Y.; Sinha, S. B.; Sharninghausen, L. S.; Fisher, K. J.; Lant, H. M. C.; Crabtree, R. H.; Brudvig, G. W. A Pyridine Alkoxide Chelate Ligand That Promotes Both Unusually High Oxidation States and Water-Oxidation Catalysis. *Acc. Chem. Res.* **2017**, *50*, 952−959.
(341) Fisher, K. J.; Materna, K. L.; Mercado, B. Q.; Crabtree, R. H.; Brudvig, G. W. Electrocatalytic Water Oxidation by a Copper(Ii) Complex of an Oxidation-Resistant Ligand. *ACS Catal.* **2017**, *7*, 3384−3387.
(342) Bohra, D.; Chaudhry, J. H.; Burdyny, T.; Pidko, E. A.; Smith, W. A. Modeling the Electrical Double Layer to Understand the Reaction Environment in a Co2 Electrocatalytic System. *Energy Environ. Sci.* **2019**, *12*, 3380−3389.
(343) Fu, K. Y.; Kwon, S. R.; Han, D.; Bohn, P. W. Single Entity Electrochemistry in Nanopore Electrode Arrays: Ion Transport Meets Electron Transfer in Confined Geometries. *Acc. Chem. Res.* **2020**, *53*, 719−728.

https://doi.org/10.1021/acs.chemrev.1c00069
Chem. Rev. 2021, 121, 9450−9501

(344) Lis, D.; Backus, E. H. G.; Hunger, J.; Parekh, S. H.; Bonn, M. Liquid Flow Along a Solid Surface Reversibly Alters Interfacial Chemistry. *Science* **2014**, *344*, 1138−1142.
(345) Liu, M.; Pang, Y.; Zhang, B.; De Luna, P.; Voznyy, O.; Xu, J.; Zheng, X.; Dinh, C. T.; Fan, F.; Cao, C.; et al. Enhanced Electrocatalytic Co2 Reduction Via Field-Induced Reagent Concentration. *Nature* **2016**, *537*, 382−386.
(346) Resasco, J.; Chen, L. D.; Clark, E.; Tsai, C.; Hahn, C.; Jaramillo, T. F.; Chan, K.; Bell, A. T. Promoter Effects of Alkali Metal Cations on the Electrochemical Reduction of Carbon Dioxide. *J. Am. Chem. Soc.* **2017**, *139*, 11277−11287.
(347) Park, C.; Fenter, P. A.; Nagy, K. L.; Sturchio, N. C. Hydration and Distribution of Ions at the Mica-Water Interface. *Phys. Rev. Lett.* **2006**, *97*, 016101.
(348) Bourg, I. C.; Lee, S. S.; Fenter, P.; Tournassat, C. Stern Layer Structure and Energetics at Mica-Water Interfaces. *J. Phys. Chem. C* **2017**, *121*, 9402−9412.
(349) Lee, S. S.; Park, C.; Sturchio, N. C.; Fenter, P. Nonclassical Behavior in Competitive Ion Adsorption at a Charged Solid-Water Interface. *J. Phys. Chem. Lett.* **2020**, *11*, 4029−4035.
(350) Tiede, D. M.; Kwon, G.; He, X.; Mulfort, K. L.; Martinson, A. B. F. Characterizing Electronic and Atomic Structures for Amorphous and Molecular Metal Oxide Catalysts at Functional Interfaces by Combining Soft X-Ray Spectroscopy and High-Energy X-Ray Scattering. *Nanoscale* **2020**, *12*, 13276−13296.
(351) He, X.; Waldman, R. Z.; Mandia, D. J.; Jeon, N.; Zaluzec, N. J.; Borkiewicz, O. J.; Ruett, U.; Darling, S. B.; Martinson, A. B. F.; Tiede, D. M. Resolving the Atomic Structure of Sequential Infiltration Synthesis Derived Inorganic Clusters. *ACS Nano* **2020**, *14*, 14846−14860.
(352) Kwon, G.; Cho, Y.-H.; Kim, K.-B.; Emery, J. D.; Kim, I. S.; Zhang, X.; Martinson, A. B. F.; Tiede, D. M. Microfluidic Electrochemical Cell for in-Situ Structural Characterization of Amorphous Thin-Film Catalysts Using High-Energy X-Ray Scattering. *J. Synchrotron Radiat.* **2019**, *26* (5), 1600−1611.
(353) Kwon, G.; Jang, H.; Lee, J.-S.; Mane, A.; Mandia, D. J.; Soltau, S. R.; Utschig, L. M.; Martinson, A. B. F.; Tiede, D. M.; Kim, H.; et al. Resolution of Electronic and Structural Factors Underlying Oxygen-Evolving Performance in Amorphous Cobalt Oxide Catalysts. *J. Am. Chem. Soc.* **2018**, *140*, 10710−10720.
(354) Mulfort, K. L.; Mukherjee, A.; Kokhan, O.; Du, P. W.; Tiede, D. M. Structure-Function Analyses of Solar Fuels Catalysts Using in-Situ X-Ray Scattering. *Chem. Soc. Rev.* **2013**, *42*, 2215−2227.
(355) Egami, T.; Billinge, S. J. L. *Underneath the Bragg Peaks: Structural Analysis of Complex Materials*; Pergamon: Oxford, U.K., 2012.
(356) Laaziri, K.; Kycia, S.; Roorda, S.; Chicoine, M.; Robertson, J. L.; Wang, J.; Moss, S. C. High-Energy X-Ray Diffraction Study of Pure Amorphous Silicon. *Phys. Rev. B: Condens. Matter Mater. Phys.* **1999**, *60*, 13520−13533.
(357) Billinge, S. J. L.; Kanatzidis, M. G. Beyond Crystallography: The Study of Disorder, Nanocrystallinity and Crystallographically Challenged Materials with Pair Distribution Functions. *Chem. Commun.* **2004**, 749−760.
(358) Billinge, S. J. L. The Rise of the X-Ray Atomic Pair Distribution Function Method: A Series of Fortunate Events. *Philos. Trans. R. Soc., A* **2019**, *377*, 20180413.
(359) Ren, Y.; Zuo, X. B. Synchrotron X-Ray and Neutron Diffraction, Total Scattering, and Small-Angle Scattering Techniques for Rechargeable Battery Research. *Small Methods* **2018**, *2*, 1800064.
(360) Newton, M. A. Time Resolved Operando X-Ray Techniques in Catalysis, a Case Study: Co Oxidation by O-2 over Pt Surfaces and Alumina Supported Pt Catalysts. *Catalysts* **2017**, *7*, 58.
(361) Benmore, C. A Review of High-Energy X-Ray Diffraction from Glasses and Liquids. *ISRN Materials Science* **2012**, *2012*, 1−19.
(362) Chupas, P. J.; Chapman, K. W.; Chen, H. L.; Grey, C. P. Application of High-Energy X-Rays and Pair-Distribution-Function Analysis to Nano-Scale Structural Studies in Catalysis. *Catal. Today* **2009**, *145*, 213−219.
(363) Petkov, V. Nanostructure by High-Energy X-Ray Diffraction. *Mater. Today* **2008**, *11*, 28−38.
(364) Lebedev, D.; Pineda-Galvan, Y.; Tokimaru, Y.; Fedorov, A.; Kaeffer, N.; Coperet, C.; Pushkar, Y. The Key Ru-V = O Intermediate of Site-Isolated Mononuclear Water Oxidation Catalyst Detected by in Situ X-Ray Absorption Spectroscopy. *J. Am. Chem. Soc.* **2018**, *140*, 451−458.
(365) Gorlin, Y.; Lassalle-Kaiser, B.; Benck, J. D.; Gul, S.; Webb, S. M.; Yachandra, V. K.; Yano, J.; Jaramillo, T. F. In Situ X-Ray Absorption Spectroscopy Investigation of a Bifunctional Manganese Oxide Catalyst with High Activity for Electrochemical Water Oxidation and Oxygen Reduction. *J. Am. Chem. Soc.* **2013**, *135*, 8525−8534.
(366) Chatterjee, R.; Weninger, C.; Loukianov, A.; Gul, S.; Fuller, F. D.; Cheah, M. H.; Fransson, T.; Pham, C. C.; Nelson, S.; Song, S.; et al. Xanes and Exafs of Dilute Solutions of Transition Metals at Xfels. *J. Synchrotron Radiat.* **2019**, *26*, 1716−1724.
(367) Drevon, D.; Görlin, M.; Chernev, P.; Xi, L.; Dau, H.; Lange, K. M. Uncovering the Role of Oxygen in Ni-Fe(Oxhy) Electrocatalysts Using in Situ Soft X-Ray Absorption Spectroscopy During the Oxygen Evolution Reaction. *Sci. Rep.* **2019**, *9*, 1532.
(368) Bordiga, S.; Groppo, E.; Agostini, G.; van Bokhoven, J. A.; Lamberti, C. Reactivity of Surface Species in Heterogeneous Catalysts Probed by in Situ X-Ray Absorption Techniques. *Chem. Rev.* **2013**, *113*, 1736−1850.
(369) van Oversteeg, C. H. M.; Doan, H. Q.; de Groot, F. M. F.; Cuk, T. In Situ X-Ray Absorption Spectroscopy of Transition Metal Based Water Oxidation Catalysts. *Chem. Soc. Rev.* **2017**, *46*, 102−125.
(370) Bergmann, A.; Jones, T. E.; Martinez Moreno, E.; Teschner, D.; Chernev, P.; Gliech, M.; Reier, T.; Dau, H.; Strasser, P. Unified Structural Motifs of the Catalytically Active State of Co(Oxyhydr)-Oxides During the Electrochemical Oxygen Evolution Reaction. *Nature Catalysis* **2018**, *1*, 711−719.
(371) Risch, M.; Ringleb, F.; Kohlhoff, M.; Bogdanoff, P.; Chernev, P.; Zaharieva, I.; Dau, H. Water Oxidation by Amorphous Cobalt-Based Oxides: In Situ Tracking of Redox Transitions and Mode of Catalysis. *Energy Environ. Sci.* **2015**, *8*, 661−674.
(372) Kanan, M. W.; Yano, J.; Surendranath, Y.; Dinca, M.; Yachandra, V. K.; Nocera, D. G. Structure and Valency of a Cobalt-Phosphate Water Oxidation Catalyst Determined by in Situ X-Ray Spectroscopy. *J. Am. Chem. Soc.* **2010**, *132*, 13692−13701.
(373) Waldman, R. Z.; Choudhury, D.; Mandia, D. J.; Elam, J. W.; Nealey, P. F.; Martinson, A. B. F.; Darling, S. B. Sequential Infiltration Synthesis of Al2o3 in Polyethersulfone Membranes. *JOM* **2019**, *71*, 212−223.
(374) Roelsgaard, M.; Dippel, A.-C.; Borup, K. A.; Nielsen, I. G.; Broge, N. L. N.; Roh, J. T.; Gutowski, O.; Iversen, B. B. Time-Resolved Grazing-Incidence Pair Distribution Functions During Deposition by Radio-Frequency Magnetron Sputtering. *IUCrJ* **2019**, *6*, 299−304.
(375) Dippel, A.-C.; Gutowski, O.; Klemeyer, L.; Boettger, U.; Berg, F.; Schneller, T.; Hardtdegen, A.; Aussen, S.; Hoffmann-Eifert, S.; Zimmermann, M. V. Evolution of Short-Range Order in Chemically and Physically Grown Thin Film Bilayer Structures for Electronic Applications. *Nanoscale* **2020**, *12*, 13103−13112.
(376) Dippel, A.-C.; Roelsgaard, M.; Boettger, U.; Schneller, T.; Gutowski, O.; Ruett, U. Local Atomic Structure of Thin and Ultrathin Films Via Rapid High-Energy X-Ray Total Scattering at Grazing Incidence. *IUCrJ* **2019**, *6*, 290−298.
(377) Bard, A. J.; Falkner, L. R. *Electroanalytical Methods: Fundamentals and Applications*, 2nd ed.; John Wiley & Sons, Inc.: New York, 2001.
(378) Elgrishi, N.; Rountree, K. J.; McCarthy, B. D.; Rountree, E. S.; Eisenhart, T. T.; Dempsey, J. L. A Practical Beginner's Guide to Cyclic Voltammetry. *J. Chem. Educ.* **2018**, *95*, 197−206.
(379) Lee, K. J.; McCarthy, B. D.; Dempsey, J. L. On Decomposition, Degradation, and Voltammetric Deviation: The Electrochemist's Field Guide to Identifying Precatalyst Transformation. *Chem. Soc. Rev.* **2019**, *48*, 2927−2945.

https://doi.org/10.1021/acs.chemrev.1c00069
Chem. Rev. 2021, 121, 9450−9501

(380) Costentin, C.; Savéant, J.-M. Homogeneous Molecular Catalysis of Electrochemical Reactions: Catalyst Benchmarking and Optimization Strategies. *J. Am. Chem. Soc.* **2017**, *139*, 8245−8250.
(381) Jackson, M. N.; Surendranath, Y. Molecular Control of Heterogeneous Electrocatalysis through Graphite Conjugation. *Acc. Chem. Res.* **2019**, *52*, 3432−3441.
(382) Stamenkovic, V. R.; Strmcnik, D.; Lopes, P. P.; Markovic, N. M. Energy and Fuels from Electrochemical Interfaces. *Nat. Mater.* **2017**, *16*, 57−69.
(383) Waegele, M. M.; Gunathunge, C. M.; Li, J.; Li, X. How Cations Affect the Electric Double Layer and the Rates and Selectivity of Electrocatalytic Processes. *J. Chem. Phys.* **2019**, *151*, 160902.
(384) Parsons, R. The Electrical Double Layer: Recent Experimental and Theoretical Developments. *Chem. Rev.* **1990**, *90*, 813−826.
(385) Das, S.; Chakraborty, S.; Mitra, S. K. Redefining Electrical Double Layer Thickness in Narrow Confinements: Effect of Solvent Polarization. *Phys. Rev. E* **2012**, *85*, 051508.
(386) Misra, R. P.; Das, S.; Mitra, S. K. Electric Double Layer Force between Charged Surfaces: Effect of Solvent Polarization. *J. Chem. Phys.* **2013**, *138*, 114703.
(387) Ge, A.; Videla, P. E.; Lee, G. L.; Rudshteyn, B.; Song, J.; Kubiak, C. P.; Batista, V. S.; Lian, T. Interfacial Structure and Electric Field Probed by in Situ Electrochemical Vibrational Stark Effect Spectroscopy and Computational Modeling. *J. Phys. Chem. C* **2017**, *121*, 18674−18682.
(388) Johansson, P. G.; Kopecky, A.; Galoppini, E.; Meyer, G. J. Distance Dependent Electron Transfer at Tio2 Interfaces Sensitized with Phenylene Ethynylene Bridged Ruii-Isothiocyanate Compounds. *J. Am. Chem. Soc.* **2013**, *135*, 8331−8341.
(389) Beh, E. S.; Basun, S. A.; Feng, X.; Idehenre, I. U.; Evans, D. R.; Kanan, M. W. Molecular Catalysis at Polarized Interfaces Created by Ferroelectric Batio3. *Chemical Science* **2017**, *8*, 2790−2794.
(390) Gorin, C. F.; Beh, E. S.; Bui, Q. M.; Dick, G. R.; Kanan, M. W. Interfacial Electric Field Effects on a Carbene Reaction Catalyzed by Rh Porphyrins. *J. Am. Chem. Soc.* **2013**, *135*, 11257−11265.
(391) Gorin, C. F.; Beh, E. S.; Kanan, M. W. An Electric Field-Induced Change in the Selectivity of a Metal Oxide-Catalyzed Epoxide Rearrangement. *J. Am. Chem. Soc.* **2012**, *134*, 186−189.
(392) Thämer, M.; De Marco, L.; Ramasesha, K.; Mandal, A.; Tokmakoff, A. Ultrafast 2d Ir Spectroscopy of the Excess Proton in Liquid Water. *Science* **2015**, *350*, 78−82.
(393) Dahms, F.; Fingerhut, B. P.; Nibbering, E. T.; Pines, E.; Elsaesser, T. Large-Amplitude Transfer Motion of Hydrated Excess Protons Mapped by Ultrafast 2d Ir Spectroscopy. *Science* **2017**, *357*, 491−495.
(394) Fournier, J. A.; Carpenter, W. B.; Lewis, N. H.; Tokmakoff, A. Broadband 2d Ir Spectroscopy Reveals Dominant Asymmetric H 5 O 2+ Proton Hydration Structures in Acid Solutions. *Nat. Chem.* **2018**, *10*, 932−937.
(395) Yan, C.; Nishida, J.; Yuan, R.; Fayer, M. D. Water of Hydration Dynamics in Minerals Gypsum and Bassanite: Ultrafast 2d Ir Spectroscopy of Rocks. *J. Am. Chem. Soc.* **2016**, *138*, 9694−9703.
(396) Yamada, S. A.; Shin, J. Y.; Thompson, W. H.; Fayer, M. D. Water Dynamics in Nanoporous Silica: Ultrafast Vibrational Spectroscopy and Molecular Dynamics Simulations. *J. Phys. Chem. C* **2019**, *123*, 5790−5803.
(397) Roget, S. A.; Kramer, P. L.; Thomaz, J. E.; Fayer, M. D. Bulk-Like and Interfacial Water Dynamics in Nafion Fuel Cell Membranes Investigated with Ultrafast Nonlinear Ir Spectroscopy. *J. Phys. Chem. B* **2019**, *123*, 9408−9417.
(398) Huber, C. J.; Egger, S. M.; Spector, I. C.; Juelfs, A. R.; Haynes, C. L.; Massari, A. M. 2d-Ir Spectroscopy of Porous Silica Nanoparticles: Measuring the Distance Sensitivity of Spectral Diffusion. *J. Phys. Chem. C* **2015**, *119*, 25135−25144.
(399) Thompson, W. H. Perspective: Dynamics of Confined Liquids. *J. Chem. Phys.* **2018**, *149*, 170901.
(400) Agmon, N.; Bakker, H. J.; Campen, R. K.; Henchman, R. H.; Pohl, P.; Roke, S.; Thämer, M.; Hassanali, A. Protons and Hydroxide Ions in Aqueous Systems. *Chem. Rev.* **2016**, *116*, 7642−7672.
(401) Laage, D.; Thompson, W. H. Reorientation Dynamics of Nanoconfined Water: Power-Law Decay, Hydrogen-Bond Jumps, and Test of a Two-State Model. *J. Chem. Phys.* **2012**, *136*, 044513.
(402) Thompson, W. H. Solvation Dynamics and Proton Transfer in Nanoconfined Liquids. *Annu. Rev. Phys. Chem.* **2011**, *62*, 599−619.
(403) Chen, L.; Shi, G.; Shen, J.; Peng, B.; Zhang, B.; Wang, Y.; Bian, F.; Wang, J.; Li, D.; Qian, Z. Ion Sieving in Graphene Oxide Membranes Via Cationic Control of Interlayer Spacing. *Nature* **2017**, *550*, 380−383.
(404) Park, H. B.; Kamcev, J.; Robeson, L. M.; Elimelech, M.; Freeman, B. D. Maximizing the Right Stuff: The Trade-Off between Membrane Permeability and Selectivity. *Science* **2017**, *356*, eaab0530.
(405) Darling, S. B.; Yang, H.-C. Introduction to Molecular Engineering for Water Technologies. *Molecular Systems Design & Engineering* **2020**, *5*, 900−901.
(406) Velasco-Velez, J.-J.; Wu, C. H.; Pascal, T. A.; Wan, L. F.; Guo, J.; Prendergast, D.; Salmeron, M. The Structure of Interfacial Water on Gold Electrodes Studied by X-Ray Absorption Spectroscopy. *Science* **2014**, *346*, 831−834.
(407) Ryczko, K.; Tamblyn, I. Structural Characterization of Water-Metal Interfaces. *Phys. Rev. B: Condens. Matter Mater. Phys.* **2017**, *96*, 064104.
(408) Cicero, G.; Grossman, J. C.; Schwegler, E.; Gygi, F.; Galli, G. Water Confined in Nanotubes and between Graphene Sheets: A First Principle Study. *J. Am. Chem. Soc.* **2008**, *130*, 1871−1878.
(409) Pham, T. A.; Ping, Y.; Galli, G. Modelling Heterogeneous Interfaces for Solar Water Splitting. *Nat. Mater.* **2017**, *16*, 401−408.
(410) Dufils, T.; Jeanmairet, G.; Rotenberg, B.; Sprik, M.; Salanne, M. Simulating Electrochemical Systems by Combining the Finite Field Method with a Constant Potential Electrode. *Phys. Rev. Lett.* **2019**, *123*, 195501.
(411) Sayer, T.; Sprik, M.; Zhang, C. Finite Electric Displacement Simulations of Polar Ionic Solid-Electrolyte Interfaces: Application to Nacl (111)/Aqueous Nacl Solution. *J. Chem. Phys.* **2019**, *150*, 041716.
(412) Zhang, C.; Sayer, T.; Hutter, J.; Sprik, M. Modelling Electrochemical Systems with Finite Field Molecular Dynamics. *Journal of Physics: Energy* **2020**, *2*, 032005.
(413) Zhang, C.; Hutter, J. R.; Sprik, M. Coupling of Surface Chemistry and Electric Double Layer at Tio2 Electrochemical Interfaces. *J. Phys. Chem. Lett.* **2019**, *10*, 3871−3876.
(414) Gerosa, M.; Gygi, F.; Govoni, M.; Galli, G. The Role of Defects and Excess Surface Charges at Finite Temperature for Optimizing Oxide Photoabsorbers. *Nat. Mater.* **2018**, *17*, 1122−1127.
(415) Smart, T. J.; Pham, T. A.; Ping, Y.; Ogitsu, T. Optical Absorption Induced by Small Polaron Formation in Transition Metal Oxides: The Case of Co 3 O 4. *Phys. Rev. Mater.* **2019**, *3*, 102401.
(416) Hegner, F. S.; Forrer, D.; Galán-Mascarós, J. R.; López, N.; Selloni, A. Versatile Nature of Oxygen Vacancies in Bismuth Vanadate Bulk and (001) Surface. *J. Phys. Chem. Lett.* **2019**, *10*, 6672−6678.
(417) Ping, Y.; Goddard, W. A.; Galli, G. A. Energetics and Solvation Effects at the Photoanode/Catalyst Interface: Ohmic Contact Versus Schottky Barrier. *J. Am. Chem. Soc.* **2015**, *137*, 5264−5267.
(418) Kohn, W.; Sham, L. J. Self-Consistent Equations Including Exchange and Correlation Effects. *Phys. Rev.* **1965**, *140*, A1133−A1138.
(419) Heyd, J.; Scuseria, G. E.; Ernzerhof, M. Hybrid Functionals Based on a Screened Coulomb Potential. *J. Chem. Phys.* **2003**, *118*, 8207−8215.
(420) Heyd, J.; Scuseria, G. E.; Ernzerhof, M. Erratum:"Hybrid Functionals Based on a Screened Coulomb Potential. *J. Chem. Phys.* **2003**, *118*, 8207; *J. Chem. Phys.* **2006**, *124*, 219906.
(421) Skone, J. H.; Govoni, M.; Galli, G. Self-Consistent Hybrid Functional for Condensed Systems. *Phys. Rev. B: Condens. Matter Mater. Phys.* **2014**, *89*, 195112.
(422) Car, R.; Parrinello, M. Unified Approach for Molecular Dynamics and Density-Functional Theory. *Phys. Rev. Lett.* **1985**, *55*, 2471−2474.
(423) Cicero, G.; Grossman, J. C.; Catellani, A.; Galli, G. Water at a Hydrophilic Solid Surface Probed by Ab Initio Molecular Dynamics:

https://doi.org/10.1021/acs.chemrev.1c00069
Chem. Rev. 2021, 121, 9450−9501

Inhomogeneous Thin Layers of Dense Fluid. *J. Am. Chem. Soc.* **2005**, *127*, 6830−6835.
(424) Selcuk, S.; Selloni, A. Facet-Dependent Trapping and Dynamics of Excess Electrons at Anatase Tio 2 Surfaces and Aqueous Interfaces. *Nat. Mater.* **2016**, *15*, 1107−1112.
(425) Wang, W.; Strohbeen, P. J.; Lee, D.; Zhou, C.; Kawasaki, J. K.; Choi, K.-S.; Liu, M.; Galli, G. The Role of Surface Oxygen Vacancies in Bivo4. *Chem. Mater.* **2020**, *32*, 2899−2909.
(426) Hörmann, N. G.; Guo, Z.; Ambrosio, F.; Andreussi, O.; Pasquarello, A.; Marzari, N. Absolute Band Alignment at Semiconductor-Water Interfaces Using Explicit and Implicit Descriptions for Liquid Water. *npj Computational Materials* **2019**, *5*, 1−6.
(427) Ping, Y.; Rocca, D.; Galli, G. Electronic Excitations in Light Absorbers for Photoelectrochemical Energy Conversion: First Principles Calculations Based on Many Body Perturbation Theory. *Chem. Soc. Rev.* **2013**, *42*, 2437−2469.
(428) Harmon, K. J.; Letchworth-Weaver, K.; Gaiduk, A. P.; Giberti, F.; Gygi, F.; Chan, M. K. Y.; Fenter, P.; Galli, G. Validating First-Principles Molecular Dynamics Calculations of Oxide/Water Interfaces with X-Ray Reflectivity Data. *Phys. Rev. Mater.* **2020**, *4*, 113085.
(429) Rozsa, V.; Pham, T. A.; Galli, G. Molecular Polarizabilities as Fingerprints of Perturbations to Water by Ions and Confinement. *J. Chem. Phys.* **2020**, *152*, 124501.
(430) Schmitt, U. W.; Voth, G. A. Multistate Empirical Valence Bond Model for Proton Transport in Water. *J. Phys. Chem. B* **1998**, *102*, 5547−5551.
(431) Schmitt, U. W.; Voth, G. A. The Computer Simulation of Proton Transport in Water. *J. Chem. Phys.* **1999**, *111*, 9361−9381.
(432) Wu, Y.; Chen, H.; Wang, F.; Paesani, F.; Voth, G. A. An Improved Multistate Empirical Valence Bond Model for Aqueous Proton Solvation and Transport. *J. Phys. Chem. B* **2008**, *112*, 467−482.
(433) Yamashita, T.; Peng, Y.; Knight, C.; Voth, G. A. Computationally Efficient Multiconfigurational Reactive Molecular Dynamics. *J. Chem. Theory Comput.* **2012**, *8*, 4863−4875.
(434) Day, T. J. F.; Soudackov, A. V.; Cuma, M.; Schmitt, U. W.; Voth, G. A. A Second Generation Multistate Empirical Valence Bond Model for Proton Transport in Aqueous Systems. *J. Chem. Phys.* **2002**, *117*, 5839−5849.
(435) Knight, C.; Lindberg, G. E.; Voth, G. A. Multiscale Reactive Molecular Dynamics. *J. Chem. Phys.* **2012**, *137*, 22A525.
(436) de Grotthuss, C. J. T. Sur La Décomposition De L'eau Et Des Corps Qu'elle Tient En Dissolution À L'aide De L'éLectricité Galvanique. *Annals of Chemistry and of Physics* **1806**, *58*, 54−73.
(437) Knight, C.; Voth, G. A. The Curious Case of the Hydrated Proton. *Acc. Chem. Res.* **2012**, *45*, 101−109.
(438) Brewer, M. L.; Schmitt, U. W.; Voth, G. A. The Formation and Dynamics of Proton Wires in Channel Environments. *Biophys. J.* **2001**, *80*, 1691−1702.
(439) Dellago, C.; Hummer, G. Kinetics and Mechanism of Proton Transport across Membrane Nanopores. *Phys. Rev. Lett.* **2006**, *97*, 245901.
(440) Peng, Y.; Swanson, J. M.; Kang, S. G.; Zhou, R.; Voth, G. A. Hydrated Excess Protons Can Create Their Own Water Wires. *J. Phys. Chem. B* **2015**, *119*, 9212−9218.
(441) Ma, X.; Li, C.; Martinson, A. F. B.; Voth, G. A. Water-Assisted Proton Transport in Confined Nanochannels. *J. Phys. Chem. C* **2020**, *124*, 16186−16201.
(442) Olson, D. H.; Kokotailo, G. T.; Lawton, S. L.; Meier, W. M. Crystal Structure and Structure-Related Properties of Zsm-5. *J. Phys. Chem.* **1981**, *85*, 2238−2243.
(443) van Santen, R. A.; Kramer, G. J. Reactivity Theory of Zeolitic Broensted Acidic Sites. *Chem. Rev.* **1995**, *95*, 637−660.
(444) Ryder, J. A.; Chakraborty, A. K.; Bell, A. T. Density Functional Theory Study of Proton Mobility in Zeolites: Proton Migration and Hydrogen Exchange in Zsm-5. *J. Phys. Chem. B* **2000**, *104*, 6998−7011.
(445) Franke, M. E.; Simon, U. Solvate-Supported Proton Transport in Zeolites. *ChemPhysChem* **2004**, *5*, 465−472.
(446) Kletnieks, P. W.; Ehresmann, J. O.; Nicholas, J. B.; Haw, J. F. Adsorbate Clustering and Proton Transfer in Zeolites: Nmr Spectroscopy and Theory. *ChemPhysChem* **2006**, *7*, 114−116.
(447) Alberti, A.; Martucci, A. Proton Transfer Mediated by Water: Experimental Evidence by Neutron Diffraction. *J. Phys. Chem. C* **2010**, *114*, 7767−7773.
(448) Van Speybroeck, V.; Hemelsoet, K.; Joos, L.; Waroquier, M.; Bell, R. G.; Catlow, C. R. A. Advances in Theory and Their Application within the Field of Zeolite Chemistry. *Chem. Soc. Rev.* **2015**, *44*, 7044−7111.
(449) Franke, M. E.; Simon, U. Proton Mobility in H-Zsm5 Studied by Impedance Spectroscopy. *Solid State Ionics* **1999**, *118*, 311−316.
(450) Zygmunt, S. A.; Curtiss, L. A.; Iton, L. E.; Erhardt, M. K. Computational Studies of Water Adsorption in the Zeolite H-Zsm-5. *J. Phys. Chem.* **1996**, *100*, 6663−6671.
(451) Olson, D. H.; Zygmunt, S. A.; Erhardt, M. K.; Curtiss, L. A.; Iton, L. E. Evidence for Dimeric and Tetrameric Water Clusters in Hzsm-5. *Zeolites* **1997**, *18*, 347−349.
(452) Franke, M. E.; Sierka, M.; Simon, U.; Sauer, J. Translational Proton Motion in Zeolite H-Zsm-5. Energy Barriers and Jump Rates from Dft Calculations. *Phys. Chem. Chem. Phys.* **2002**, *4*, 5207−5216.
(453) Jones, A. J.; Iglesia, E. The Strength of Brønsted Acid Sites in Microporous Aluminosilicates. *ACS Catal.* **2015**, *5*, 5741−5755.
(454) Li, Y.-P.; Gomes, J.; Mallikarjun Sharada, S.; Bell, A. T.; Head-Gordon, M. Improved Force-Field Parameters for Qm/Mm Simulations of the Energies of Adsorption for Molecules in Zeolites and a Free Rotor Correction to the Rigid Rotor Harmonic Oscillator Model for Adsorption Enthalpies. *J. Phys. Chem. C* **2015**, *119*, 1840−1850.
(455) Patet, R. E.; Caratzoulas, S.; Vlachos, D. G. Adsorption in Zeolites Using Mechanically Embedded Oniom Clusters. *Phys. Chem. Chem. Phys.* **2016**, *18*, 26094−26106.
(456) Mi, Q.; Ping, Y.; Li, Y.; Cao, B.; Brunschwig, B. S.; Khalifah, P. G.; Galli, G. A.; Gray, H. B.; Lewis, N. S. Thermally Stable N2-Intercalated Wo3 Photoanodes for Water Oxidation. *J. Am. Chem. Soc.* **2012**, *134*, 18318−18324.
(457) Govoni, M.; Galli, G. Large Scale Gw Calculations. *J. Chem. Theory Comput.* **2015**, *11*, 2680−2696.
(458) Hohenberg, P.; Kohn, W. Inhomogeneous Electron Gas. *Phys. Rev.* **1964**, *136*, B864−B871.
(459) Martin, R. M. *Electronic Structure: Basic Theory and Practical Methods*; Cambridge University Press, 2004.
(460) Perdew, J. P.; Ernzerhof, M.; Burke, K. Rationale for Mixing Exact Exchange with Density Functional Approximations. *J. Chem. Phys.* **1996**, *105*, 9982−9985.
(461) Zheng, H.; Govoni, M.; Galli, G. Dielectric-Dependent Hybrid Functionals for Heterogeneous Materials. *Phys. Rev. Mater.* **2019**, *3*, 073803.
(462) Wan, Q.; Galli, G. First-Principles Framework to Compute Sum-Frequency Generation Vibrational Spectra of Semiconductors and Insulators. *Phys. Rev. Lett.* **2015**, *115*, 246404.
(463) Voth, G. A. *Coarse-Graining of Condensed Phase and Biomolecular Systems*; CRC Press, 2008.
(464) Sevgen, E.; Giberti, F.; Sidky, H.; Whitmer, J. K.; Galli, G.; Gygi, F.; de Pablo, J. J. Hierarchical Coupling of First-Principles Molecular Dynamics with Advanced Sampling Methods. *J. Chem. Theory Comput.* **2018**, *14*, 2881−2888.
(465) Sidky, H.; Colón, Y. J.; Helfferich, J.; Sikora, B. J.; Bezik, C.; Chu, W.; Giberti, F.; Guo, A. Z.; Jiang, X.; Lequieu, J.; et al. Ssages: Software Suite for Advanced General Ensemble Simulations. *J. Chem. Phys.* **2018**, *148*, 044104.
(466) Shaffer, P.; Valsson, O.; Parrinello, M. Enhanced, Targeted Sampling of High-Dimensional Free-Energy Landscapes Using Variationally Enhanced Sampling, with an Application to Chignolin. *Proc. Natl. Acad. Sci. U. S. A.* **2016**, *113*, 1150−1155.
(467) Guo, A. Z.; Sevgen, E.; Sidky, H.; Whitmer, J. K.; Hubbell, J. A.; de Pablo, J. J. Adaptive Enhanced Sampling by Force-Biasing Using Neural Networks. *J. Chem. Phys.* **2018**, *148*, 134108.
(468) Sevgen, E.; Guo, A. Z.; Sidky, H.; Whitmer, J. K.; de Pablo, J. J. Combined Force-Frequency Sampling for Simulation of Systems

https://doi.org/10.1021/acs.chemrev.1c00069
Chem. Rev. 2021, 121, 9450−9501

Having Rugged Free Energy Landscapes. *J. Chem. Theory Comput.* **2020**, *16*, 1448−1455.
(469) Pham, T. A. Ab Initio Simulations of Liquid Electrolytes for Energy Conversion and Storage. *Int. J. Quantum Chem.* **2019**, *119*, No. e25795.
(470) Ong, M. T.; Bhatia, H.; Gyulassy, A. G.; Draeger, E. W.; Pascucci, V.; Bremer, P.-T.; Lordi, V.; Pask, J. E. Complex Ion Dynamics in Carbonate Lithium-Ion Battery Electrolytes. *J. Phys. Chem. C* **2017**, *121*, 6589−6595.
(471) Kim, S. J.; Wang, Y.-C.; Lee, J. H.; Jang, H.; Han, J. Concentration Polarization and Nonlinear Electrokinetic Flow near a Nanofluidic Channel. *Phys. Rev. Lett.* **2007**, *99*, 044501.
(472) Schoch, R. B.; Han, J.; Renaud, P. Transport Phenomena in Nanofluidics. *Rev. Mod. Phys.* **2008**, *80*, 839−883.
(473) Pan, D.; Galli, G. A First Principles Method to Determine Speciation of Carbonates in Supercritical Water. *Nat. Commun.* **2020**, *11*, 421.
(474) Choi, W.; Ulissi, Z. W.; Shimizu, S. F.; Bellisario, D. O.; Ellison, M. D.; Strano, M. S. Diameter-Dependent Ion Transport through the Interior of Isolated Single-Walled Carbon Nanotubes. *Nat. Commun.* **2013**, *4*, 2397.
(475) Wang, Z.; Parrondo, J.; He, C.; Sankarasubramanian, S.; Ramani, V. Efficient Ph-Gradient-Enabled Microscale Bipolar Interfaces in Direct Borohydride Fuel Cells. *Nature Energy* **2019**, *4*, 281−289.
(476) King, L. A.; Hubert, M. A.; Capuano, C.; Manco, J.; Danilovic, N.; Valle, E.; Hellstern, T. R.; Ayers, K.; Jaramillo, T. F. A Non-Precious Metal Hydrogen Catalyst in a Commercial Polymer Electrolyte Membrane Electrolyser. *Nat. Nanotechnol.* **2019**, *14*, 1071−1074.
(477) Lin, K.; Gómez-Bombarelli, R.; Beh, E. S.; Tong, L.; Chen, Q.; Valle, A.; Aspuru-Guzik, A.; Aziz, M. J.; Gordon, R. G. A Redox-Flow Battery with an Alloxazine-Based Organic Electrolyte. *Nature Energy* **2016**, *1*, 16102.
(478) Eastman, S. A.; Kim, S.; Page, K. A.; Rowe, B. W.; Kang, S.; Soles, C. L.; Yager, K. G. Effect of Confinement on Structure, Water Solubility, and Water Transport in Nafion Thin Films. *Macromolecules* **2012**, *45*, 7920−7930.
(479) Zhou, C.; Segal-Peretz, T.; Oruc, M. E.; Suh, H. S.; Wu, G.; Nealey, P. F. Fabrication of Nanoporous Alumina Ultrafiltration Membrane with Tunable Pore Size Using Block Copolymer Templates. *Adv. Funct. Mater.* **2017**, *27*, 1701756.
(480) Bundschuh, M.; Filser, J.; Lüderwald, S.; McKee, M. S.; Metreveli, G.; Schaumann, G. E.; Schulz, R.; Wagner, S. Nanoparticles in the Environment: Where Do We Come from, Where Do We Go To? *Environ. Sci. Eur.* **2018**, *30*, 6.
(481) Zobel, M.; Neder, R. B.; Kimber, S. A. J. Universal Solvent Restructuring Induced by Colloidal Nanoparticles. *Science* **2015**, *347*, 292−294.
(482) Simeonidis, K.; Martinez-Boubeta, C.; Zamora-Pérez, P.; Rivera-Gil, P.; Kaprara, E.; Kokkinos, E.; Mitrakas, M. Implementing Nanoparticles for Competitive Drinking Water Purification. *Environ. Chem. Lett.* **2019**, *17*, 705−719.
(483) Warkiani, M. E.; Bhagat, A. A. S.; Khoo, B. L.; Han, J.; Lim, C. T.; Gong, H. Q.; Fane, A. G. Isoporous Micro/Nanoengineered Membranes. *ACS Nano* **2013**, *7*, 1882−1904.
(484) Feng, X.; Kawabata, K.; Kaufman, G.; Elimelech, M.; Osuji, C. O. Highly Selective Vertically Aligned Nanopores in Sustainably Derived Polymer Membranes by Molecular Templating. *ACS Nano* **2017**, *11*, 3911−3921.
(485) Phillip, W. A.; O'Neill, B.; Rodwogin, M.; Hillmyer, M. A.; Cussler, E. Self-Assembled Block Copolymer Thin Films as Water Filtration Membranes. *ACS Appl. Mater. Interfaces* **2010**, *2*, 847−853.
(486) Phillip, W. A.; Dorin, R. M.; Werner, J. R.; Hoek, E. M.; Wiesner, U.; Elimelech, M. Tuning Structure and Properties of Graded Triblock Terpolymer-Based Mesoporous and Hybrid Films. *Nano Lett.* **2011**, *11*, 2892−2900.
(487) Kambe, Y.; Arges, C. G.; Czaplewski, D. A.; Dolejsi, M.; Krishnan, S.; Stoykovich, M. P.; de Pablo, J. J.; Nealey, P. F. Role of Defects in Ion Transport in Block Copolymer Electrolytes. *Nano Lett.* **2019**, *19*, 4684−4691.
(488) Bates, F. S.; Hillmyer, M. A.; Lodge, T. P.; Bates, C. M.; Delaney, K. T.; Fredrickson, G. H. Multiblock Polymers: Panacea or Pandora's Box? *Science* **2012**, *336*, 434−440.
(489) Barry, E.; McBride, S. P.; Jaeger, H. M.; Lin, X.-M. Ion Transport Controlled by Nanoparticle-Functionalized Membranes. *Nat. Commun.* **2014**, *5*, 5847.
(490) Zhang, Y.; Almodovar-Arbelo, N. E.; Weidman, J. L.; Corti, D. S.; Boudouris, B. W.; Phillip, W. A. Fit-for-Purpose Block Polymer Membranes Molecularly Engineered for Water Treatment. *npj Clean Water* **2018**, *1*, 2.
(491) Stuart, M. A. C.; Huck, W. T.; Genzer, J.; Müller, M.; Ober, C.; Stamm, M.; Sukhorukov, G. B.; Szleifer, I.; Tsukruk, V. V.; Urban, M.; et al. Emerging Applications of Stimuli-Responsive Polymer Materials. *Nat. Mater.* **2010**, *9*, 101−113.
(492) Wang, Z.; Yang, X.; Cheng, Z.; Liu, Y.; Shao, L.; Jiang, L. Simply Realizing "Water Diode" Janus Membranes for Multifunctional Smart Applications. *Mater. Horiz.* **2017**, *4*, 701−708.
(493) Guo, W.; Cao, L.; Xia, J.; Nie, F. Q.; Ma, W.; Xue, J.; Song, Y.; Zhu, D.; Wang, Y.; Jiang, L. Energy Harvesting with Single-Ion-Selective Nanopores: A Concentration-Gradient-Driven Nanofluidic Power Source. *Adv. Funct. Mater.* **2010**, *20*, 1339−1344.
(494) Yang, H. C.; Xie, Y.; Hou, J.; Cheetham, A. K.; Chen, V.; Darling, S. B. Janus Membranes: Creating Asymmetry for Energy Efficiency. *Adv. Mater.* **2018**, *30*, 1801495.
(495) Zhang, Z.; Kong, X.-Y.; Xiao, K.; Liu, Q.; Xie, G.; Li, P.; Ma, J.; Tian, Y.; Wen, L.; Jiang, L. Engineered Asymmetric Heterogeneous Membrane: A Concentration-Gradient-Driven Energy Harvesting Device. *J. Am. Chem. Soc.* **2015**, *137*, 14765−14772.
(496) Waldman, R. Z.; Yang, H. C.; Mandia, D. J.; Nealey, P. F.; Elam, J. W.; Darling, S. B. Janus Membranes Via Diffusion-Controlled Atomic Layer Deposition. *Adv. Mater. Interfaces* **2018**, *5*, 1800658.
(497) Bishop, K. J. M.; Wilmer, C. E.; Soh, S.; Grzybowski, B. A. Nanoscale Forces and Their Uses in Self-Assembly. *Small* **2009**, *5*, 1600−1630.
(498) Walker, D. A.; Kowalczyk, B.; de la Cruz, M. O.; Grzybowski, B. A. Electrostatics at the Nanoscale. *Nanoscale* **2011**, *3*, 1316−1344.
(499) Kamysbayev, V.; Srivastava, V.; Ludwig, N. B.; Borkiewicz, O. J.; Zhang, H.; Ilavsky, J.; Lee, B.; Chapman, K. W.; Vaikuntanathan, S.; Talapin, D. V. Nanocrystals in Molten Salts and Ionic Liquids: Experimental Observation of Ionic Correlations Extending Beyond the Debye Length. *ACS Nano* **2019**, *13*, 5760−5770.
(500) Smith, A. M.; Lee, A. A.; Perkin, S. The Electrostatic Screening Length in Concentrated Electrolytes Increases with Concentration. *J. Phys. Chem. Lett.* **2016**, *7*, 2157−2163.
(501) Israelachvili, J. N. *Intermolecular and Surface Forces*; Academic press, 2011.
(502) Zhang, H.; Dasbiswas, K.; Ludwig, N. B.; Han, G.; Lee, B.; Vaikuntanathan, S.; Talapin, D. V. Stable Colloids in Molten Inorganic Salts. *Nature* **2017**, *542*, 328−331.
(503) Grasso, D.; Subramaniam, K.; Butkus, M.; Strevett, K.; Bergendahl, J. A Review of Non-Dlvo Interactions in Environmental Colloidal Systems. *Rev. Environ. Sci. Bio/Technol.* **2002**, *1*, 17−38.
(504) Lee, A. A.; Perez-Martinez, C. S.; Smith, A. M.; Perkin, S. Scaling Analysis of the Screening Length in Concentrated Electrolytes. *Phys. Rev. Lett.* **2017**, *119*, 026002.
(505) Yin, Y.; Alivisatos, A. P. Colloidal Nanocrystal Synthesis and the Organic-Inorganic Interface. *Nature* **2005**, *437*, 664−670.
(506) Boles, M. A.; Ling, D.; Hyeon, T.; Talapin, D. V. The Surface Science of Nanocrystals. *Nat. Mater.* **2016**, *15*, 141−153.
(507) Kim, D.; Kim, J.; Park, Y. I.; Lee, N.; Hyeon, T. Recent Development of Inorganic Nanoparticles for Biomedical Imaging. *ACS Cent. Sci.* **2018**, *4*, 324−336.
(508) Wu, S.; Han, G.; Milliron, D. J.; Aloni, S.; Altoe, V.; Talapin, D. V.; Cohen, B. E.; Schuck, P. J. Non-Blinking and Photostable Upconverted Luminescence from Single Lanthanide-Doped Nanocrystals. *Proc. Natl. Acad. Sci. U. S. A.* **2009**, *106*, 10917−10921.

https://doi.org/10.1021/acs.chemrev.1c00069
Chem. Rev. 2021, 121, 9450−9501

(509) Bruns, O. T.; Bischof, T. S.; Harris, D. K.; Franke, D.; Shi, Y.; Riedemann, L.; Bartelt, A.; Jaworski, F. B.; Carr, J. A.; Rowlands, C. J.; et al. Next-Generation in Vivo Optical Imaging with Short-Wave Infrared Quantum Dots. *Nature Biomedical Engineering* **2017**, *1*, 1−11.
(510) Hu, J.; Li, L.-S.; Yang, W.; Manna, L.; Wang, L.-W.; Alivisatos, A. P. Linearly Polarized Emission from Colloidal Semiconductor Quantum Rods. *Science* **2001**, *292*, 2060−2063.
(511) Huang, Y.; Duan, X.; Wei, Q.; Lieber, C. M. Directed Assembly of One-Dimensional Nanostructures into Functional Networks. *Science* **2001**, *291*, 630−633.
(512) Cunningham, P. D.; Souza, J. B.; Fedin, I.; She, C.; Lee, B.; Talapin, D. V. Assessment of Anisotropic Semiconductor Nanorod and Nanoplatelet Heterostructures with Polarized Emission for Liquid Crystal Display Technology. *ACS Nano* **2016**, *10*, 5769−5781.
(513) Attia, M. F.; Wallyn, J.; Anton, N.; Vandamme, T. F. Inorganic Nanoparticles for X-Ray Computed Tomography Imaging. *Crit. Rev. Ther. Drug Carrier Syst.* **2018**, *35*, 391−431.
(514) Na, H. B.; Song, I. C.; Hyeon, T. Inorganic Nanoparticles for Mri Contrast Agents. *Adv. Mater.* **2009**, *21*, 2133−2148.
(515) Simeonidis, K.; Mourdikoudis, S.; Kaprara, E.; Mitrakas, M.; Polavarapu, L. Inorganic Engineered Nanoparticles in Drinking Water Treatment: A Critical Review. *Environmental Science: Water Research & Technology* **2016**, *2*, 43−70.
(516) Pradeep, T.; Anshup. Noble Metal Nanoparticles for Water Purification: A Critical Review. *Thin Solid Films* **2009**, *517*, 6441−6478.
(517) Dankovich, T. A.; Gray, D. G. Bactericidal Paper Impregnated with Silver Nanoparticles for Point-of-Use Water Treatment. *Environ. Sci. Technol.* **2011**, *45*, 1992−1998.
(518) He, J.; Lin, X.-M.; Chan, H.; Vuković, L.; Král, P.; Jaeger, H. M. Diffusion and Filtration Properties of Self-Assembled Gold Nanocrystal Membranes. *Nano Lett.* **2011**, *11*, 2430−2435.
(519) Yesibolati, M. N.; Laganá, S.; Kadkhodazadeh, S.; Mikkelsen, E. K.; Sun, H.; Kasama, T.; Hansen, O.; Zaluzec, N. J.; Mølhave, K. Electron Inelastic Mean Free Path in Water. *Nanoscale* **2020**, *12*, 20649−20657.
(520) Bard, A. J.; Fan, F. R. F.; Kwak, J.; Lev, O. Scanning Electrochemical Microscopy. Introduction and Principles. *Anal. Chem.* **1989**, *61*, 132−138.
(521) Bard, A. J.; Denuault, G.; Lee, C.; Mandler, D.; Wipf, D. O. Scanning Electrochemical Microscopy-a New Technique for the Characterization and Modification of Surfaces. *Acc. Chem. Res.* **1990**, *23*, 357−363.
(522) Bard, A. J.; Fan, F.-R. F.; Pierce, D. T.; Unwin, P. R.; Wipf, D. O.; Zhou, F. Chemical Imaging of Surfaces with the Scanning Electrochemical Microscope. *Science* **1991**, *254*, 68−74.
(523) Gardner, C. E.; Unwin, P. R.; Macpherson, J. V. Correlation of Membrane Structure and Transport Activity Using Combined Scanning Electrochemical-Atomic Force Microscopy. *Electrochem. Commun.* **2005**, *7*, 612−618.
(524) Watkins, T. S.; Sarbapalli, D.; Counihan, M. J.; Danis, A. S.; Zhang, J.; Zhang, L.; Zavadil, K. R.; Rodríguez-López, J. A Combined Secm and Electrochemical Afm Approach to Probe Interfacial Processes Affecting Molecular Reactivity at Redox Flow Battery Electrodes. *J. Mater. Chem. A* **2020**, *8*, 15734−15745.
(525) Scott, E. R.; White, H. S.; Phipps, J. B. Scanning Electrochemical Microscopy of a Porous Membrane. *J. Membr. Sci.* **1991**, *58*, 71−87.
(526) Nugues, S.; Denuault, G. Scanning Electrochemical Microscopy: Amperometric Probing of Diffusional Ion Fluexes through Porous Membranes and Human Dentine. *J. Electroanal. Chem.* **1996**, *408*, 125−140.
(527) Bath, B. D.; Lee, R. D.; White, H. S.; Scott, E. R. Imaging Molecular Transport in Porous Membranes. Observation and Analysis of Electroosmotic Flow in Individual Pores Using the Scanning Electrochemical Microscope. *Anal. Chem.* **1998**, *70*, 1047−1058.
(528) Edwards, M.; Robinson, D.; Ren, H.; Cheyne, C.; Tan, C.; White, H. Nanoscale Electrochemical Kinetics & Dynamics: The Challenges and Opportunities of Single-Entity Measurements. *Faraday Discuss.* **2018**, *210*, 9−28.
(529) Holzinger, A.; Neusser, G.; Austen, B. J.; Gamero-Quijano, A.; Herzog, G.; Arrigan, D. W.; Ziegler, A.; Walther, P.; Kranz, C. Investigation of Modified Nanopore Arrays Using Fib/Sem Tomography. *Faraday Discuss.* **2018**, *210*, 113−130.
(530) Balme, S.; Picaud, F.; Lepoitevin, M.; Bechelany, M.; Balanzat, E.; Janot, J.-M. Unexpected Ionic Transport Behavior in Hydrophobic and Uncharged Conical Nanopores. *Faraday Discuss.* **2018**, *210*, 69−85.
(531) Bae, J. H.; Yu, Y.; Mirkin, M. V. Scanning Electrochemical Microscopy Study of Electron-Transfer Kinetics and Catalysis at Nanoporous Electrodes. *J. Phys. Chem. C* **2016**, *120*, 20651−20658.
(532) Sun, T.; Wang, D.; Mirkin, M. V. Electrochemistry at a Single Nanoparticle: From Bipolar Regime to Tunnelling. *Faraday Discuss.* **2018**, *210*, 173−188.
(533) Cao, L.; He, X.; Jiang, Z.; Li, X.; Li, Y.; Ren, Y.; Yang, L.; Wu, H. Channel-Facilitated Molecule and Ion Transport across Polymer Composite Membranes. *Chem. Soc. Rev.* **2017**, *46*, 6725−6745.
(534) Scott, E. R.; White, H. S.; Phipps, J. B. Iontophoretic Transport through Porous Membranes Using Scanning Electrochemical Microscopy: Application to in Vitro Studies of Ion Fluxes through Skin. *Anal. Chem.* **1993**, *65*, 1537−1545.
(535) Kim, J.; Izadyar, A.; Nioradze, N.; Amemiya, S. Nanoscale Mechanism of Molecular Transport through the Nuclear Pore Complex as Studied by Scanning Electrochemical Microscopy. *J. Am. Chem. Soc.* **2013**, *135*, 2321−2329.
(536) Pathirathna, P.; Balla, R. J.; Jantz, D. T.; Kurapati, N.; Gramm, E. R.; Leonard, K. C.; Amemiya, S. Probing High Permeability of Nuclear Pore Complexes by Scanning Electrochemical Microscopy: Ca2+ Effects on Transport Barriers. *Anal. Chem.* **2019**, *91*, 5446−5454.
(537) Hansma, P.; Drake, B.; Marti, O.; Gould, S.; Prater, C. The Scanning Ion-Conductance Microscope. *Science* **1989**, *243*, 641−643.
(538) Pecora, R. Dynamic Light Scattering Measurement of Nanometer Particles in Liquids. *J. Nanopart. Res.* **2000**, *2*, 123−131.
(539) Kastengren, A.; Powell, C. F. Synchrotron X-Ray Techniques for Fluid Dynamics. *Exp. Fluids* **2014**, *55*, 1−15.
(540) Svarovsky, L. in *Solid-Liquid Separation*; Elsevier, 2001, 30−65.
(541) Ross, F. M. Opportunities and Challenges in Liquid Cell Electron Microscopy. *Science* **2015**, *350*, aaa9886.
(542) Ross, F. M. *Liquid Cell Electron Microscopy*; Cambridge University Press, 2016.
(543) De Jonge, N.; Ross, F. M. Electron Microscopy of Specimens in Liquid. *Nat. Nanotechnol.* **2011**, *6*, 695−704.
(544) Kelly, D. J.; Zhou, M.; Clark, N.; Hamer, M. J.; Lewis, E. A.; Rakowski, A. M.; Haigh, S. J.; Gorbachev, R. V. Nanometer Resolution Elemental Mapping in Graphene-Based Tem Liquid Cells. *Nano Lett.* **2018**, *18*, 1168−1174.
(545) Jensen, E.; Mølhave, K. Encapsulated Liquid Cells for Transmission Electron Microscopy. *Liquid Cell Electron Microscopy* **2016**, 35−55.
(546) Tanase, M.; Winterstein, J.; Sharma, R.; Aksyuk, V.; Holland, G.; Liddle, J. A. High-Resolution Imaging and Spectroscopy at High Pressure: A Novel Liquid Cell for the Transmission Electron Microscope. *Microsc. Microanal.* **2015**, *21*, 1629−1638.
(547) Yuk, J. M.; Park, J.; Ercius, P.; Kim, K.; Hellebusch, D. J.; Crommie, M. F.; Lee, J. Y.; Zettl, A.; Alivisatos, A. P. High-Resolution Em of Colloidal Nanocrystal Growth Using Graphene Liquid Cells. *Science* **2012**, *336*, 61−64.
(548) Zaluzec, N. J.; Burke, M. G.; Haigh, S. J.; Kulzick, M. A. X-Ray Energy-Dispersive Spectrometry During in Situ Liquid Cell Studies Using an Analytical Electron Microscope. *Microsc. Microanal.* **2014**, *20*, 323−329.
(549) Verch, A.; Pfaff, M.; de Jonge, N. Exceptionally Slow Movement of Gold Nanoparticles at a Solid/Liquid Interface Investigated by Scanning Transmission Electron Microscopy. *Langmuir* **2015**, *31*, 6956−6964.
(550) Schneider, N. M.; Norton, M. M.; Mendel, B. J.; Grogan, J. M.; Ross, F. M.; Bau, H. H. Electron-Water Interactions and Implications for Liquid Cell Electron Microscopy. *J. Phys. Chem. C* **2014**, *118*, 22373−22382.

https://doi.org/10.1021/acs.chemrev.1c00069
Chem. Rev. 2021, 121, 9450−9501

(551) Schilling, S.; Janssen, A.; Zaluzec, N. J.; Burke, M. G. Practical Aspects of Electrochemical Corrosion Measurements During in Situ Analytical Transmission Electron Microscopy (Tem) of Austenitic Stainless Steel in Aqueous Media. *Microsc. Microanal.* **2017**, *23*, 741−750.
(552) Lu, J.; Aabdin, Z.; Loh, N. D.; Bhattacharya, D.; Mirsaidov, U. Nanoparticle Dynamics in a Nanodroplet. *Nano Lett.* **2014**, *14*, 2111−2115.
(553) Lewis, E. A.; Haigh, S. J.; Slater, T. J. A.; He, Z.; Kulzick, M. A.; Burke, M. G.; Zaluzec, N. J. Real-Time Imaging and Local Elemental Analysis of Nanostructures in Liquids. *Chem. Commun.* **2014**, *50*, 10019−10022.
(554) Jensen, E.; Burrows, A.; Mølhave, K. Monolithic Chip System with a Microfluidic Channel for in Situ Electron Microscopy of Liquids. *Microsc. Microanal.* **2014**, *20*, 445−451.
(555) Yesibolati, M. N.; Laganà, S.; Sun, H.; Beleggia, M.; Kathmann, S. M.; Kasama, T.; Mølhave, K. Mean Inner Potential of Liquid Water. *Phys. Rev. Lett.* **2020**, *124*, 065502.
(556) Chu, W.; Webb, M. A.; Deng, C.; Colón, Y. J.; Kambe, Y.; Krishnan, S.; Nealey, P. F.; De Pablo, J. J. Understanding Ion Mobility in P2vp/Nmp+ I-Polymer Electrolytes: A Combined Simulation and Experimental Study. *Macromolecules* **2020**, *53*, 2783−2792.
(557) Pfister, L.; Savenije, H. H. G.; Fenicia, F. *Leonardo Da Vinci's Water Theory: On the Origin and Fate of Water*; International Association of Hydrological Sciences Press, 2009.

https://doi.org/10.1021/acs.chemrev.1c00069
Chem. Rev. 2021, 121, 9450−9501